

University of Montana

ScholarWorks at University of Montana

Graduate Student Theses, Dissertations, &
Professional Papers

Graduate School

1981

Petrology of Cretaceous and Tertiary intrusive rocks Red Mountains-Bull Trout Point area Boise Valley and Custer Counties Idaho

Stephen T. Luthy
The University of Montana

Follow this and additional works at: <https://scholarworks.umt.edu/etd>

Let us know how access to this document benefits you.

Recommended Citation

Luthy, Stephen T., "Petrology of Cretaceous and Tertiary intrusive rocks Red Mountains-Bull Trout Point area Boise Valley and Custer Counties Idaho" (1981). *Graduate Student Theses, Dissertations, & Professional Papers*. 7565.
<https://scholarworks.umt.edu/etd/7565>

This Thesis is brought to you for free and open access by the Graduate School at ScholarWorks at University of Montana. It has been accepted for inclusion in Graduate Student Theses, Dissertations, & Professional Papers by an authorized administrator of ScholarWorks at University of Montana. For more information, please contact scholarworks@mso.umt.edu.

COPYRIGHT ACT OF 1976

THIS IS AN UNPUBLISHED MANUSCRIPT IN WHICH COPYRIGHT SUBSISTS. ANY FURTHER REPRINTING OF ITS CONTENTS MUST BE APPROVED BY THE AUTHOR.

MANSFIELD LIBRARY
UNIVERSITY OF MONTANA
DATE: 1981

PETROLOGY OF CRETACEOUS AND TERTIARY INTRUSIVE
ROCKS, RED MOUNTAIN - BULL TROUT POINT AREA,
BOISE, VALLEY, AND CUSTER COUNTIES, IDAHO

by

Stephen T. Luthy

B.A., University of California, Santa Barbara,
1977

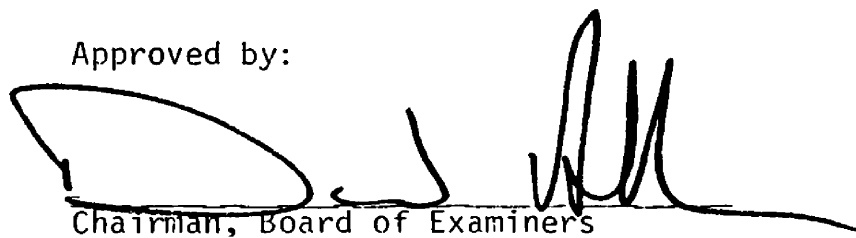
Presented in partial fulfillment of the
requirements for the degree of


Master of Science

UNIVERSITY OF MONTANA

1981

Approved by:


Chairman, Board of Examiners


Dean, Graduate School

Date

6-8-81

UMI Number: EP38366

All rights reserved

INFORMATION TO ALL USERS

The quality of this reproduction is dependent upon the quality of the copy submitted.

In the unlikely event that the author did not send a complete manuscript and there are missing pages, these will be noted. Also, if material had to be removed, a note will indicate the deletion.



UMI EP38366

Published by ProQuest LLC (2013). Copyright in the Dissertation held by the Author.

Microform Edition © ProQuest LLC.

All rights reserved. This work is protected against
unauthorized copying under Title 17, United States Code



ProQuest LLC.
789 East Eisenhower Parkway
P.O. Box 1346
Ann Arbor, MI 48106 - 1346

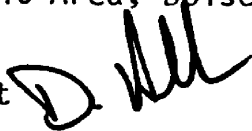
ABSTRACT

Luthy, Stephen T., M.S., Spring, 1981

Geology

Petrology of Cretaceous and Tertiary Intrusive Rocks, Red Mountain-Bull Trout Point Area, Boise, Valley and Custer Counties, Idaho

Director: David Alt



Field, petrographic, and chemical data indicate that four mineralogically and texturally distinct Cretaceous rock units exist in the Red Mountain-Bull Trout Point area, Idaho. Although contact relations are obscure, megacryst-bearing foliated granodiorite may be a deformed and partly remobilized early phase emplaced at relatively high levels in the batholith. Later batholithic phases include granodiorite porphyry and granodiorite which is the most abundant rock type. Leucocratic granite is a late-stage differentiate emplaced along structural planes of weakness in older batholithic rocks including a west-northwest trending shear zone north of Red Mountain. In this area, a swarm of leucocratic granite dikes and surrounding older batholithic rocks contain magnetite megacrysts. The megacrysts were formed during localization of a water-rich melt phase late in the crystallization history of these dikes.

Two intrusive assemblages of probable Eocene age are recognized: a quartz diorite stock with associated latite and quartz latite dikes; and a pink granite pluton with a differentiated cap and marginal facies of alaskite and related rhyolite dikes. In addition to their close chemical affinities, members of each of the two groups have a similar mineralogy and display consistent spatial and temporal relations. In each case, dikes ramified from their larger plutonic source and were injected before, during, and after final emplacement of the related pluton. North- to northeast-trending high-angle normal faults and fractures controlled emplacement of the plutons and their associated dike rocks. Approximately 35 percent northwest-southeast crustal extension is indicated based upon the cumulative thickness of dike rocks in the area. Each intrusive center was forcibly emplaced to depths of less than 2 kilometers in this north- to northeast-trending extensional zone which is interpreted as an incipient crustal rift.

ACKNOWLEDGMENTS

Special thanks are given to Thor Kiilsgaard and Dave Alt for continued advice, enlightenment and encouragement both in and out of the field. Considerable time and effort were given by Gray Thompson and Ken Watson during their critical review of the manuscript. Mike Wilson and Jerry Zieg offered inspirational insight on various matters pertaining to the thesis, and to them I am grateful. Judi and Heather Whitley provided endless support and unbending faith throughout the frequently winding course of this work.

TABLE OF CONTENTS

	Page
ABSTRACT.	ii
ACKNOWLEDGMENTS	iii
LIST OF TABLES.	vii
LIST OF FIGURES	viii
LIST OF PLATES.	ix
 CHAPTER	
I. INTRODUCTION.	1
Location of Study Area.	2
Previous Work	3
This Study.	4
II. REGIONAL GEOLOGY.	6
Lithologies	6
Precambrian(?) Rocks.	6
Paleozoic(?) Rocks.	9
Idaho Batholith	10
Leucocratic Quartz Monzonite.	12
Tertiary Granitic Rocks	13
Tertiary Dikes.	14
Idaho Porphyry Belt	15
III. DESCRIPTION OF MAP UNITS.	19
Precambrian Metamorphic Rocks	19
Marble.	19
Undifferentiated Metamorphic Rocks.	20

CHAPTER	Page
Discussion.	20
Cretaceous Granitic Rocks	26
Foliated Granodiorite	26
Granodiorite Porphyry	32
Granodiorite.	35
Leucocratic Granite	36
Tertiary Granitic Rocks	38
Quartz Diorite.	38
Discussion.	42
Pink Granite.	46
Alaskite.	49
Tertiary Dike Rocks	53
Quartz Latite-Latite Porphyry	55
Rhyolite.	57
Diabase	59
Discussion.	61
Quaternary Deposits	61
Alluvium.	61
Moraine	61
IV. WHOLE-ROCK COMPOSITIONS	62
Ternary Diagrams.	65
Silica Variation Diagrams	69
Depth of Emplacement of Tertiary Intrusions	73
Summary	75

CHAPTER	Page
V. STRUCTURAL FRAMEWORK.	78
Pink Granite-Cretaceous Granodiorite Contact.	78
Faults.	79
Dikes	83
Summary	85
VI. VAPOR PHASE CRYSTALLIZATION IN LEUCOCRATIC GRANITE.	88
Discussion.	96
VII. CONCLUSIONS	102
Cretaceous Rocks.	102
Tertiary Rocks.	103
REFERENCES CITED.	105

LIST OF TABLES

Table	Page
1. Mineralogy of the Cretaceous granitic units	33
2. Mineralogy of the quartz diorite, quartz latite, and latite units.	41
3. Mineralogy of the pink granite, alaskite, and rhyo- lite units.	47
4. Whole-rock XRF chemical analyses.	63

LIST OF FIGURES

Figure	Page
1. Location of study area.	2
2. Regional geology.	8
3. Outline of Idaho Porphyry Belt.	17
4. Photograph of marble roof pendant	23
5. Photograph of marble near Spring Creek.	23
6. Photograph of migmatite near Spring Creek	23
7. Rock classification chart	27
8. Photograph of foliated granodiorite	30
9. Photograph of granodiorite porphyry	30
10. Photograph of granodiorite.	30
11. Photograph of leucocratic granite	30
12. Compositional plot of foliated granodiorite and grano- diorite porphyry.	31
13. Compositional plot of granodiorite and leucocratic granite	31
14. Compositional plot of Tertiary quartz diorite and pink granite	39
15. Photomicrograph of rounded quartz phenocryst in quartz diorite	43
16. Photomicrograph of synneusis texture in quartz diorite. .	43
17. Pressure-weight percent H ₂ O phase assemblage diagram for synthetic granite	44
18. Sketch of development of synneusis aggregate.	45
19. Photomicrograph of pink granite	51
20. Photomicrograph of alaskite	51

LIST OF FIGURES (Continued)

Figure	Page
21. Photograph of quartz latite dike.	51
22. AFM ternary diagram	66
23. Normative CaO-K ₂ O-Na ₂ O ternary diagram.	68
24. Normative An-Or-Ab ternary diagram.	68
25. Variation diagram	71
26. Normative Ab-Or-Qz ternary diagram.	74
27. Photograph of pink granite-granodiorite contact	80
28. Photograph of fault near head of Cat Creek.	80
29. Schematic block diagram of Red Mountain Bull Trout Point area.	86
30. Photograph of cluster of magnetite megacrysts	91
31. Photograph of aligned quartz-feldspar halos	91
32. Microphotograph of magnetite megacryst.	91
33. Temperature-fO ₂ diagram for compositions of coexisting ilmenite-titanomagnetite pairs.	93
34. Schematic diagram of leucocratic dikes.	98
35. Schematic diagram for formation of magnetite megacrysts .	100

LIST OF PLATES

Plate	Page
I Geologic map, scale 1:24,000	In Pocket

CHAPTER I

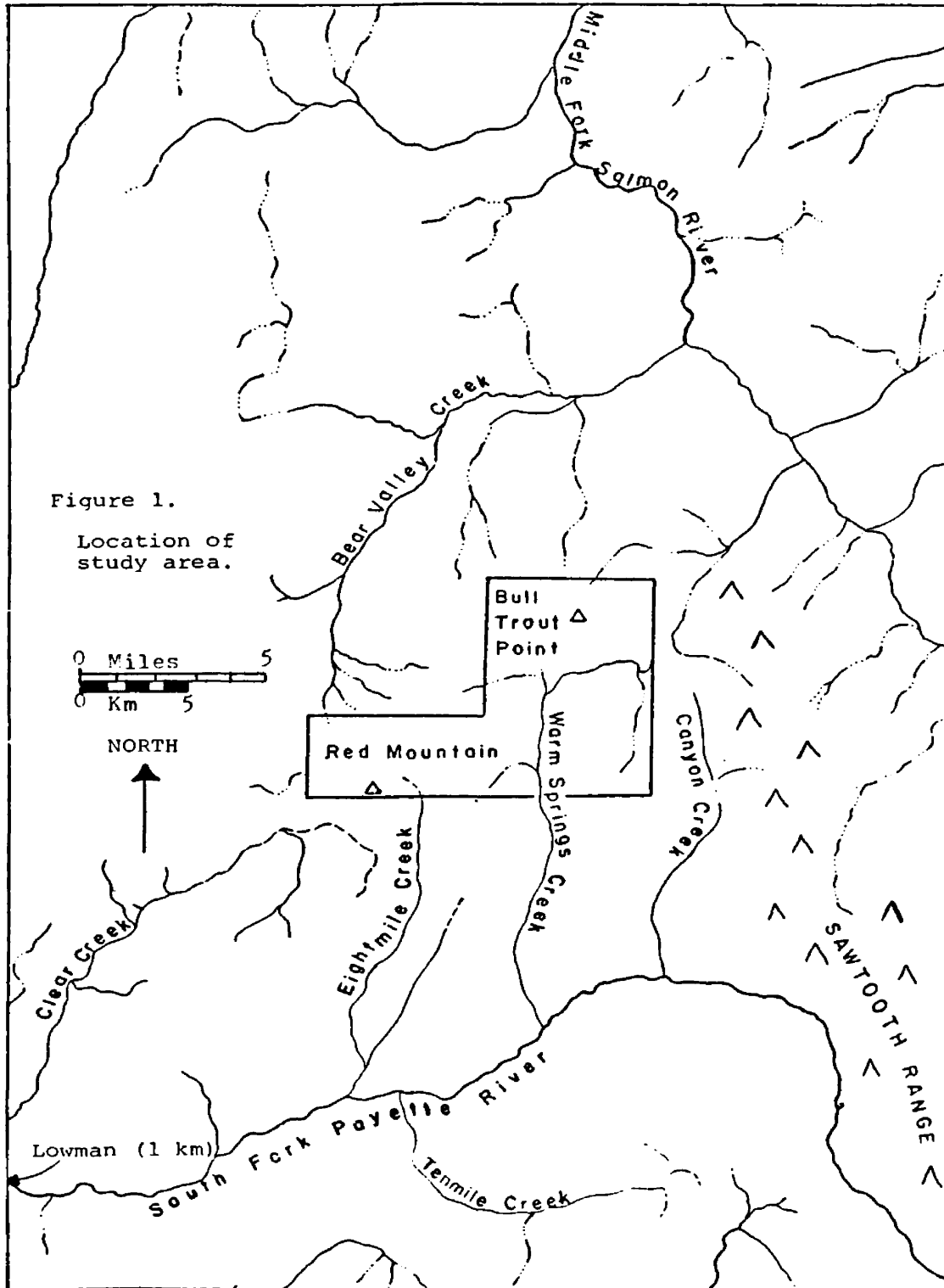
INTRODUCTION

The primary objectives of this study were to describe the petrography and field relations of a sequence of Cretaceous and Tertiary intrusive rocks in south-central Idaho and use this information to determine the intrusive history of the area. This report presents field, petrographic, and chemical data on these rocks in terms of a possible tectono-magmatic environment.

The area is underlain by granitic rocks of the Cretaceous-age Idaho batholith which are intruded by granitic and dike rocks of early- to mid-Tertiary age. Granitic rocks in the area range in composition from granite to quartz diorite. Dike rocks vary in composition from rhyolite to basalt, however, most dikes are between latite and rhyolite in composition. Other lithologies present in the area include Precambrian(?) metamorphic rocks and unconsolidated Quaternary deposits.

Location of Study Area

The study area is in the Challis and Boise National Forests, approximately 30 kilometers northeast of Lowman, Idaho (Fig. 1). Bull Trout Point lies near the northeastern corner and Red Mountain occupies the southwestern corner of the map area. Access to the area may be gained by Clear Creek Road leading northeast from Lowman or by Forest Service roads leading into Bull Trout Lake from Route 21. Forest



Service-maintained pack trails enter into the area from these roads.

The irregularly-shaped field area is bordered on the east by the 115°15' longitudinal line and on the south by the 44°15' latitudinal line. Northern and western boundaries reflect logistical limitations. Approximately 64 square kilometers were mapped during the months of July and August.

Previous Work

Rocks in the area have received cursory examination in previous reconnaissance geologic mapping. The geologic map of Idaho (Bond, 1978) shows that undifferentiated Cretaceous-age granitic rocks underly most of the area with patches of Tertiary granitic rocks north of Bull Trout Lake and a swarm of northeast-trending dikes in the vicinity of Red Mountain. A geologic study of rare earth placer deposits in the Bear Valley district made by Mackin and Schmidt (1953) mentions three types of bedrock: medium-grained and coarse-grained granite and granite porphyry, with all gradations between them. Their study revealed a distinctly later system of porphyry dikes, ranging from acidic to basic, well-exposed in the cirque walls on the north and east sides of Red Mountain.

Reconnaissance mapping by Olson (1968) revealed a small Tertiary stock of quartz monzonite near Red Mountain and two larger masses of Tertiary pink granite north and west of Bull Trout Lake. A northeast-trending swarm of latite, quartz latite, and rhyolite dikes forms a conspicuous geologic element. Olson suggested that at least some of

the dikes in the Red Mountain area are related to the Tertiary quartz monzonite stock. The strong northeast trend of the dikes was attributed to pervasive northeast fracturing within older batholithic rocks.

In reconnaissance geologic studies to the east and southeast, Reid (1963) and Kiilsgaard (1970) describe coarse-grained, Tertiary pink granite of the Sawtooth batholith and a variety of Tertiary dikes ranging from rhyolite to basalt. Both authors also describe granitic rocks of the Cretaceous Idaho batholith including leucocratic quartz monzonite which was interpreted as a late-stage differentiate of older batholithic rocks.

This Study

The present study was part of a United States Geological Survey investigation of the mineral resource potential of the Challis two-degree quadrangle, Idaho. Financial aid and logistical support were provided by the U. S. Geological Survey. Field data were recorded onto 1:24,000 topographic base maps. Aerial photos were used for preliminary identification of intrusive contacts, faults, and Quaternary deposits. The area of this study is contained on U. S. Geological Survey Bull Trout Point and Cache Creek 7½' quadrangle sheets.

Thirteen major bedrock lithologic units were mapped (Plate 1). All units were differentiated in the field on the basis of hand specimen and outcrop characteristics. In a few cases, later thin-section examination resulted in the reclassification of particular outcrops. Outcrops of most lithologic units are abundant, particularly at higher elevations, and structural data in these areas is reliable. At lower

elevations, or where there is abundant vegetative cover, units were mapped primarily on the basis of "rubble"--loose, unconsolidated material presumed to be locally derived on the basis of lithologic continuity or geographic location.

CHAPTER II

REGIONAL GEOLOGY

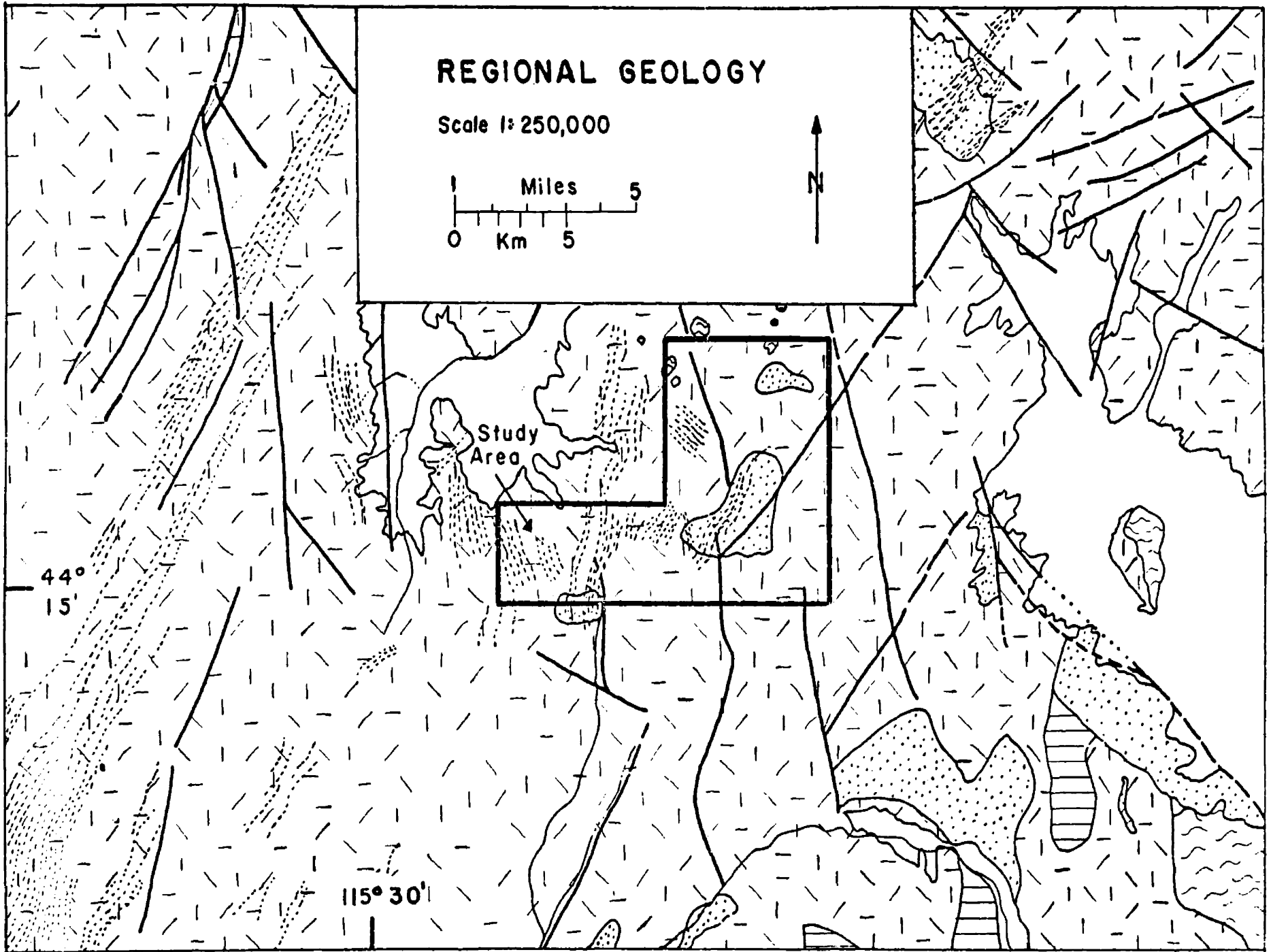
Lithologies

The region is underlain by rocks of the Cretaceous Idaho batholith and by Tertiary intrusive bodies, including shallow level plutons, hypabyssal stocks, and dikes. Exposures of Precambrian(?) metamorphic rocks exist throughout the core of the Idaho Porphyry Belt. Figure 2 shows the regional geology and Figure 3 shows the outline of the Idaho Porphyry Belt.

Precambrian(?) Rocks

The oldest known rocks in the region, the metamorphosed rocks of the Thompson Peak Formation (Reid, 1963) are found locally along 16 kilometers of the eastern front of the Sawtooth Mountains. The nearest exposures of the rocks are approximately seven miles east of Bull Trout Lake. Feldspathic schist, feldspar-rich granofels, and lime-silicate granofels comprise most of the Thompson Peak Formation in the Sawtooth Range. Xenoliths are found locally within the Idaho and Sawtooth batholiths. Reid (1963) considered those metamorphic rocks, which show more complex deformation and higher grade metamorphism than nearby Paleozoic rocks, to be Precambrian in age because they resemble the Wallace Formation of the Proterozoic Belt Supergroup in northern Idaho.

Figure 2. Regional geology. Precambrian metamorphic rocks shown in wavy dashed pattern, granitic rocks of the Idaho batholith in crystalline pattern, leucocratic quartz monzonite of Cretaceous age in ruled pattern, and Tertiary plutonic rocks in stippled pattern. Dikes (short dashes) shown schematically. Modified from Rember and Bennett, 1979.



Paleozoic(?) Rocks

Remnants and roof pendants of undifferentiated metamorphosed sedimentary rocks are exposed north of a line between Bull Trout Lake and Red Mountain. Their ages are uncertain. Olson (1968) considered these rocks to be lower Paleozoic and possibly Ordovician in age because they resemble the Kinnikinic Quartzite and because Ross (1934) considered nearby rocks to be Ordovician(?). Finely-laminated quartzite intercalated with marble and calc-silicate members comprise most of these rocks.

In the Casto quadrangle, Ross (1934) found schists which lay unconformably under limestone and quartzite of possible Ordovician, or as Ross (1962) later suggested, of possible Beltian age. The pronounced angular unconformity at the top of the schists led Ross to assign them an Algonkian age. Mapping farther to the southwest in the Seafoam Mining District, Treves and Melear (1953) mention highly foliated and contorted schists gradational into quartzites which they designate as Algonkian and Ordovician, respectively.

Ages of 58 ± 1.7 m.y. (biotite) and 63.6 ± 1.9 m.y. (muscovite) were obtained by Rychener (pers. comm., in Olson, 1968) on a muscovite biotite schist about 17 miles northwest of Stanley. These minimum ages may reflect Mesozoic metamorphism during emplacement of the Idaho batholith or partial argon release during emplacement of the nearby Sawtooth batholith.

Idaho Batholith

The Idaho batholith is a composite body, consisting of numerous granitic to granodioritic plutons (Hyndman and Williams, 1977; Williams, 1977; Nold, 1974). Evidence for a mesozonal to catazonal depth of emplacement includes: regionally concordant and gradational contacts with surrounding high-grade regionally metamorphosed sedimentary rocks, subsolvus mineralogy of most plutonic rocks, abundant migmatitic textures, and the absence of genetically-related volcanic rocks (Hyndman, 1972). The anomalous position of this major pluton east of the Cordilleran batholithic trend, and its division into two geographically-distinct parts, renders it unique among Cordilleran batholiths. The two parts of the body are separated by 1500 m.y.-old high-grade metamorphic rocks of the Salmon River Arch (Armstrong, 1975). The northern and southern parts of the batholith have been called the Bitterroot and Atlanta Lobes, respectively.

Country rocks adjoining the Atlanta lobe on the north and northeast are Belt and pre-Belt basement schists and gneisses; those on the east are locally Precambrian(?) metamorphic rocks (Dover, 1969; Reid, 1963). Along the western border, the country rocks are metamorphosed submarine volcanic rocks of probable Permo-Triassic age. Devonian to Permian marine clastic rocks are thrust eastward away from the batholith. Much of the Atlanta lobe-country rock interface is covered by younger rocks, predominantly Tertiary continental volcanic rocks. Miocene flood basalts and Pliocene fluvial and lacustrine sediments occur west of the Atlanta lobe; on the south are Pliocene

welded tuffs and Pleistocene Snake River Plain flood basalts. Challis volcanics of Eocene age and related shallow-level plutonic bodies overlap the batholith along its eastern margin.

Much of the region (Fig. 2) is underlain by rocks comprising the Atlanta Lobe of the Cretaceous-age Idaho batholith. Armstrong (1976) suggests that the age of the Atlanta Lobe may be between 75-100 m.y. Ages of 69.6 ± 2 m.y. (biotite), 71.2 ± 2 m.y. (biotite), and 77 ± 4 m.y. (Rb-Sr, whole rock) were reported by Armstrong (1975) for medium-grained, porphyritic biotite granodiorite and adamellite rocks belonging to the Idaho batholith on Bear Valley Mountain approximately 6 kilometers north of Red Mountain. These ages presumably represent minimum ages due to a profound igneous-hydrothermal-tectonic event in Eocene time which partially-to-totally reset K/Ar dates to approximately 50 m.y. (Criss, 1980; Criss and Taylor, 1978; Armstrong, 1976).

In the Sawtooth Primitive Area, the batholith is composed of granodiorite and quartz monzonite, and minor quartz diorite (Kills-gaard, 1970). Reid (1963) mentions compositional zones in the same area with more alkali-rich phases concentrated towards the east. Schmidt (1964) recognized five gradational belts along a 35 mile section in the latitudes of McCall and Cascade. His reconnaissance petrographic sampling suggested that a border zone of basic quartz diorite migmatite and gneiss gives way eastward to successively more alkali-rich phases culminating in a quartz monzonite belt in the Warm Lake area. Textural variations range from medium- and fine-grained varieties to striking porphyritic textures featuring large megacrysts of K-feldspar, and in some cases, quartz.

Leucocratic Quartz Monzonite

Significant amounts of fine- to medium-grained, equigranular leucocratic quartz monzonite exist within the region. Such rocks have been reported by Ross (1934) in the Casto quadrangle, Anderson (1947) east of Idaho City in the Boise Basin, Reid (1963) and Kiilsgaard (1970) in the Sawtooth Mountains, and Bennett (1973) in the White Cloud Wilderness. The unit is characterized by a deficiency of mafic constituents, particularly biotite. Similar mineralogies have led some workers to interpret the leucocratic unit as a late stage differentiate of Idaho batholithic rocks, and this unit consistently cuts all other batholithic phases. The leucocratic rock commonly occurs as discordant sheets and irregularly-shaped masses.

Absolute ages of the leucocratic rock are unknown. Reid (1963) noted that the unit generated a suite of pegmatite and aplite phases distinctly different from those of the Idaho batholith. Kiilsgaard (1970) reported angular xenoliths of batholith-related granodiorite within the younger quartz monzonite. Field work during 1979 in the 10-Mile RARE II Wilderness noted similar relations at the head of Big Silver Creek, however, pink granite of known or suspected Eocene age (44-46 m.y.) intrudes the quartz monzonite. The leucocratic rock is, therefore, considered intermediate in age between Challis-related intrusives and Cretaceous Idaho batholithic rocks. These constraints place the age of the unit as being of very latest Cretaceous or Early-Tertiary age.

Tertiary Granitic Rocks

Tertiary granitic rocks form coarse-grained, epizonal stocks and plutons. Two groups of Tertiary batholiths and stocks exist within the region: a large group of distinctive quartz monzonite-granite plutons and a smaller but significant number of quartz diorite to quartz monzonite intrusions (Bennett, 1980).

The most easily recognized of the Tertiary plutonic rocks are pink biotite granite stocks and batholiths which are widespread in both the Bitterroot and Atlanta lobes (Bennett, 1980; Hyndman and Williams, 1977). Some characteristics shared by this group, including the Sawtooth and Casto plutons, indicate shallow emplacement: miarolitic cavities containing smoky quartz crystals and sharp, discordant contacts are two such features. The quartz diorite to quartz monzonite and granodiorite group includes the Boise Basin quartz diorite (Anderson, 1947), the Trinity Mountain quartz diorite (Bennett, 1980), the Red Mountain quartz monzonite (Olson, 1968), granodiorite of Jackson Peak (Kiilsgaard, in prep.), quartz diorite in the Casto quadrangle (Ross, 1934), and several other small stocks (Kiilsgaard, pers. comm., 1980).

Many plutons that have not been dated are believed to be Tertiary in age because they closely resemble dated plutons. Cater (1973) reports that a single potassium-argon determination on mica yielded an age of 42.7 m.y. for the Casto pluton. Potassium-argon determinations on biotite gave ages of around 44 m.y. for pink granite of the Sawtooth batholith (Armstrong, 1975). Kiilsgaard (pers. comm., 1981)

reports concordant potassium-argon ages on biotite of 46 m.y. for the granodiorite of Jackson Peak.

Tertiary Dikes

Dikes are abundant throughout the region and form a nearly continuous swarm connecting the intrusive centers of the Boise Basin and the Casto quadrangle. According to Olson (1968), the dikes vary in composition from diabase, dark andesites, and fine-grained diorite through latite, quartz latite and rhyolite. Intrusion of the dikes may have followed an imperfect differentiation sequence, becoming progressively more acidic with time (Olson, 1968).

The dikes tend to concentrate in swarms of different preferred directions. Olson (1968) describes dikes swarms in the Boise Basin, Miller Creek, Red Mountain, Seafoam, Cliff Creek, Ruffneck Peak, and Beaver Creek areas. With few exceptions, he shows that dikes fall into a system of two sets; a dominant north-northeast trending set, and a secondary set trending east-northeast.

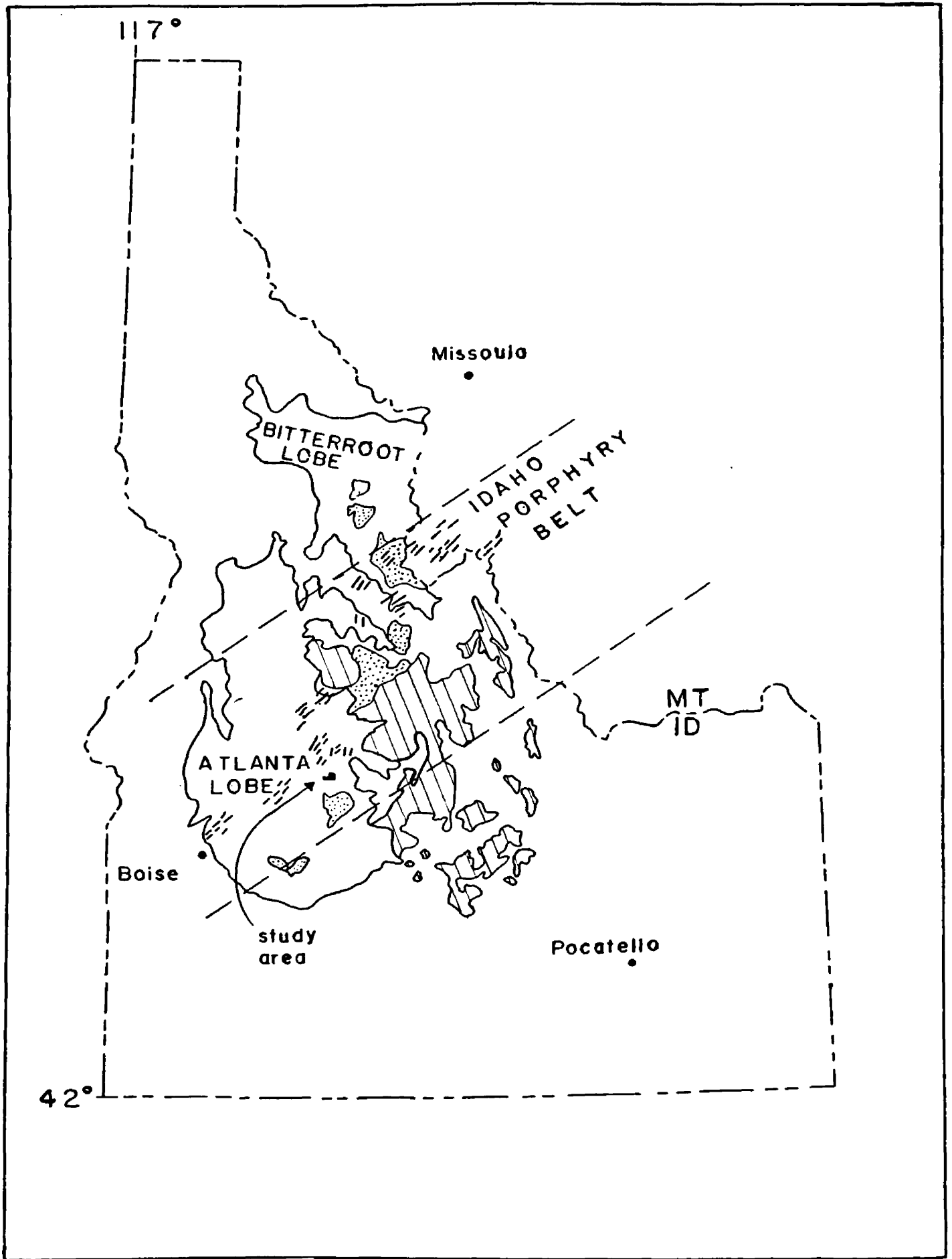
Absolute ages of the dike swarms are unknown. Most dikes crosscut Idaho batholithic rocks and are therefore Tertiary in age. A single Rb-Sr whole rock age determination of 38.5 ± 1.2 m.y. was reported by Olson (1968) on quartz latite porphyry collected adjacent to the Boise Basin dike swarm west of Lowman. Many of the swarms in the region are related spatially to intrusive masses of known or suspected Eocene age, however, some of the dikes cut these intrusives (Olson, 1968; Kiilsgaard, 1970; Reid, 1963).

Idaho Porphyry Belt

Early Tertiary dikes are concentrated in a broad northeast-trending zone throughout south-central Idaho and southwestern Montana. The dikes, which vary in composition from basalt to rhyolite, have been grouped together and called the Idaho Porphyry Belt (Fig. 3), or less commonly, the Anaconda Range Dike Swarm (Badgely, 1965). Previous workers in the Idaho Porphyry Belt include Ross (1934), Anderson (1947), Donovan (1962), Olson (1968), and Badley (1977). The "type area" for the belt is located in the Boise Basin (Anderson, 1947) and many of the dikes belonging to the belt are found in areas containing economic base and precious metal deposits. Dikes are not always found with a corresponding area of mineralization, however, the relationship between mineralization and intrusion of dikes has been described by Donovan (1962).

A pre-existing zone of structural weakness has been called upon by recent workers (Hyndman, Badley and Rebal, 1977; Olson, 1968) to account for the emplacement and length (approximately 400 km) of the Idaho Porphyry Belt. Residual Bouguer anomaly maps from surveys in central Idaho and western Montana indicate major northeast-trending lineaments defined by pronounced, localized gravity lows, extending from south-central Idaho to southwestern Montana (Smith, 1967; Eaton and others, 1978; Ballard, 1980). The belt also coincides with a broad northeast-trending oval gravity low across central Idaho which in turn coincides with an axis of high (>2,1000 m) topography (Eaton and others, 1978). This elevated topographic surface north of the

Figure 3. Map of Idaho showing outline of Idaho Porphyry Belt. Cretaceous rocks of the Idaho batholith outlined with solid line, Tertiary plutons in stippled pattern, and Challis Volcanics in ruled pattern. Study area shown in black.



central and eastern Snake River Plain is similar in location, configuration, and trend to a surface of Eocene topography reconstructed by Axelrod (1968). The broadly domed Eocene surface coincides closely with the outline of the Idaho Porphyry Belt which contains significant amounts of Eocene volcanic and intrusive rocks.

It has been suggested (Eaton and others, 1978) that these features may represent products of regional, thermo-magmatic uplift. The associated gravity low may indicate the addition of primarily Eocene low density intrusive material to this portion of the crust. Emplacement of dikes within the belt may have been caused by gentle crustal upwarping and consequent fracturing in this region during emplacement of Challis-related intrusive material.

CHAPTER III

DESCRIPTION OF MAP UNITS

The geologic map (Plate 1) shows the distribution of all major rock units within the area as well as the location and trend of major faults. In the following description, each unit is characterized by both hand specimen and thin section study, in order of age from oldest to youngest.

Precambrian(?) Metamorphic Rocks

The oldest rocks in the study are metamorphic roof pendants of marble and undifferentiated metamorphic rocks including quartzite, biotite schist, marble, and biotite quartzo-feldspathic gneiss. Age of these rocks is uncertain, and it is possible that they may be wholly or in part of Paleozoic age.

Marble -- pCm

The bulk of metamorphic rocks are composed of cream to greenish-white limestone and marble. Marble also forms the largest roof pendants which crop out on the ridge east of Spring Creek. Two such remnants exceed 300 meters in length while several others are greater than 150 meters in length. Minor amounts of calcareous schist and biotite hornfels occur within the larger marble pendants which weather to form prominent tan- to buff-colored bluff exposures. Structures within the marble are isoclinally folded layers from two to five

centimeters thick which vary in relative amounts of silica and lime. The layering is not always discernible, is generally discontinuous, and may represent primary sedimentary features or the effects of metamorphic differentiation.

In thin section, quartz (10-40 percent), diopside (30 percent), wollastonite (5-25 percent) or calcite (5 percent) are the primary mineral constituents. Minor amounts of plagioclase and/or K-feldspar may also be present. Quartz is strained but grains are not oriented whereas elongate wollastonite subhedra usually display a weak lineation. Layering is defined by quartz-rich and diopside-calcite-wollastonite-rich layers. The rock is generally fresh with little or no indication of alteration.

Undifferentiated Metamorphic Rocks -- pCu

A small, elongate cluster of relatively small metamorphic remnants crop out north of Cat Lakes in the western portion of the map area. The cluster trends approximately west-northwest and consists of quartzite, biotite schist, marble, and biotite quartzo-feldspathic gneiss. Light-tan to brown, massive quartzite and greyish-tan to rust-colored fine-grained calcareous schist make up most of the small remnants in the Cat Lakes area.

Discussion

The metamorphic roof pendants are generally composed of numerous, polygonally-shaped blocks surrounded by thick, continuous dikes of coarse-grained pegmatite and aplite. Figure 4 shows one of the larger

remnants which crop out on the ridge east of Spring Creek. The aplite and pegmatite often form sub-parallel, closely-spaced dikes and dike-lets which alternate with layers of the country rock. In several localities, the dikes display complex isoclinal folding. Axes of these folds usually parallel the dominant layering direction defined by the aplite and pegmatite dike sets which in turn follow compositional layering within the host metamorphic pendant (Fig. 5). In some cases, folding is so intense that the rock begins to take on the appearance of a migmatite (Fig. 6).

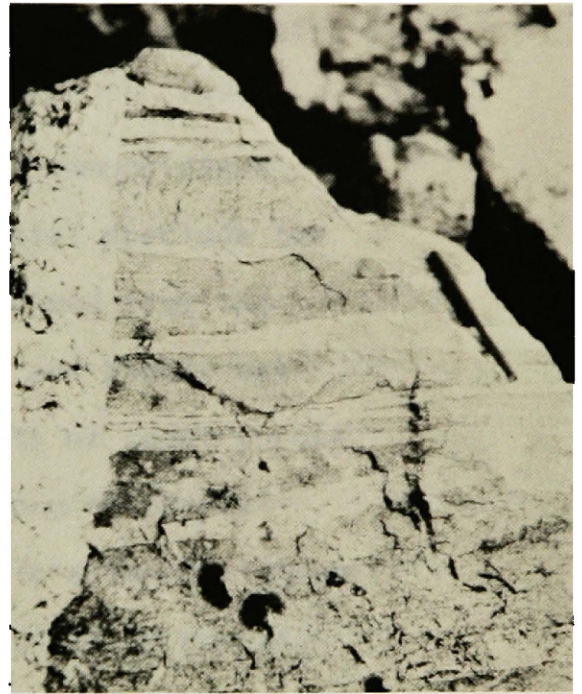
Numerous lines of evidence suggest that crystalline quartz-feldspar dikes are the result of intrusion of volatile-rich magma during block stoping and not the product of metasomatic replacement, partial melting of country rock, or metamorphic differentiation.

- 1) The thicker veins cross-cut one another (Fig. 6) producing offset of earlier formed veins. It is unlikely that metamorphic differentiation would produce vein material in such divergent orientations as shown in Figure 6. Dilation offset of earlier-formed veins argues strongly against metasomatic replacement origin for these cross-cutting veins.
- 2) Chilled margins of some veins against roof pendants indicate that the vein material was significantly hotter than the enclosing metamorphic rock during its formation. Metasomatic introduction of various elements (K, Na, etc.) to form granitic veins presumably

Figure 4. Photograph of marble roof pendant. View is toward east ridge of Spring Creek.

Figure 5. Photograph of quartz-feldspar dikes paralleling apparent lithologic layering in marble near Spring Creek.

Figure 6. Migmatitic aspect of quartz-feldspar dikes and host marble in roof pendant near Spring Creek.



requires diffusion of these elements down activity gradients (i.e. from hotter to cooler environments) and therefore could not have played a significant role in this case. A large temperature gradient between the rock and the position of the new layers hardly seems likely considering the small scale of the layers (Hyndman, 1972).

- 3) In most cases, contrasting chemical compositions between vein and country rock material preclude the possibility that the veins were derived from the country rock. Since most pendants are highly calcareous, prohibitively large amounts of country rock would necessarily be involved in forming quartz-feldspar veins by either metamorphic differentiation or partial melting of country rock. It is conceivable that some vein material originated by anatectic melting in rocks of different composition and moved far enough from their source to take on the characteristics of injection veins.

No systematic or consistent temporal relations were established between concordant veins and dikelets and discordant dikes. Exposures show concordant veins at once cutting and being cut by larger discordant dikes. Examination of some exposures suggested that the two sets of dikes were emplaced synchronously, or that the small sub-parallel veins ramified laterally from the larger discordant dikes.

In the latter case, the larger discordant dikes may have acted as "magma reservoirs" for the concordant vein material. Barrell (1907) notes that infiltration veins have been injected laterally away from associated cross-trending dikes in the Marysville stock of western Montana. Contacts between the thick, coarse-grained dikes and narrow, medium- to fine-grained veins and dikelets are marked only by gradational changes in grain size. The change in grain size may reflect different rates of cooling as determined by dike width, and not differences in composition or times of emplacement.

All levels of structural complexity exist between the planar, concordant veining shown in Figure 5, and the isoclinally folded, highly complex migmatitic structure displayed by veins in Figure 6. Since injection material presumably followed paths of least resistance in the rock, it is plausible that present vein geometry now represents orientation of pre-existing structural planes and fractures. Some veins parallel apparent lithologic changes in marble pendants near Spring Creek suggesting the veins were injected preferentially along bedding plane partings of an original calcareous unit.

Pendants in the Cat Lakes area also display features suggestive of block stoping. Small, isolated blocks have a flat or nearly flat-lying aspect. Relatively smooth, sharp sides and tops contrast markedly with very irregular, poorly defined bottoms. Whereas pegmatite and aplite dikes generally surround the blocks on all sides, injection veins and dikes preferentially penetrate from the bottom upwards. The dikes were presumably injected initially upwards along

fractures into and around the block, isolating and subsequently foundering it in volatile-rich magma.

Presence of metamorphic roof pendants indicate that the current level of exposure must be at or near the top of the batholith in this area. Emplacement of the batholith by multiple block stoping at this localized level was enhanced by the ability of surrounding country rocks to behave somewhat brittly to stresses placed upon them.

Cretaceous Granitic Rocks

The Idaho batholith has been subdivided into four textural and compositional units; foliated granodiorite, granodiorite porphyry, the widespread granodiorite unit, and leucocratic granite. Mineralogical variations control the compositions of the rocks; the IUGS classification and nomenclature for plutonic rocks (Streckeisen, 1976) are used to name the rocks and is shown in Figure 7.

Foliated Granodiorite -- Kfgd

The unit forms small fault-bounded, wedge-shaped bodies in the southeastern portion of the area. These bodies are probably remnants of an older and presumably much larger intrusive mass which was subsequently intruded by younger batholithic rocks. Nearby roof pendants attest to the relatively high level of the batholith exposed in this area, and it is suggested that the foliated granite was part of a foliated, mafic upper margin or carapace of the batholith. Similar rocks are reported near roof pendants in the Basin Creek area by Erler (1980).

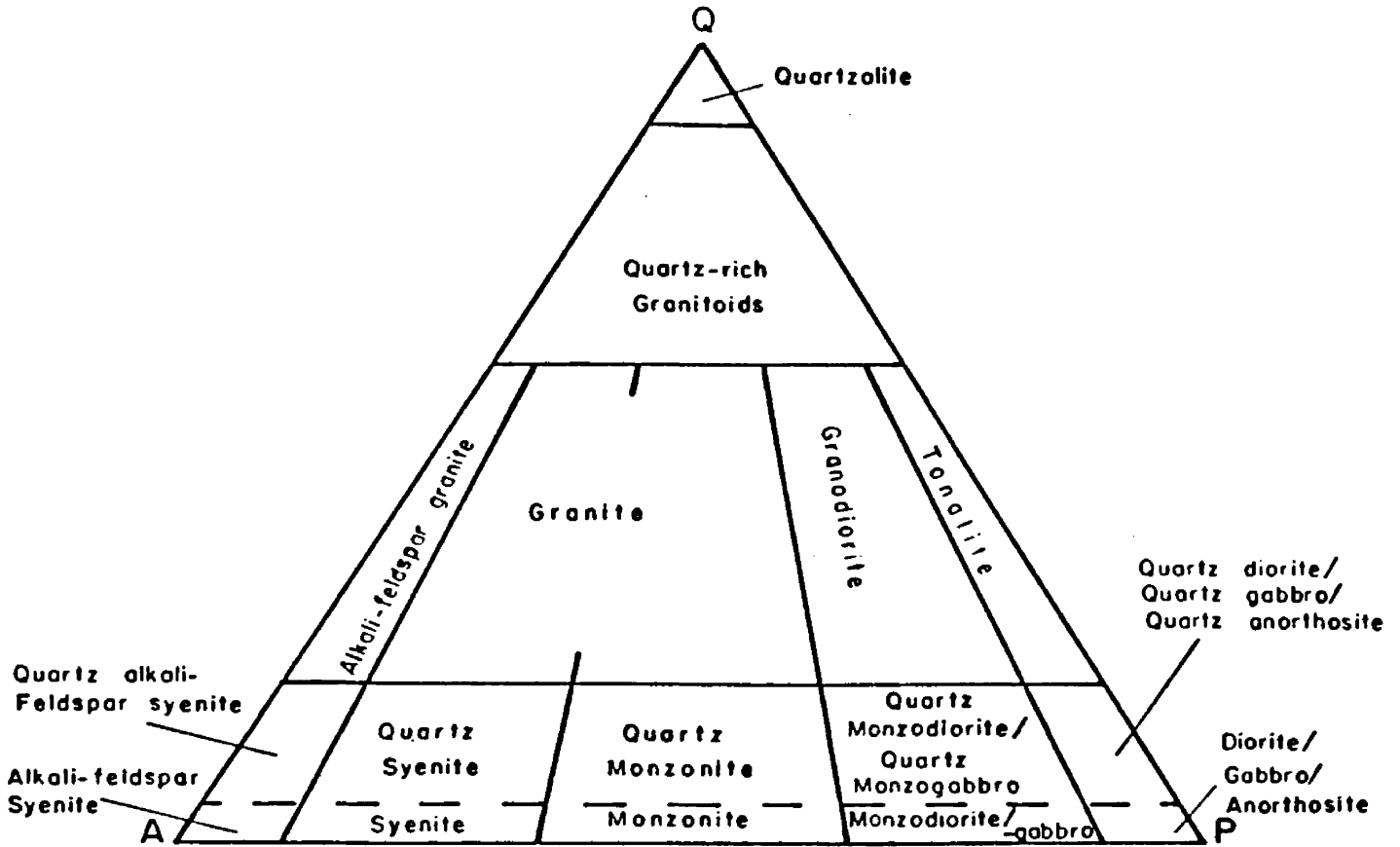


Figure 7. General classification and nomenclature of quartz-bearing plutonic rocks according to mineral content (in volume percent), after Streckeisen (1976, p. 8).

Foliated granodiorite forms fairly non-resistant, steep-sided bluffs, probably because it contains a low proportion of felsic constituents, notably K-feldspar. In hand specimen, the rock is characterized by a medium- to coarse-grained groundmass of plagioclase, K-feldspar, biotite, and quartz. Pink megacrysts of potassium feldspar are distinctive although they are not distributed uniformly throughout the unit. The megacrysts range from 2 to 8 centimeters in length, are commonly well-shaped, and range from pencil eraser pink to white. A crude foliation, defined by clots and streaks of biotite, is ubiquitous throughout the unit and trains or individual tabular megacrysts of orthoclase are generally oriented parallel to this foliation (Fig. 8).

Foliated granodiorite ranges from tonalite to granodiorite in composition but may be equivalent to the quartz diorite gneiss of Donnelly described by Schmidt (1964) and K-feldspar porphyritic granite described by Erler (1980) in the Basin Creek area. Mineralogy of this unit is summarized in Table 1 and modes are plotted in Figure 12.

Primary mineral components of foliated granodiorite in thin section are plagioclase (35-40 percent), quartz (20-30 percent), biotite (20 percent), potassium feldspar (5-15 percent), and hornblende (0-5 percent). Accessory minerals include apatite, sphene, and iron-oxides.

Alteration is commonly observed in thin section; up to 50 percent of the plagioclase has broken down to sericite and minor coarse-grained muscovite. Biotite has partially altered to chlorite, dusty magnetite, and sphene.

Figure 8. Hand specimen of Kfgd foliated granite showing subparallel K-feldspar megacrysts.

Figure 9. Hand specimen of Kgdp granodiorite porphyry. Mafic constituents are biotite and hornblende.

Figure 10. Hand specimen of Kgd porphyritic granodiorite. Mafic constituent is biotite.

Figure 11. Hand specimen of Klg leucocratic granite. Note fine-grained, xenomorphic texture and low content of biotite.

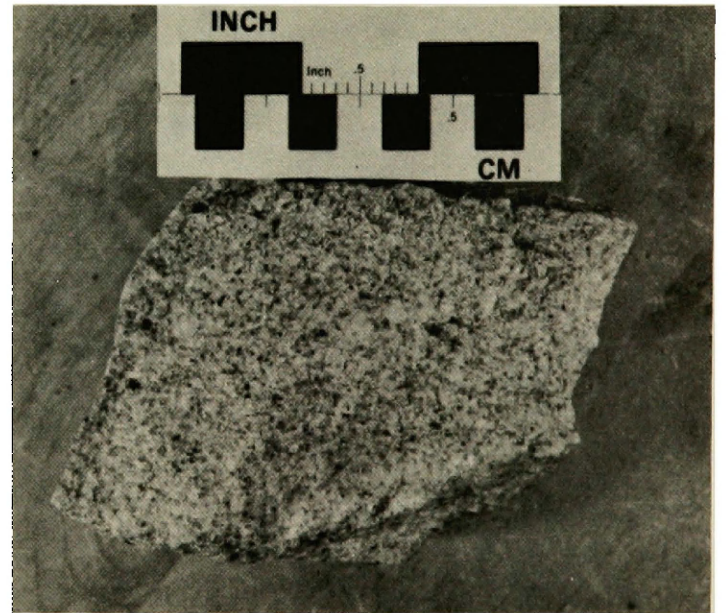
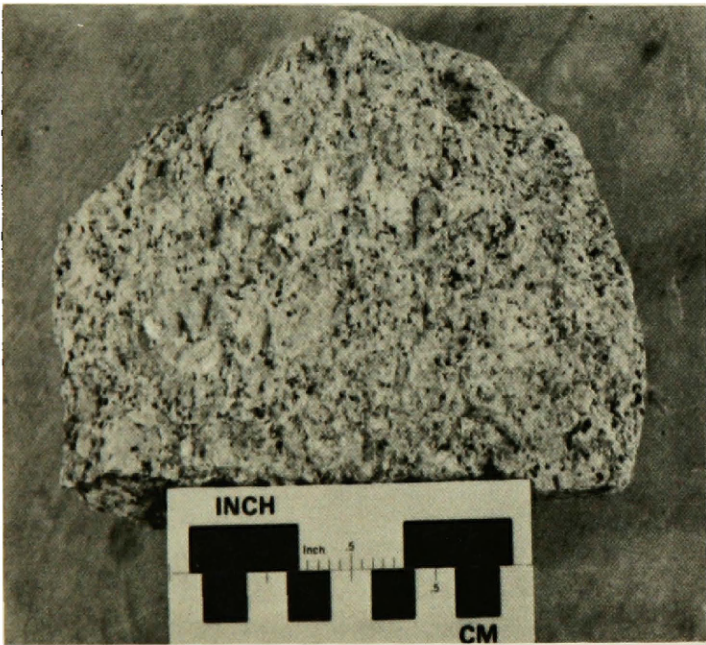
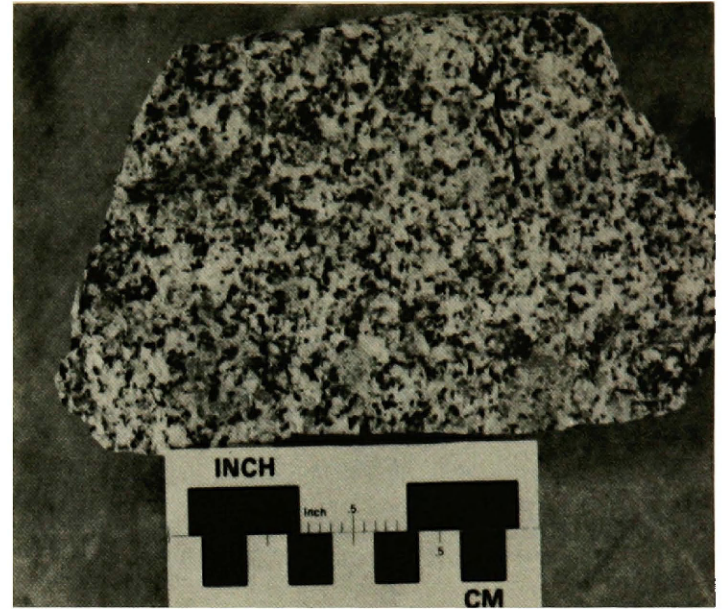
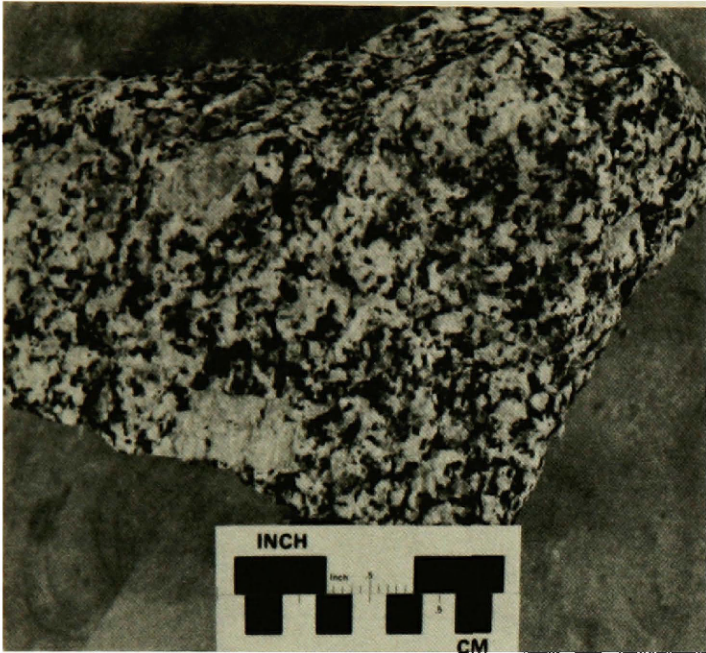


Figure 12. Compositional plot of foliated granite (triangles) and granodiorite porphyry (circles).

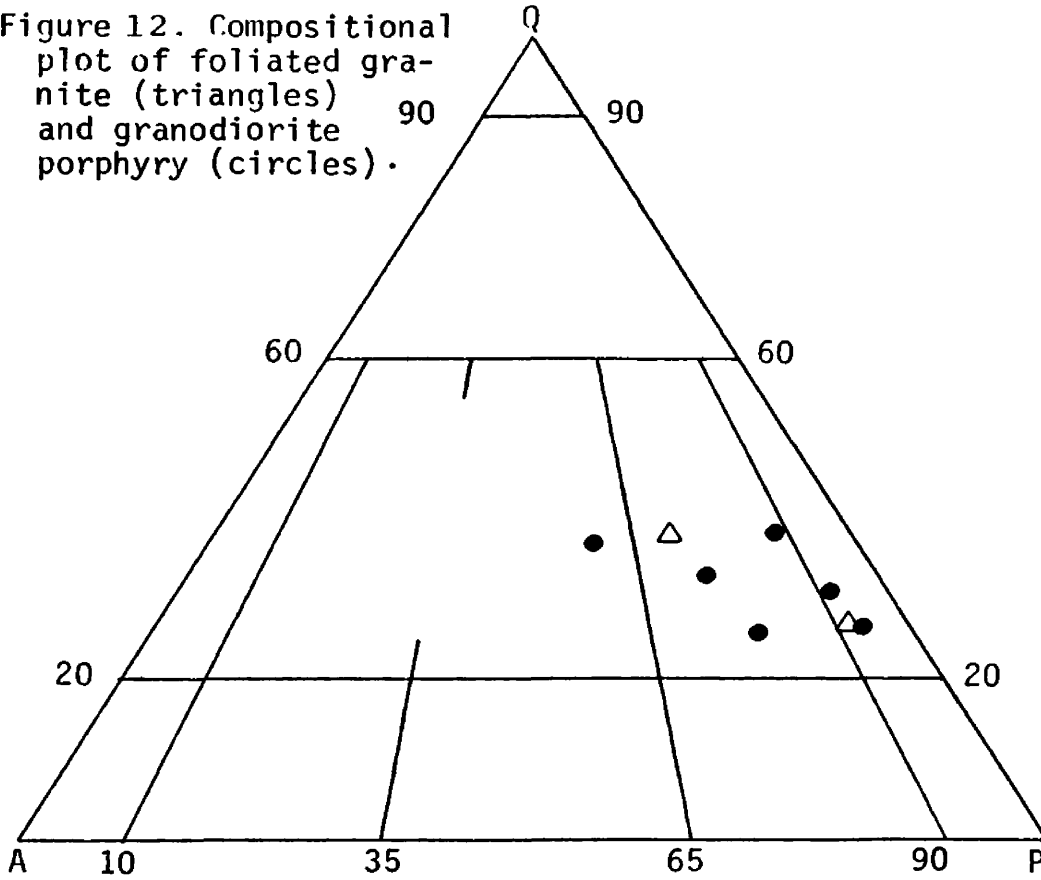
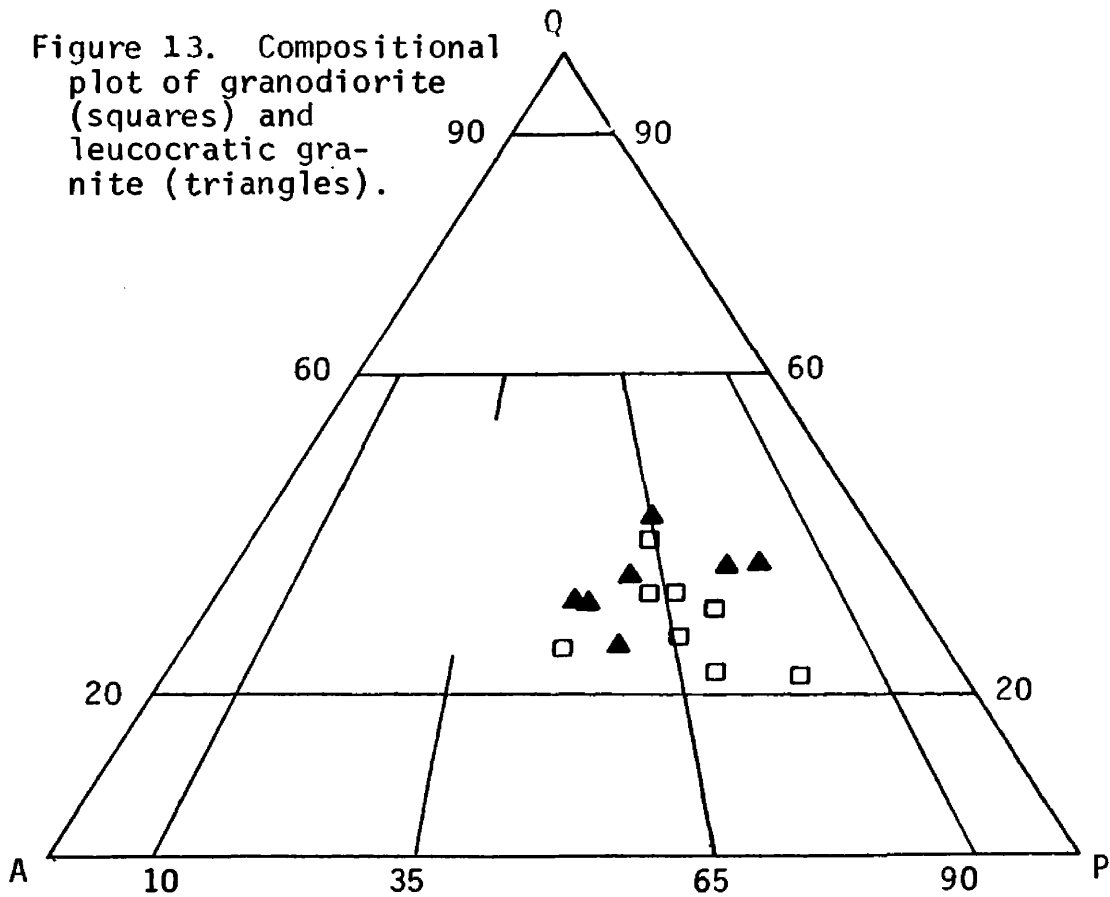


Figure 13. Compositional plot of granodiorite (squares) and leucocratic granite (triangles).



Textures in thin section include poikilitic potassium feldspar megacrysts with quartz, plagioclase, and biotite inclusions, braid and vein perthite (Heinrich, 1965) in orthoclase, and myrmekite fringing the feldspar megacrysts. A strong deformational fabric is exhibited by quartz crystals composed of numerous, optically disoriented grains with sutured grain boundaries, undulatory extinction in plagioclase, quartz, K-feldspar, and biotite grains, wavy twin lamellae in plagioclase grains, bent and kinked cleavage traces in biotite, and sutured grain boundaries between quartz, potassium feldspar, and plagioclase. Biotite foliation observable in hand specimen is probably part of this deformational fabric which may record the emplacement of subsequent batholithic intrusions or, perhaps, a completely unrelated tectonic event. Well-shaped K-feldspar megacrysts parallel this deformational fabric and are slightly deformed as seen in thin section, suggesting the megacrysts grew during the waning stages of this deformational event. Perhaps intrusion of younger batholithic magma deformed the rock and partly remobilized the low temperature K-feldspar component to form the megacrysts. Alternatively, deformation may have accompanied intrusion of the primary melt, and the megacrysts are primary crystallization products. Admittedly, these conclusions are highly speculative and further work is needed to test their validity.

Granodiorite Porphyry -- Kgdp

Medium- to coarse-grained, porphyritic, hornblende-biotite granodiorite crops out along the eastern flank of Warm Springs Creek south of the Deadman Creek-Cat Creek confluence. Age of the unit is

Table 1. Mineralogy of the Cretaceous granitic units.

MAP UNIT FEATURE	FOLIATED GRANODIORITE	GRANODIORITE PORPHYRY	GRANODIORITE	LEUCOCRATIC GRANITE
PRIMARY MINERALS Percentages shown as (%). Minerals listed in relative order of crystallization.	An 25-35 (35-40) quartz (25-30) biotite (20) K-feldspar (5-15) hornblende (0-5)	An 15-35 (35-65) quartz (25-35) K-feldspar (5-25) biotite (3-10) hornblende (2-10)	An 15-30 (25-55) quartz (20-35) K-feldspar (15-40) biotite (5-15)	An 8-20 (35-50) quartz (25-40) K-feldspar (15-40) biotite (2-5)
ACCESSORY MINERALS	apatite Fe-oxides sphene allanite	sphene allanite Fe-oxides zircon apatite	sphene allanite Fe-oxides zircon apatite muscovite	sphene allanite Fe-oxides rutile apatite
GRAIN SIZE & SHAPE	Coarse-grained equigranular or commonly porphyritic with K-feldspar megacrysts (2-5 cm).	Porphyritic with large (1-2 cm) megacrysts of poikilitic K-feldspar in a medium-grained groundmass.	Equigranular or more commonly porphyritic with K-feldspar megacrysts (1-2 cm) in a medium groundmass.	Fine-to medium-grained (.1-.5 cm). Usually xenomorphic equigranular.
ALTERATION	Intense sericitization of feldspars, particularly plag. Bio and hbl to chl Fe-oxides, sphene.	Moderate to intense sericitization of feldspar. Bio and hbl to chl, ep, Fe-oxides.	Moderate alteration of biotite to sphene Fe-oxides, chlorite and white micas.	Limited alteration of feldspars to white micas.
TEXTURES & COMMENTS	Deformed fabric defined by bent and kinked cleavage traces in biotite, sutured grain boundaries, and undulatory extinction in four primary mineral components	Glomerocrysts (.5 cm) of bio, hbl, and Fe-oxides are common as are synneusis clusters of oscillatory zoned plag grains.	Fine-scale myrmekite (quartz intergrowths in plagioclase) well developed adjacent to K-feldspar grains.	Commonly has saccharoidal texture defined by anhedral interlocking grains of feldspar and qtz. Crude foliation defined by aligned biotite flakes.

uncertain. Contacts with other batholithic units are not exposed but may be gradational. On this basis, the rock has been assigned a Cretaceous age. The presence of hornblende, however, is more characteristic of Tertiary-age intrusive rocks in the Idaho batholith than of older batholithic rocks (Hyndman, ms).

Outcrops weather to form prominent resistant cliffs which are grey to greyish-tan in color. Hand specimens (Fig. 9) are characterized by a medium-grained groundmass of plagioclase, quartz, and K-feldspar subhedra enclosing resistant megacrysts of K-feldspar. The angular megacrysts range in color from steel-grey in the western portion of the intrusive to light-pink in the more eastern parts, but are remarkably uniform in size, averaging about 1.5 cm in length, and shape. Concentrations of yellow, tabular sphene seem to increase systematically from west to east.

Table 1 gives the average mineral percentages and Figure 12 gives modes obtained by visual estimation of relative percentages. Plagioclase (An_{20-35}) comprises between 40 and 60 percent of the rock and quartz (25-35 percent), K-feldspar (5-15 percent), biotite (3-10 percent), and hornblende (2-15 percent) are the other essential constituents. Sphene, allanite, and apatite are common accessory minerals. Textures in thin section include oscillatory zoning and complex twinning patterns in plagioclase whereas quartz and K-feldspar occur as interstitial anhedral. Poikilitic K-feldspar megacrysts contain inclusions of plagioclase, quartz, biotite, and hornblende. Brown biotite and green hornblende occur as individual 1-2 mm euhedra and as

3-5 mm clusters which together with Fe-oxides, enclose smaller felsic constituents. Most samples show intense sericitization of feldspars whereas biotite is only partially altered to chlorite and Fe-oxides. Pseudomorphs of iron-oxides after sphene are common and hornblende shows limited alteration to chlorite, opaques and epidote.

Granodiorite -- Kgd

Coarse-grained, porphyritic biotite granodiorite underlies approximately 50 percent of the field area. Porphyritic and non-porphyritic, equigranular varieties are present in nearly equal amounts, but no attempt was made to map them separately.

Outcrops of the rock are deeply weathered and dissected by joints and fractures. Weathered faces tend to be light-tan to tan-grey in color and are mantled by a veneer of gruss of variable thickness. The unit may also be recognized by a one- to three-meter thick dark brown soil alluvium which supports rounded, disaggregated clasts and small flat-sided pebbles of porphyritic granite.

White, euhedral phenocrysts of K-feldspar (1 centimeter) in a medium- to coarse-grained groundmass of quartz, plagioclase, and K-feldspar is a diagnostic texture of this rock in hand specimen (Fig. 10). Medium-grained flakes of biotite make up between 5-15 percent of the rock which is massive to slightly foliated. Average mineral percentages have been determined from thin sections and are given in Table 1. The rock composition plots as granodiorite to granite (Fig. 13).

Major mineral components are 35 to 55 percent plagioclase, 20 to 35 percent quartz, 20 to 40 percent K-feldspar and 5 to 15 percent biotite. Accessory minerals include allanite apatite, monazite, and zircon. Alteration of biotite to chlorite and iron-oxides is common and plagioclase has characteristically been partly altered to sericite. Irregular small crystals of sphene and white mica are disseminated throughout the rock. They may be primary accessory minerals or alteration products after biotite. K-feldspar and quartz occur as interstitial grains lacking external crystalline form. Potassium feldspar also forms phenocrysts which contain small anhedral grains of plagioclase, quartz, and biotite. Subhedral grains of plagioclase show normal zoning and simple twinning patterns. Textures observed in thin section are fine scale myrmekite and strained grains of quartz or K-feldspar. Plagioclase twins may show wavy extinction or are offset.

Leucocratic Granite -- Klg

Leucocratic granite lies on the ridge between the North and South Forks of Cat Creek and forms a discontinuous swarm of northwest-trending dikes and dikelets in the Cat Lakes-Lost Lakes region. Individual dikes were generally too small to be shown at map scale, however, width of the swarm is approximately correct. The contact between leucocratic granite and porphyritic granite on the ridge between North and South Forks of Cat Creek is nearly flat-lying. The contact is gradational over a vertical span of 100 feet as rock with relatively high proportions of leucocratic granite grades downwards to rock with increasing proportions of porphyritic granite.

Contacts between the two are sharp, however, on the scale of a hand specimen.

In contrast to other phases of the Idaho batholith, this unit forms fairly resistant outcrops that typically have parallel, closely spaced joints and joint faces. Weathered outcrops are usually light-tan to buff in color. Similar rocks were observed by the writer south of the area on the ridge west of Warm Springs Creek.

The rock is cream to pinkish-white in color and has a massive to slightly foliated, fine- to medium-grained (0.1-0.5 cm), equigranular texture. There are slight differences in mineralogy and texture between the dikes and the sill of leucocratic granite in the area, however similarities between the two are greater than their differences. Both units contain a notably low amount of mafic material, particularly biotite. In each case, the rock generally contains less than 5 percent biotite. In hand specimen, the flat-lying sill of leucocratic granite is distinctive in its light color and saccharoidal texture defined by a mosaic of rounded, interlocking anhedral grains of quartz, K-feldspar, and plagioclase (Fig. 11). Grain size is slightly coarser in the dike rocks, and there is less K-feldspar in this rock than in the sill-like body. Foliation in the dike rock is defined by aligned flakes of biotite.

In thin section, the primary minerals are plagioclase (An_{5-15} ; 35-50 percent), quartz (25-40 percent), microcline (10-30 percent), and biotite (less than 5 percent). Table 1 gives the average mineral percentages and Figure 13 gives the visually estimated modes for each

thin section. The rock is noticeably more fine-grained and equigranular than other phases of the batholith. Allanite, apatite, and sphene are accessory minerals in both localities. Euhedral magnetite is an accessory in both areas, but the unusual occurrence of magnetite in the dike rocks is distinctive and will be the subject of Chapter VI. Alteration minerals include chlorite and Fe-oxides after biotite and limited sericitization of plagioclase. Quartz often shows extreme undulose extinction, sometimes becoming segmented into optically discontinuous grains.

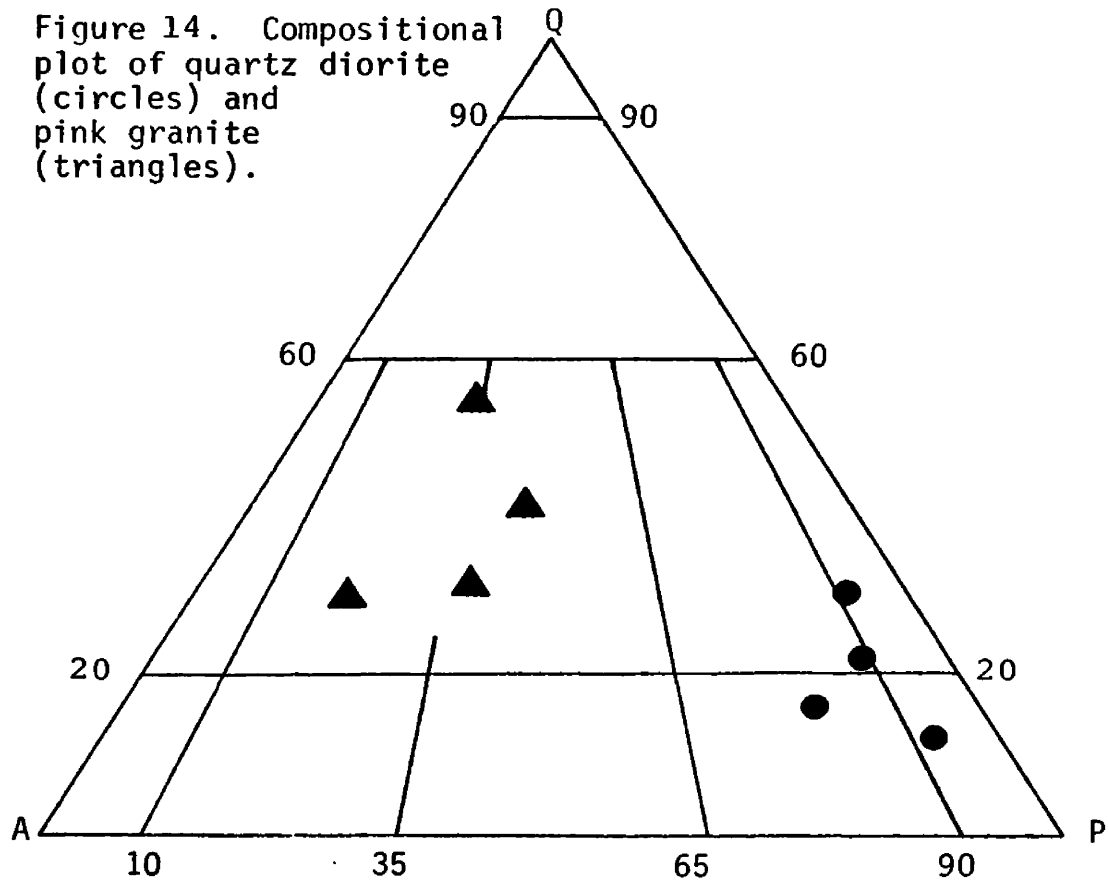
Tertiary Granitic Rocks

Three intrusive stocks of known or probable Tertiary age were mapped in the area. The three rock types differ in both texture and composition. Ranges of compositions are given in Tables 2 and 3 and visually estimated modes for each thin section are given in Figure 14.

Quartz Diorite -- Tqd

Biotite-hornblende quartz diorite underlies approximately 2.5 square kilometers in the vicinity of Red Mountain. The unit varies from medium- to coarse-grained, equigranular quartz diorite near its margins to porphyritic granite and granodiorite towards the core of the stock. Contacts with surrounding porphyritic granodiorite dip steeply outward at angles of around 50 to 75°. Contacts are typically razor-sharp and well-exposed along the east side of Red Mountain. Alteration of country rock near the contact is virtually absent but many of these same rocks show granulated crush zones of quartz and K-feldspar

Figure 14. Compositional plot of quartz diorite (circles) and pink granite (triangles).



in thin section. These textures are indicative of incipient cataclasis presumably brought about by forcible emplacement of the Tertiary stock. The stock has a chilled mafic margin approximately 3 meters thick which is cut by several dikes of quartz latite porphyry that emanate from the stock and penetrate older batholithic rocks.

The pluton may belong to a group of quartz diorite to granodioritic plutons within the Atlanta lobe of the Idaho batholith recognized by Bennett (1980). Direct comparison of the Red Mountain stock with a granodiorite stock in the 10-Mile RARE II Wilderness (Kiilsgaard, in prep.) show similar features. Distinctive characteristics of this rock in hand sample include the presence of large laths of hornblende, a fine- to medium-grained groundmass with pink color, and a peculiar mottled texture in finer-grained facies defined by white euhedral laths of plagioclase and smaller euhedra of magnetite. Concordant ages of 46 m.y. on biotite from two samples of the 10-Mile stock (Kiilsgaard, pers. comm., 1981) suggest an Eocene age for the Red Mountain stock.

The rock is characterized by a bimodal grain size in thin section. Medium- to coarse-grained phenocrysts of plagioclase, quartz, and K-feldspar, biotite, and hornblende account for approximately 80 percent of the rock volume. A fine-grained groundmass (less than .25 mm) of anhedral K-feldspar quartz and minor amounts of plagioclase, biotite, and hornblende makes up the rest of the rock. Alteration products include minor amounts of iron-oxides and chlorite after biotite, sericite after plagioclase, and iron-oxides, chlorite and epidote after hornblende.

Table 2. Mineralogy of the quartz diorite, quartz latite, and latite units.

MAP UNIT FEATURE	QUARTZ DIORITE	QUARTZ LATITE	LATITE
PRIMARY MINERALS Percentages shown as (%). Minerals listed in relative order of crystallization	plagioclase An_{30-40} (55-65) hornblende (5-10) biotite (5-10) quartz (5-15) K-feldspar (0-5) Groundmass (0-5)	Phenocrysts (30-60) plagioclase An_{25-30} (25-40) hornblende (3-5) biotite (3-10) quartz (3-5) K-feldspar (3-5) Groundmass (5-50)	Phenocrysts (50-90) plagioclase An_{25-40} (35-60) hornblende (10-20) biotite (5-10) Groundmass (5-50)
ACCESSORY MINERALS	allanite apatite sphene Fe-oxides	allanite apatite sphene Fe-oxides	allanite apatite sphene Fe-oxides
GRAIN SIZE & SHAPE	Fine-to medium-grained (1-5 mm); slightly porphyritic to equigranular and generally hypidiomorphic.	Porphyritic: Subhedral phenocrysts (2-4 mm) in a very fine-grained groundmass (.025 mm).	Phenocrysts: Subhedral or euhedral (2-4 mm) Groundmass: Xenomorphic (.025).
ALTERATION	Biotite and hornblende altered to chlorite and Fe-oxides. Weak sericitization of plagioclase grains.	Moderate to intense alteration of biotite and hornblende to Fe-oxides, chlorite, and epidote.	Biotite and hornblende altered to Fe-oxides, chlorite, epidote, and sphene.
TEXTURES & COMMENTS	Commonly has a bimodal grain size with an interstitial xenomorphic groundmass surrounding larger subhedra of feldspar and quartz. Synneusis structure defined by oscillatory zoned plagioclase grains.	Rounded, deeply embayed quartz phenocrysts are common. Glomerocrysts of plagioclase or hornblende and biotite are locally abundant.	Synneusis structure defined by oscillatory zoned plagioclase grains is prevalent. Biotite and hornblende clusters form small glomerocrysts to 2mm.

Distinctive textures of the rock include rounded, embayed quartz crystals (Fig. 15), clusters of oscillatory zoned plagioclase subhedra (Fig. 16), and clusters of biotite, hornblende, and iron-oxides.

Discussion. Clustering of phenocryst species and the formation of rounded, embayed quartz grains are important indicators as to the cooling history of an igneous rock.

Corrosion of quartz phenocrysts is thought to occur when a decrease in pressure causes the melt to cross the phase boundary marking the disappearance of the quartz (Fig. 17). The corrosion is augmented by the increased solubility of silica in quartz-undersaturated melts at lower pressures (Whitney, 1975). This process commonly occurs in rocks with a moderately high silica content and the synthetic granite on which Figure 17 is based contains 73.98 percent silica. This relatively rapid decrease in pressure may also explain the bimodal grain size of the quartz diorite as seen in thin section.

Clustering of individual phenocryst species, in which pairs, or larger groups, of crystals are concentrically zoned and the centers of zoning are offset from the mutual boundary, is also known as synneusis structure (Vance, 1969; Dowty, 1980). Where more than one phenocryst species is involved, the resultant cluster is called a glomerocryst. Irregularity and disparity in size of the individuals and parallelism of prominent crystal faces along the mutual boundary between grains have also been advanced as criteria for recognizing these textures (Vance, 1969). Dowty (1980) has recently shown that most synneusis structures may be explained more simply as the result of growth

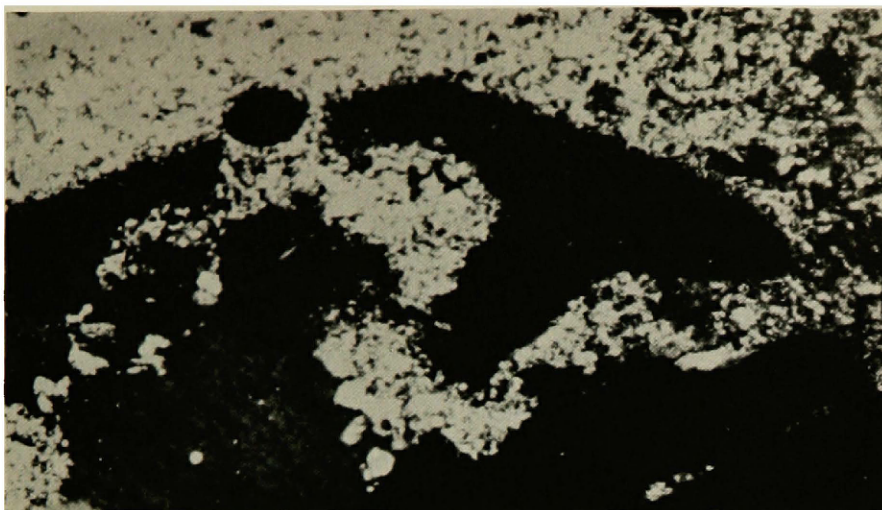


Figure 15. Photomicrograph of marginal facies of Tqd quartz diorite showing rounded, embayed quartz phenocryst in fine-grained groundmass. 10x, crossed nicols.

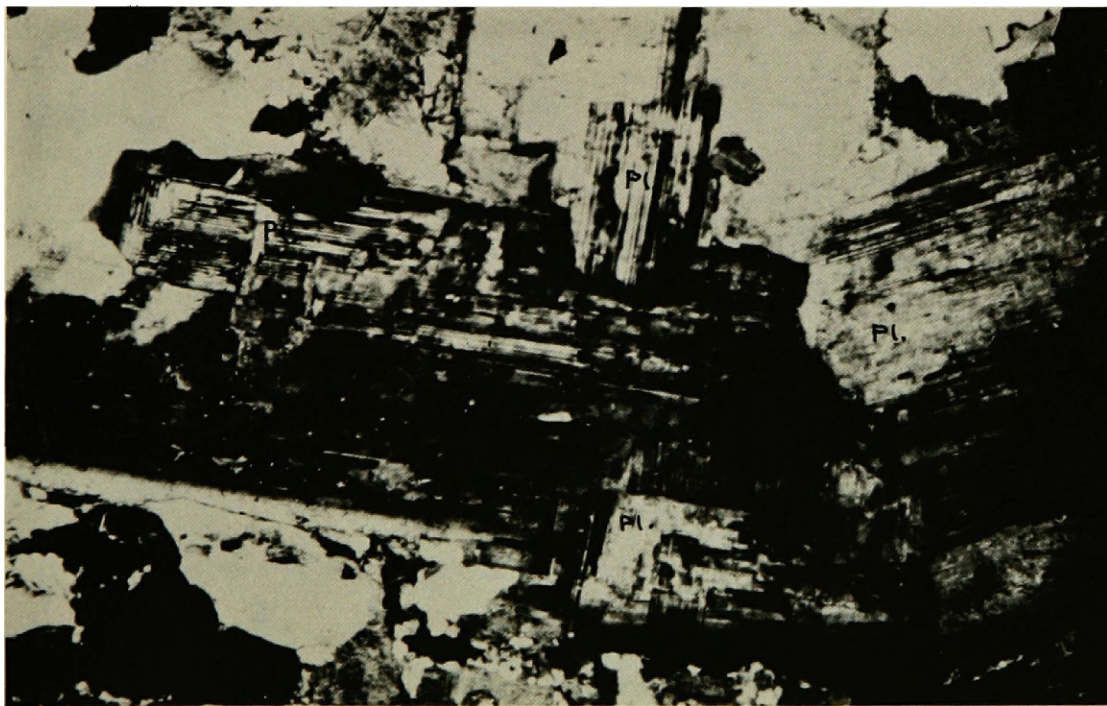


Figure 16. Photomicrograph of Tqd quartz diorite showing synneusis texture of oscillatory zoned plagioclase grains. 10x, crossed nicols.

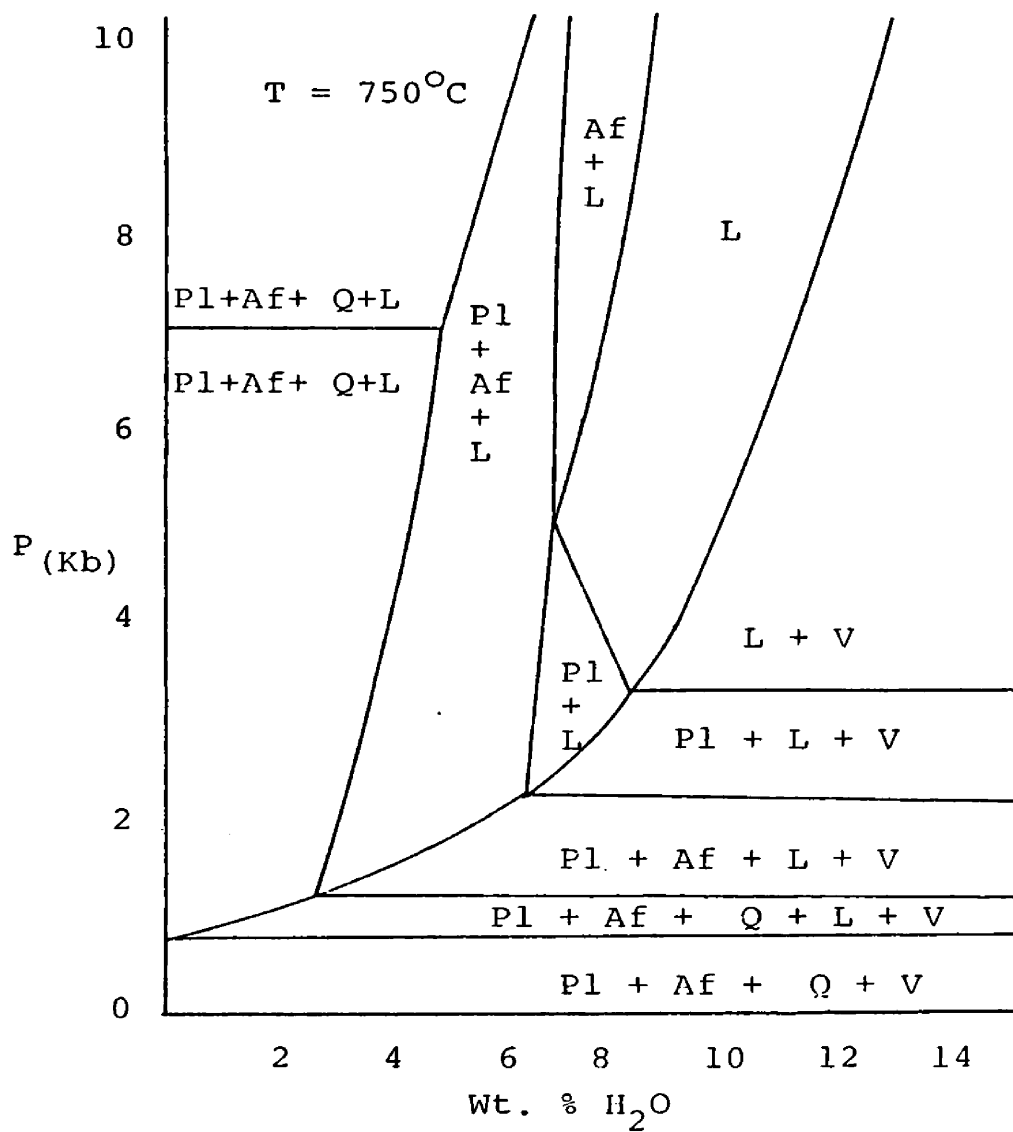


Figure 17. Pressure versus weight percent H₂O for synthetic granite (after Whitney, 1975).

processes than as the result of grain adhesion. Commonly, synneusis twins can be distinguished from growth twins by misfit and irregularities of the common boundary. Most grain clusters in the Tqd unit display irregular mutual boundaries and are interpreted as synneusis or glomerocryst structures.

Both structures are thought to form as crystals drift together and attach themselves to one another (Fig. 18). They are presumably indicative of magmatic origin for those rocks which contain them, requiring a medium fluid enough to allow unrestricted movement of phenocrysts. They are thought to originate through episodic magmatic turbulence early in the crystallization of the magma and are often found in volcanic rocks (Vance, 1969).

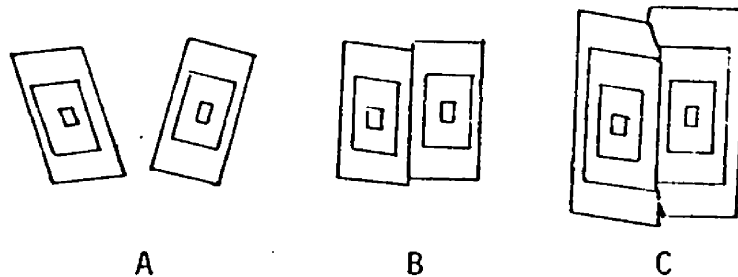


Figure 18 A-C. Stages in development of synneusis aggregates. A. Two isolated crystals. B. Drifting together and union. C. Post-syneusis overgrowth (From Vance, 1969, p. 9).

The textures described above indicate an early period in the crystallization history of this rock characterized by a relatively rapid decrease in pressure and simultaneous turbulent activity within the parent magma. These features may have originated during emplacement of dikes which emanate from the stock. As dikes cut through the

mafic margin of the source pluton, real volume of the magma chamber increased, thereby decreasing internal pressure and creating disruptive turbulence within the melt. Incipient cataclasis of country rocks may have been generated just prior to injection of the dikes, during a period of "swelling" of the pluton, when crystallization of anhydrous phases caused drastic increases in P_{H_2O} of the melt. Alternatively, swelling may have been caused by the addition of new melt into the partly crystallized magma chamber as shown by Sylvester (1978) for the epizonal Papoose Flat pluton in the Inyo Mountains of California.

Pink Granite -- Tpg

Pink granite is found as an elongate body extending from the confluence of Deadman Creek and Cat Creek to the northern map boundary and underlies nearly 30 percent of the map area. This body probably represents an outlier of the larger Sawtooth batholith which lies to the southeast (Olson, 1968). Comparison of rocks from the two areas show nearly identical textural and mineralogical characteristics. Contacts between pink granite and Cretaceous granitic rocks are generally sharp. Pervasive alteration aureoles locally extend from the contact into both the Tertiary and Cretaceous granitic rocks. The halos are defined by a pervasive green color and almost total obliteration of grain boundaries up to 100 meters from the intrusive contact.

The pink granite weathers to form prominent cliffs and angular outcrops owing to high-angle jointing. Coarse-grained pink K-feldspar

weathers out of the rock to form gneiss that thinly mantles fairly resistant weathered slopes. The overall pinkish color of this granite readily distinguishes it from Idaho batholithic rocks. Other distinctive features of this rock in hand specimen include small 1-2 mm microlitic cavities, a coarse-grained equigranular texture, and smokey-colored quartz grains.

In texture and composition, rocks of the Tpg unit are comparable to epizonal granites mapped elsewhere in the Atlanta and Bitterroot lobes of the Idaho batholith (Bennett, 1980).

The rock varies between 35-50 percent perthitic K-feldspar in thin section and plots well within the granite field. Quartz (30-40 percent), plagioclase (20-30 percent), and biotite (2-5 percent) are the other primary constituents. Accessory minerals include allanite, colorless, isotropic fluorite, sphene, apatite, monazite, and zircon.

Potassium feldspar contains approximately 35 percent vein and braid perthite composed of nearly pure albite which displays distinctive albite twinning. Twinned albite also occurs as interstitial material, forming narrow rims around larger grains of quartz and K-feldspar (Fig. 19). K-feldspar forms interstitial anhedral between large, embayed grains of quartz and plagioclase subhedra. Plagioclase (An_{8-15}) is normally zoned and contains subhedral inclusions of quartz. Quartz grains are usually large (3-4 mm), subhedral, contain mild strain shadows, and are embayed by plagioclase and K-feldspar anhedral.

Table 3. Mineralogy of the pink granite, alaskite, and rhyolite units.

MAP UNIT FEATURE	PINK GRANITE	ALASKITE	RHYOLITE
<p>PRIMARY MINERALS</p> <p>Percentages shown as (%). Minerals listed in relative order of crystallization</p>	<p>plagioclase An₁₀₋₂₀ (20-30)</p> <p>K-feldspar (30-50)</p> <p>quartz (30-40)</p> <p>biotite (2- 5)</p>	<p>plagioclase An₅₋₁₀ (2- 3)</p> <p>microperthite (40-50)</p> <p>quartz (40-50)</p> <p>biotite (1- 2)</p>	<p>Phenocrysts (0- 5)</p> <p>plagioclase (2- 3)</p> <p>sanidine (0- 1)</p> <p>quartz (0- 1)</p> <p>Groundmass (95-100)</p>
<p>ACCESSORY MINERALS</p>	<p>Fe-oxide fluorite</p> <p>allanite zircon</p> <p>monazite muscovite</p>	<p>Fe-oxides</p>	<p>biotite fluorite</p> <p>Fe-oxides zircon</p> <p>allanite</p>
<p>GRAIN SIZE & SHAPE</p>	<p>Medium- to coarse-grained (5-10 mm).</p> <p>Hypidiomorphic-equigranular.</p>	<p>Fine-grained (.5-1.5 mm).</p> <p>Xenomorphic-equigranular.</p>	<p>Phenocrysts: Subhedral or euhedral (.5-2 mm).</p> <p>Groundmass: Fine-grained</p>
<p>ALTERATION</p>	<p>Limited alteration of biotite to chlorite, Fe-oxides.</p>	<p>Limited sericitization of feldspars. Extensive martitization of Fe-oxides. Biotite to Fe-oxides, chlorite.</p>	<p>Locally intense alteration of feldspars to clays and carbonate. Biotite to Fe-oxides, chlorite.</p>
<p>TEXTURES & COMMENTS</p>	<p>Albitic rims on plagioclase grains.</p> <p>Interstitial anheda (.025 mm) of albite between larger subhedra of K-feldspar.</p> <p>Prominent perthitic texture in K-feldspar.</p>	<p>Pervasive granophyric texture defined by graphic quartz blebs within and around larger feldspar grains.</p> <p>Prominent perthitic texture K-feldspar.</p>	<p>Rounded, deeply embayed phenocrysts of quartz are in-filled by microcrystalline groundmass.</p>

Alaskite -- Ta

Fine-grained, equigranular alaskite underlies approximately .5 km² in the vicinity of Bull Trout Point. In hand sample, the rock is pinkish-white to light-buff colored on fresh surfaces. The rock weathers to form platey or more commonly blocky-shaped angular rubble with light tan to brownish-red surfaces and commonly displays iron oxide staining on weathered and fracture surfaces. Conspicuous miarolitic cavities with iron oxide stain are disseminated throughout the rock.

In thin section, the primary components of the rock are 50-60 percent microperthite (orthoclase with about 40-50 percent exsolved albite) and 40-50 percent quartz. Anhedra Fe-oxide grains with hematite rims and biotite anhedra compose less than 2 percent of the rock.

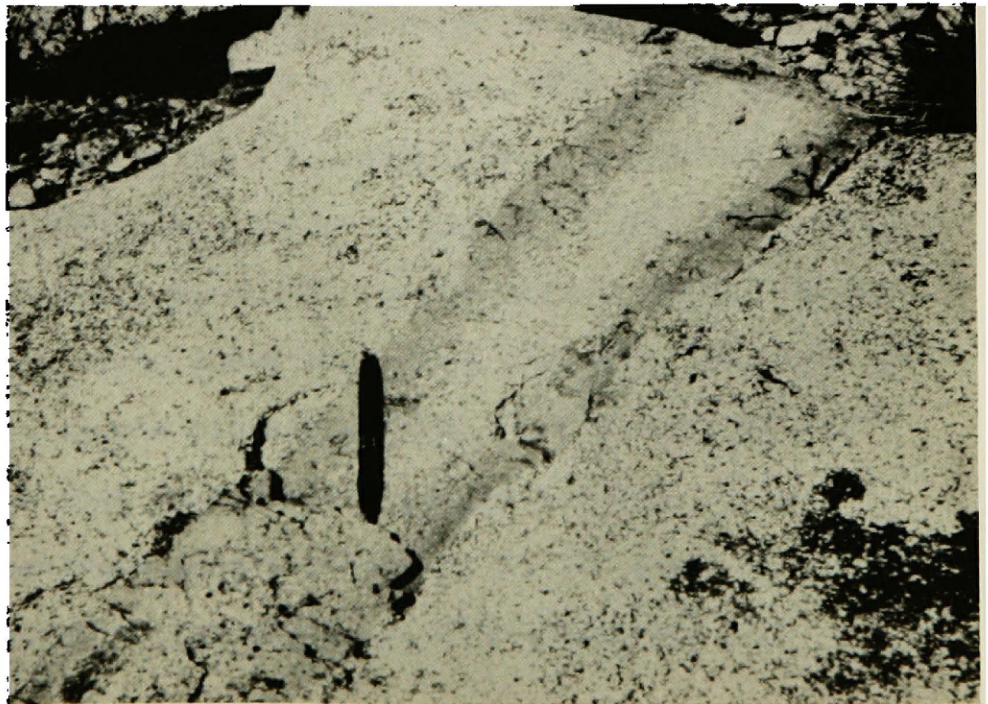
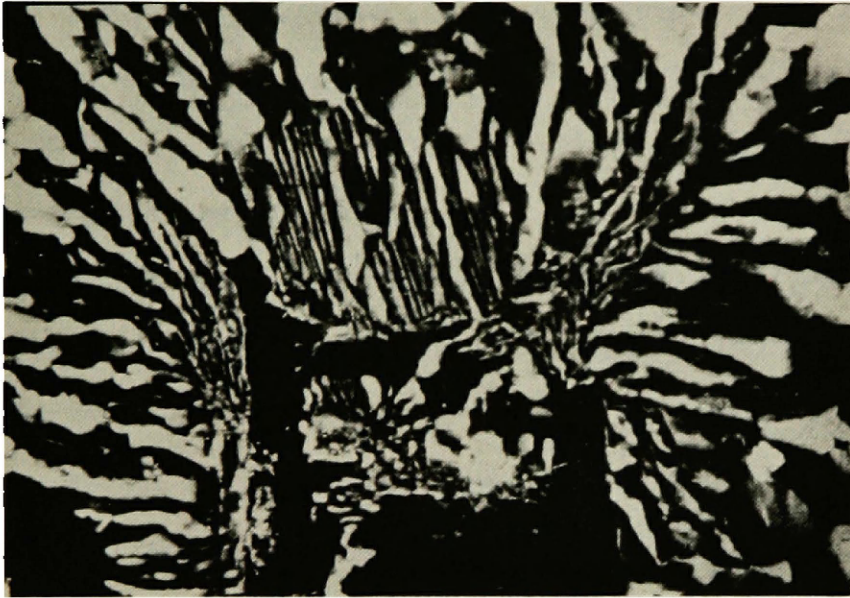
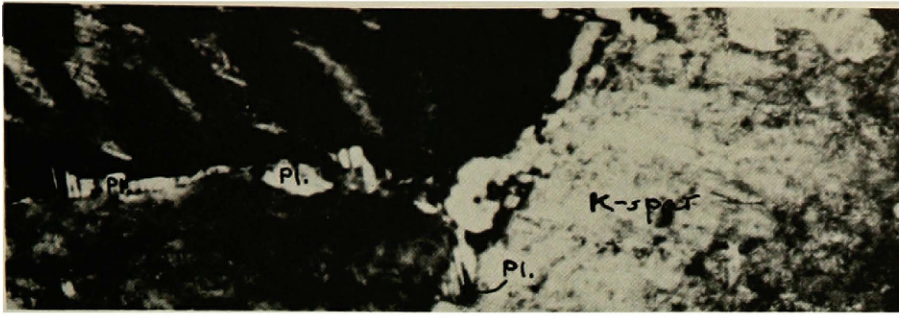
Both field relations and petrographic similarities suggest that the unit may represent a differentiated high-silica roof zone of pink granite. Contacts between the underlying pink granite and alaskite are gradational. Both rock types contain miarolitic cavities and are composed of the same primary phases; quartz, albitic plagioclase, and microperthite. In both units, K-feldspar appears to have crystallized relatively early with regard to other primary phases (Table 3).

The dominant texture of the rock in thin section is a granophyric intergrowth of quartz and microperthite (Figure 20). Optically continuous clusters of quartz up to 3 mm in diameter are intergrown with one or several grains of microperthite. The clusters are commonly radially arranged and composed of triangular or polyhedral blebs and

Figure 19. Photomicrograph of Tpg pink granite showing narrow rims of interstitial albite between larger grains of K-feldspar. 10x, crossed nicols.

Figure 20. Photomicrograph of Ta alaskite showing granophyric intergrowths of quartz and microperthite. 10x, crossed nicols.

Figure 21. Photograph of quartz latite dike cutting Tqd quartz diorite stock showing gradational porphyritic to equigranular texture from margin to core. Pen for scale.



prisms of quartz. Larger (2-3 mm) continuous anhedral of quartz have mild undulose extinction.

The origin of granophyric texture is uncertain, but arguments have been proposed in favor of origin by replacement and by crystallization at a eutectic (Hyndman, ms.). No phenocrysts or relict grains were observed in thin section, and the fine-grained, xenomorphic texture of the rock may indicate that this rock formed by crystallization of melt of eutectic composition.

One simple method of generating a melt of this eutectic composition is to allow crystallization of a "normal" granitic magma until the residual melt lies in the eutectic isobaric minimum quartz-K-feldspar-albite. Separation and concentration of this late melt phase would presumably crystallize to form a granophyric rock similar to the Ta unit. Separation and concentration of this last melt phase may have taken place before significant crystallization of the parent melt; the only requirement for the generation of the last melt phase would be that all three mineral phases (quartz, orthoclase, and albite) had begun crystallizing in the parent magma. Kennedy (1955) showed that alkali silicates alone among the rock-forming mineral components are highly soluble in water vapor under high pressures and that water and other volatile species should migrate upwards in a stabilized magma chamber. He suggested that upward migration of alkali-silica rich solutions should concentrate alkali-silicates in the upper parts of intrusions where they could crystallize as orthoclase and other alkali-rich minerals.

Several authors have postulated the existence of strongly differentiated "caps" in shallow level magma chambers based upon the studies of ash-flow deposits (Hildreth, 1979; Smith, 1979). Numerous authors including Cater (1969) and Fiske (1963) have reported related shallow level plutons and overlying, strongly differentiated granophyric caps. Buddington (1959) notes that granophyre is often found as a domical roof facies and that it is almost exclusively found in the epizone.

I interpret the alaskite as a strongly differentiated cap and marginal facies of the pink granite. Crystallization of the granite and near-simultaneous upwards removal of the rest magma concentrated alkalis and silica in a water and halogen-enriched roof zone which crystallized to form granophyric alaskite. Chemical data presented in Chapter IV is consistent with this interpretation and indicates that crystallization of this roof zone magma may have taken place at depths of less than 1.8 km.

Tertiary Dike Rocks

Dikes of Tertiary age are ubiquitous throughout the region. Dikes within the field area are part of a larger system of Tertiary dikes labeled the Red Mountain swarm by Olson (1968). Compositions are variable and range from dikes more basic than latite to rhyolite. Most dikes within the map area trend north-northeast although a few in the eastern part of the area trend northwest.

Whereas some dikes were mapped continuously for lengths of up to three or four kilometers, most could only be traced for a few hundred

meters. Trends of a single dike vary as much as 45° within the span of an outcrop but are much more consistent at map scale. Thicknesses of dikes vary by 50 percent within the span of an outcrop. Dikes narrower than 15 meters could not be shown at map scale but constitute a significant proportion of total dike rock in the area.

Inspection of Plate 1 shows a fairly non-uniform distribution of dike rocks in the area. Dikes of latite to quartz latite composition are concentrated within the Red Mountain area whereas rhyolite is found in and around the Warm Springs Creek drainage basin and just south of the pink granite stock. The distribution of dikes and their compositions is consistent with the distribution of Eocene-aged plutons in the area. This association suggests that the latite-quartz latite and rhyolite dike suites are genetically related to the Tertiary quartz diorite and pink granite stocks, respectively.

Temporal relations of the dikes are also consistent with the inferred timing of the emplacement of the two Tertiary plutons. Age data on similar rocks from nearby areas indicate that the quartz diorite stock may be 2-4 million years older than the nearby pink granite. Accordingly, rhyolite dikes consistently cross-cut presumably older dikes of the latite-quartz latite assemblage.

Field relations suggest that the dikes were emplaced at about the same time as the Tertiary stocks. Whereas most of the dikes are near the granitic intrusives, few cut the stocks. Many apparently die out or are truncated at the intrusive contacts as shown on Plate 1. A few of the dikes cut the stocks, however, indicating that the dikes were emplaced before, during, and after final emplacement of the related pluton.

Olson (1968) suggests that dikes of the Red Mountain swarm are part of a system of dikes emanating from the quartz diorite intrusive center. Relations such as those shown in Figure 21 suggest that at least some of the quartz latite-latite dikes in the Red Mountain area are directly related to the quartz diorite stock. The dike pictured in Figure 21 is approximately 25 cm in width and cuts rocks of the quartz diorite stock of Red Mountain. Margins of the dike display typical porphyritic texture which becomes increasingly coarse-grained and equigranular towards the center of the dike. The middle of the dike is composed of a rock very similar in composition and texture to the surrounding quartz diorite host. Presumably, magma derived from deeper, less crystallized portions of the magma chamber was injected into a more solidified carapace of the stock. Rapid quenching of the marginal dike material yielded a normal porphyritic texture. Crystallization of internal portions may have proceeded more slowly, presumably at nearly the same rate of crystallization as the surrounding granitic material and within the same magmatic range of temperatures. The peculiar granitic texture of the dike at its core suggests the solid (or nearly solid) quartz diorite host may have been relatively hot compared to surrounding older batholithic rocks. Dikes of similar width and composition have typical porphyritic texture across their width where they intrude older and presumably cooler batholithic rocks.

Quartz Latite-Latite Porphyry

Although quartz latite porphyry and latite porphyry were mapped separately in the field, thin section study shows that their

similarities are greater than their differences (Table 2). I have, therefore, chosen to describe the two groups of dikes collectively to emphasize the likenesses between them and to simplify their relationship with the quartz diorite stock.

The dikes are greyish to light greenish-grey rocks with an aphanitic groundmass, numerous white feldspar phenocrysts, and smaller crystals of biotite, and hornblende. The greatest difference between quartz latite and latite is the presence or absence of small (1-2 mm) quartz phenocrysts in hand specimen. The rocks are similar to some of the rocks described by Ross (1934) and Anderson (1947) as dacite porphyry as well as the latite and quartz latite porphyries of Olson (1968). The dikes show considerable textural and mineralogical variation and often show chilling and other contact effects. Some of the narrower dikes and/or contact facies are difficult to distinguish from rhyolite. Many of the dikes contain mafic inclusions composed of hornblende, biotite, \pm plagioclase. Other dikes contain inclusions which are recognizable xenoliths of older dikes. Some of these inclusions may reflect an earlier period of autobrecciation of the dikes. Microbreccias along the margins of some dikes are composed of finely comminuted angular shards and fragments of wall rock surrounded by a chilled, aphanitic groundmass.

Phenocryst species of the quartz latite-latite assemblage are plagioclase (An_{20-30} ; 60-70 percent of total phenocrysts present), biotite (15-30 percent of all phenocrysts), hornblende (5-10 percent of all phenocrysts), quartz (0-5 percent of all phenocrysts), and

K-feldspar (0-10%). The microcrystalline anhedral groundmass comprises between 10 and 50 percent of the rock and is composed of K-feldspar, quartz and subordinate amounts of plagioclase, hornblende, and biotite. The apparent order of crystallization for these rocks was plagioclase, hornblende, and biotite, quartz, and finally K-feldspar. This sequence was determined from thin sections based on the presence and/or absence of various phenocryst species, euhedral crystals, crystal size, composition of inclusions and composition of the groundmass. The positions of accessory minerals including allanite, Fe-oxides, sphene and epidote within this paragenetic sequence were not determined. Alteration minerals include chlorite and Fe-oxides after biotite, chlorite, Fe-oxides, and epidote after hornblende, and sericite, carbonate and clay from feldspar.

Other textures visible in thin section include rounded, embayed quartz phenocrysts, oscillatory zoning in plagioclase grains and synneusis structure. Synneusis is recognized in plagioclase crystal clusters and clusters of optically discontinuous grains of biotite and hornblende are numerous.

Both the mineralogy and textures of these dikes are similar to those found in the quartz diorite stock (Table 2). Both units are characterized by synneusis texture and corrosion of early-formed quartz grains indicating strong disturbances of the primary melt.

Rhyolite

Rhyolite dikes are the most abundant of all dikes in the area. The swarm of rhyolite dikes along Warm Springs Creek forms conspicuous

outcrops on the precipitous valley walls. In other portions of the area, rhyolite dikes have inconspicuous outcrops, and typically form a platy rubble similar to that of quartz latite porphyry. The dikes commonly show extensive alteration, especially of feldspar grains, and generally have a reddish-orange stain on weathered surfaces owing to oxidation of disseminated pyrite anhedral.

In hand specimen, the rock varies from light-tan to yellow-white and pink, is commonly equigranular, and has a fine-grained to aphanitic groundmass which may be flow banded. Quartz and feldspar phenocrysts are generally small, rarely attaining lengths greater than 3 mm.

In thin section, quartz, sanidine, and albitic plagioclase are the only phenocrystic species and also comprise most of the fine-grained groundmass. Quartz phenocrysts are commonly rounded but some show clear hexagonal outlines. The phenocrysts, which are between .5-1 mm in diameter, are commonly embayed and in-filled with a fine-grained, quartz-rich groundmass. Plagioclase phenocrysts are heavily sericitized and vary from .5 to 1 mm in size. Clusters of optically discontinuous plagioclase phenocrysts are suggestive of synneusis structure, however, absence of visible zonation patterns in most grains precludes the positive identification of this texture.

The groundmass in the rhyolites consists of very fine-grained intergrowths of feldspar and a silica mineral. The intergrowths may take the form of 1) discrete patches, 2) massive felsite, or 3) feathery spherulites 0.25-0.5 mm in diameter which in many cases nucleate on phenocrysts or clots of "dusty" quartz. Granophyric intergrowths

of quartz blebs in sanidine are quite common. Phenocrysts in the groundmass have sharp, irregular grain boundaries. Flow banding is caused by alternating spherulitic and granular quartz-feldspar-rich layers. Quartz-feldspar layers are composed of very fine-grained anhedral of quartz and feldspar. Disseminated anhedral of isotropic fluorite are common within quartz-feldspar-rich layers. Accessory, fine flakes of ragged, red-brown biotite are heavily altered to chlorite. Tiny (.5-1 mm) miarolitic cavities are disseminated throughout the rock and are visible both in hand specimen and thin section.

The rhyolite dikes share a number of petrographic features with the pink granite and granite which indicate a co-magmatic origin for the three units (Table 3). These features: 1) nearly identical primary mineralogies; 2) crystallization of K-feldspar relatively early in the paragenetic sequence; 3) presence of fluorite as an accessory mineral; 4) granophyric texture; and 5) separation of a discrete volatile phase indicated by miarolitic cavities.

Diabase

Diabase dikes form a relatively small percentage of dike rock in the area, but are perhaps the most distinctive. Many are too small to map at the present scale. The greatest concentration of diabase occurs along the ridge crest west of Deadman Creek. Contacts with surrounding host rocks are usually sharp and parallel, and thicknesses of the dikes range from 2-5 meters. Most of these dikes are deeply weathered and are usually covered. Spherulitic weathering and rough weathered surfaces are distinctive features. In hand specimen, the

dikes are light-grey to black, fine-grained and equigranular.

In thin section, the diabase is fine-grained and inconspicuously porphyritic, generally consisting of subequal amounts of plagioclase and pyroxene. Most dikes have been so extensively altered that original dark minerals are not easily identified and do not stand out sharply. Green asbestiform actinolite and chlorite partly to totally replace pyroxene grains. Relict sub-ophitic texture, in which pseudomorphs of chlorite and actinolite after pyroxene envelop the ends of laths of plagioclase, is common in both groundmass and phenocrysts. This distinctive texture is attributed to simultaneous crystallization of plagioclase and pyroxene (Walker, 1957). Plagioclase, pseudomorphic intergrowths of actinolite and chlorite after pyroxene, and pseudomorphic intergrowths of carbonate, Fe-oxides, and chlorite after pyroxene(?) are the dominant phenocrystic species. An aphanitic groundmass supports trachytic feldspar microlites (.25 mm), slender laths of chlorite and actinolite, and interstitial anhedral chlorite, quartz and Fe-oxides. Secondary calcite, chlorite, and epidote anhedral form veinlets and round clusters which cut discordantly through the rock.

Diabase dikes cross-cut all other intrusive phases in the area and are presumably post-Eocene in age. Similar relations have been noted by Reid (1963) in the Sawtooth area, Anderson (1947) in the Boise Basin, Ross (1937) in the Bayhorse region, and Ross (1934) in the Casto quadrangle. Diabase sills and, less commonly, dikes are widespread common features in and around regions of flood basalts (Hyndman, 1972).

Discussion

Tertiary intrusive rocks of suspected Eocene age are characterized by two distinct plutonic-dike assemblages in the Red Mountain-Bull Trout Point area. The associations have been made on the basis of spatial, temporal and petrographic similarities. An earlier generation of dikes and plutonic rocks were derived from a relatively dry quartz diorite to granodiorite magma characterized by discordant contacts, and the absence of a separate vapor phase or contact alteration aureoles. A separate, more felsic and presumably water-rich magma was later emplaced in the vicinity of Bull Trout Point, producing the pink granite-alaskite-rhyolite dikes assemblage. This assemblage is characterized by relatively wide contact aureoles around larger intrusive bodies and by miarolitic cavities. In addition to strong mineralogical and textural affinities which define each assemblage, chemical evidence discussed in the next chapter independently delineates the two assemblages.

Quaternary Deposits

Alluvium -- Qa1

Undifferentiated Quaternary deposits consist of morainal material, possible lake sediments, and alluvium.

Moraine -- Qm

Ground moraine is composed of nonsorted, nonstratified glacial drift material. The moraines typically contain large angular or subrounded erratics set within finer-grained glacial debris.

CHAPTER IV

WHOLE-ROCK COMPOSITIONS

Table 4 gives whole-rock major-element chemical analyses for 18 intrusive rocks including 5 samples of Tertiary dike rock and 5 samples of Tertiary granitic rocks. All analyses were done at Washington State University, Pullman, using a Phillips PW140-00 X-ray fluorescence spectrometer with an XRG 3000 X-ray generator. Beads were prepared by fusing 7 grams of lithium tetraborate with 3.5 grams of pulverized sample at 1000°C in graphite crucibles. Values reported in Table 4 are in weight percent. Normative minerals were calculated using the NORM2 computer program at the University of Montana.

All samples contain greater than 66 percent silica and may be classified as acidic or felsic igneous rocks. Of the dike rocks, three contain silica in the range 65-72 percent, including two dikes mapped as latite and one mapped as quartz latite, one contains 72-76 percent silica, and one contains silica in excess of 76 percent. The divisions correspond to the "quartz latite", "low silica rhyolite" and "high silica rhyolite" categories used by Byers and others (1976) for rocks of the Timber Mountain-Oasis Valley caldera complex of southern Nevada. For ease of comparison, dikes containing between 65-72 percent silica are referred to as quartz latite and those containing greater than 72 percent silica are called rhyolites.

Table 4A. Whole-rock XRF chemical analyses of study area rocks.

	133 Kfgd	112 Kgdp	001 Kgd	118B Kgd	113B Klg	131 Klg	035 Tl	050 Tl	058 Tql
SiO ₂	68.79	70.51	73.84	73.06	75.51	76.06	65.89	66.34	69.77
Al ₂ O ₃	15.80	15.51	14.91	15.18	14.59	15.07	17.09	16.20	16.34
Feo	1.83	1.63	0.66	0.43	0.06	0.06	3.04	2.24	1.47
Fe ₂ O ₃	1.60	1.42	0.57	0.37	0.05	0.05	2.65	1.96	1.29
MnO	0.08	0.05	0.03	0.03	0.01	0.00	0.07	0.06	0.03
MgO	1.41	1.34	0.48	0.31	0.30	0.35	2.69	1.75	1.20
CaO	3.30	2.60	1.60	1.20	0.64	1.03	4.43	3.25	1.59
Na ₂ O	2.93	3.39	3.79	3.76	3.38	3.58	3.47	3.11	3.38
K ₂ O	2.89	3.65	2.82	4.03	4.10	3.95	3.43	3.82	4.51
P ₂ O ₅	0.14	0.15	0.04	0.03	0.01	0.02	0.26	0.20	0.15
TiO ₂	0.53	0.47	0.16	0.13	0.05	0.04	0.78	0.60	0.44
TOTAL	99.31	100.72	98.91	98.54	98.70	100.22	103.80	99.54	100.16

	081 Tqd	128B Tqd	129 Tqd	024 Tpg	160 Tpg	166 Ta	169 Ta	013 Tr	191 Tr
SiO ₂	66.40	67.35	68.14	74.72	76.70	76.34	77.98	72.36	76.93
Al ₂ O ₃	16.18	15.94	15.94	14.38	13.14	12.77	12.69	12.43	12.43
FeO	2.17	2.18	1.87	0.83	0.48	0.34	0.16	0.34	0.43
Fe ₂ O ₃	1.89	1.90	1.63	0.72	0.42	0.29	0.14	0.30	0.38
MnO	0.07	0.07	0.06	0.03	0.02	0.00	0.00	0.03	0.01
MgO	1.88	1.92	1.59	0.56	0.27	0.15	0.16	0.30	0.18
CaO	3.60	3.57	3.17	1.06	0.16	0.09	0.14	4.32	0.14
Na ₂ O	2.98	3.46	3.04	2.81	3.11	2.98	3.19	2.70	2.09
K ₂ O	3.63	3.57	3.63	5.14	4.96	4.54	4.81	4.41	5.34
P ₂ O ₅	0.19	0.20	0.17	0.06	0.01	0.00	0.01	0.02	0.00
TiO ₂	0.61	0.61	0.53	0.23	0.08	0.05	0.09	0.11	0.07
TOTAL	99.60	100.78	99.78	100.54	99.37	97.55	99.38	97.31	98.01

Table 4b. Normative mineral content of study area samples. Norms calculated using NORM2 computer program, University of Montana.

	133 Kfgd	112 Kgdp	001 Kgd	118B Kgd	113B Klg	131 Klg	035 Tl	050 Tl	058 Tql
Q	31.31	29.16	36.73	32.67	38.36	37.44	18.79	23.88	27.64
OR	17.08	21.57	16.67	23.82	24.23	23.34	20.27	22.58	26.65
AB	24.79	28.69	32.07	31.82	28.60	30.29	29.36	26.32	28.60
AN	15.46	11.92	7.68	5.76	3.11	4.98	20.28	14.82	6.91
HY	4.32	4.47	1.73	1.10	0.75	0.87	8.93	5.97	3.95
MT	2.32	2.06	0.83	0.54	0.07	0.07	3.84	2.84	1.87
IL	1.01	0.89	0.30	0.25	0.09	0.08	1.48	1.14	0.84
AP	0.32	0.35	0.09	0.07	0.02	0.05	0.60	0.46	0.35
C	2.19	1.61	2.81	2.52	3.45	3.08	0.24	1.52	3.37

	081 Tqd	128B Tqd	129 Tqd	024 Tpg	160 Tpg	166 Ta	169 Ta	013 Tr	191 Tr
Q	24.29	22.90	27.28	35.49	38.71	41.07	40.49	32.72	43.59
OR	21.45	21.10	21.45	30.38	29.31	26.83	28.43	26.06	31.56
AB	25.22	29.28	25.72	23.78	26.32	25.22	26.99	22.85	17.69
AN	16.62	16.41	14.62	4.87	0.73	0.45	0.63	8.77	0.69
HY	6.23	6.34	5.28	2.00	1.11	0.68	0.43	-----	0.83
MT	2.74	2.75	2.36	1.04	0.61	0.42	0.20	0.43	0.55
IL	1.16	1.16	1.01	0.44	0.15	0.09	0.17	0.21	0.13
AP	0.44	0.46	0.39	0.14	0.02	-----	0.02	0.05	-----
C	1.26	0.37	1.65	2.14	2.39	2.79	2.01	-----	2.96

Ternary Diagrams

Normalized three component systems are plotted to observe the mutual relations of the components. An AFM diagram (Fig. 22) shows the expected calc-alkaline alkali-enrichment trend for both Cretaceous and Tertiary rocks and strong clustering of Tertiary samples by association. The Skaergaard iron-enrichment trend and Mount Lassen calc-alkaline trend are shown for comparison. The calc-alkaline trend is commonly ascribed to relatively high partial pressures of oxygen in the magma (Hyndman, ms.). With high PO_2 , iron is oxidized, thereby being removed as magnetite during crystallization of the magma.

Two other ternary plots, the Na_2O-K_2O-CaO and Ab-Or-An diagrams (Figures 23,24) show fairly distinct clusters of samples. The rhyolite-alaskite-pink granite assemblage shows considerable enrichment in potassium relative to the other rocks in the area. Sample LCr 122 was deleted from these diagrams as thin section analysis showed minor calcite veining within the rock. The Tertiary quartz diorite stock and related dikes contain distinctly more CaO than all other samples.

Cretaceous-aged Idaho batholithic samples show alkali enrichment but contain distinctly more sodium than the Tertiary samples. Similar trends and enrichment patterns are found in the Ab-Or-An diagram, but clustering of data by assemblage is more pronounced here. The quartz latite-latite-quartz diorite assemblage shows relative enrichment in normalized An, the rhyolite-alaskite-pink granite association contains greater amounts of normalized orthoclase whereas older batholithic rocks contain more albite end-member.

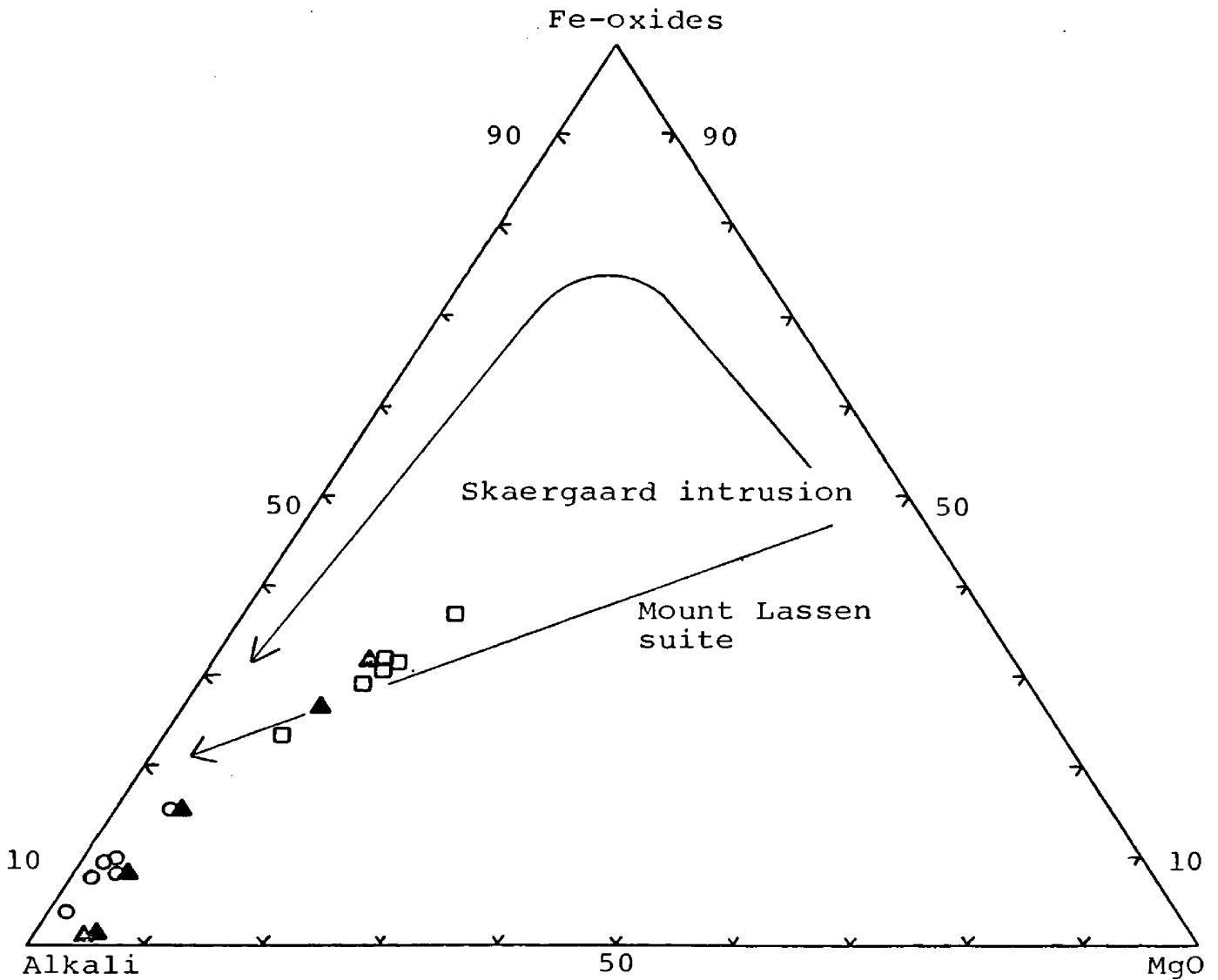
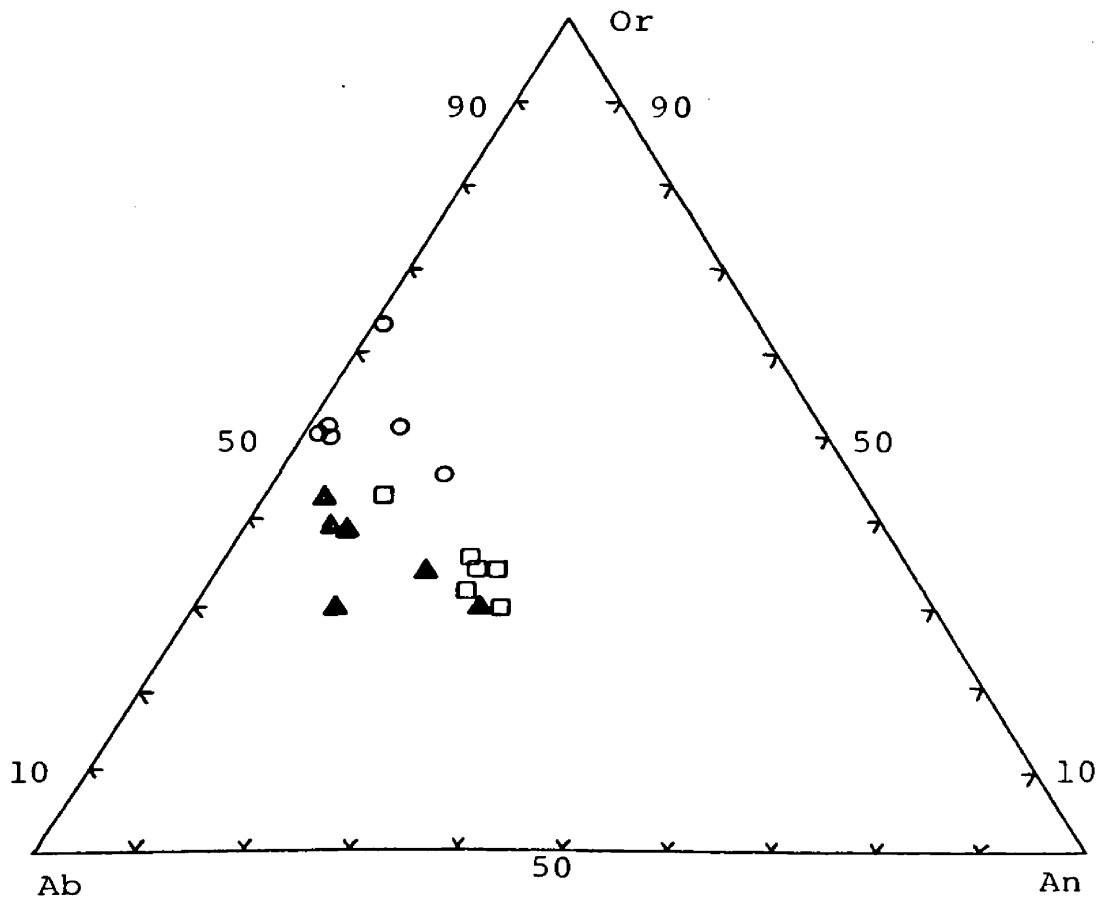
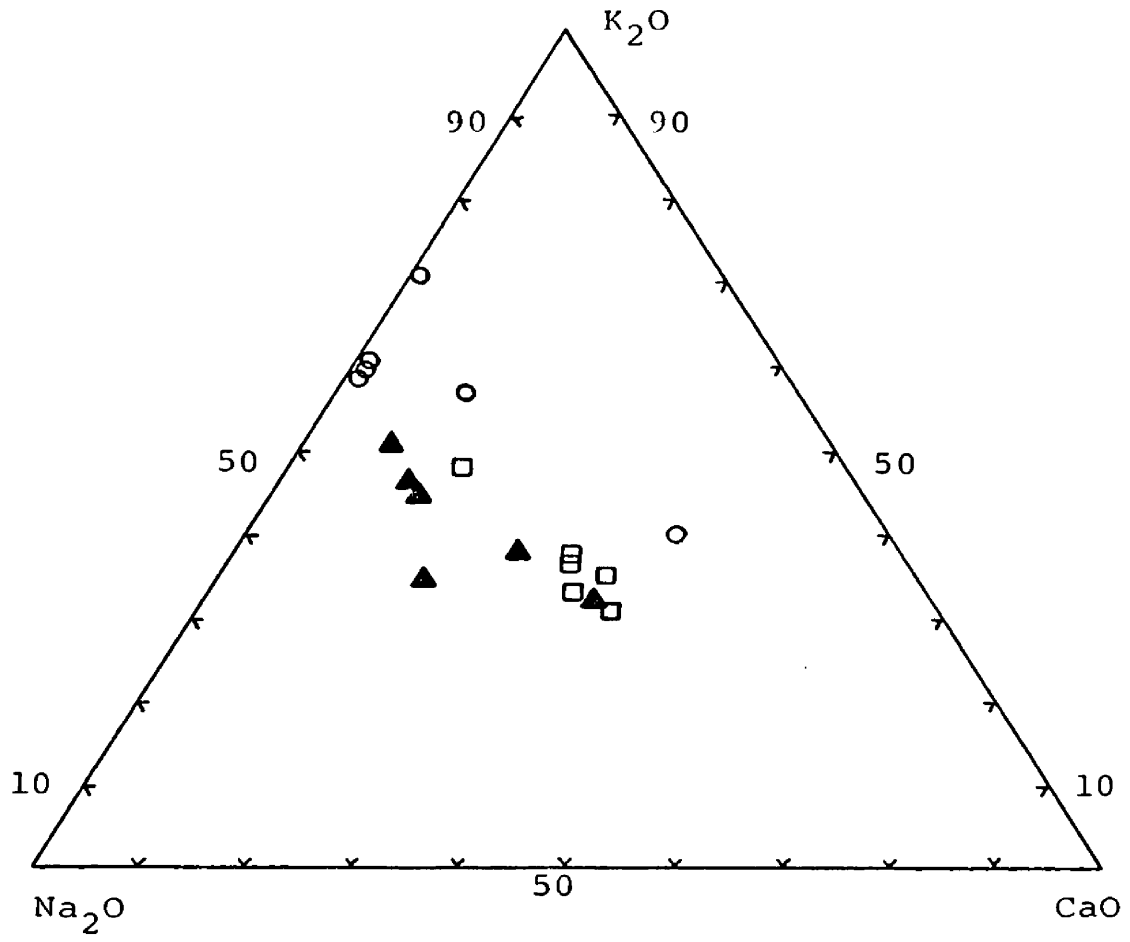


Figure 22. AFM diagram of Cretaceous-age batholithic rocks (triangles), latite, quartz latite, quartz diorite rocks (boxes), and rhyolite, pink granite, alaskite rocks (circles).

Figure 23. CaO-K₂O-Na₂O plot of Cretaceous-age rocks² (triangles), latite, quartz latite, quartz diorite rocks (boxes), and rhyolite, pink granite, alaskite (circles).

Figure 24. An-Or-Ab plot of Cretaceous-age rocks (triangles), latite, quartz latite, quartz diorite rocks (boxes), and rhyolite, pink granite, alaskite (circles).



Silica Variation Diagrams

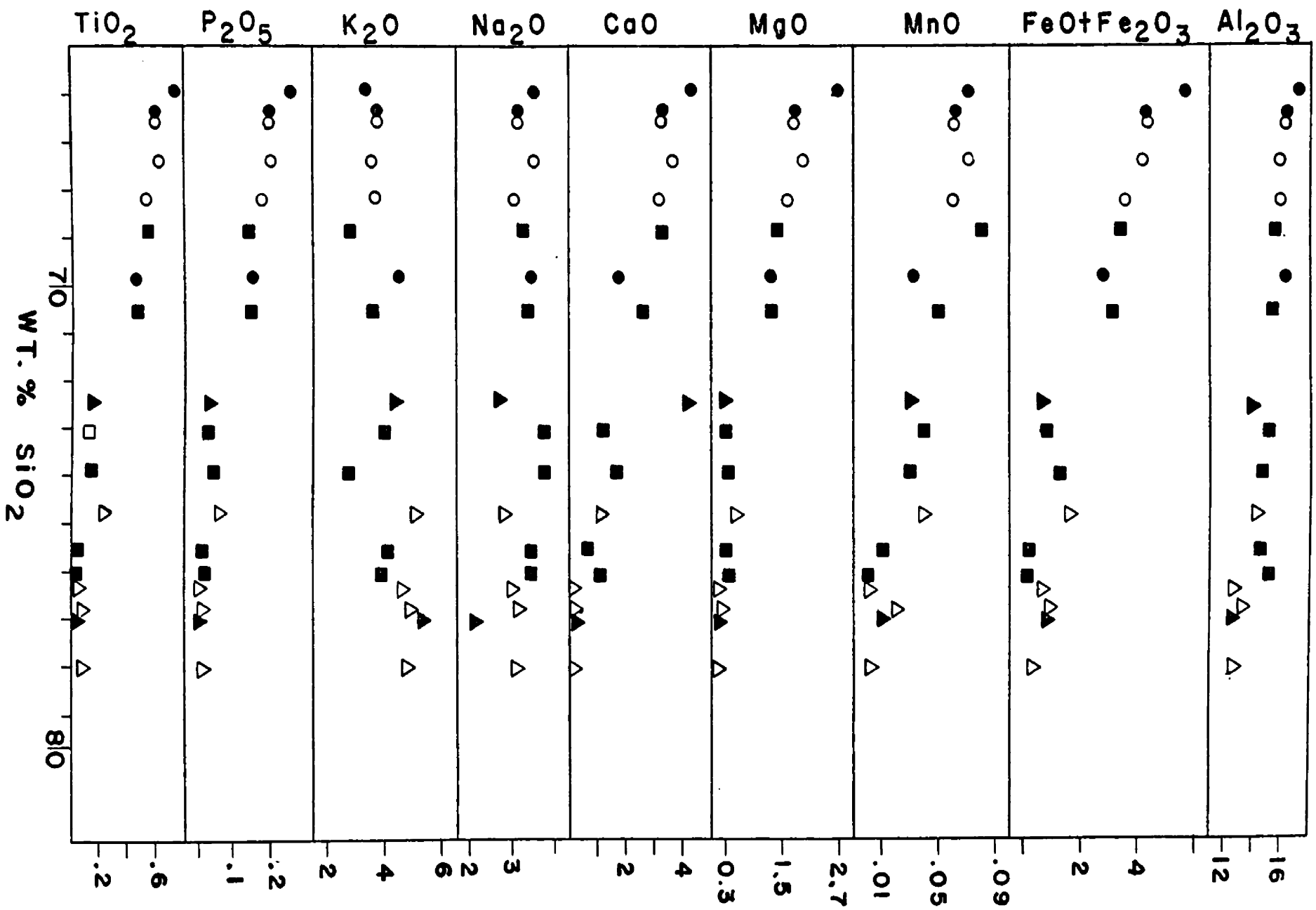
Figure 25 is a variation diagram of silica plotted against nine other oxides for the eighteen Cretaceous and Tertiary rock analyses given in Table 4. Elements which show straight line variation on such diagrams are considered to have a common derivation along the liquid line of descent (Wilcox, 1979; Hyndman, ms) and are commonly interpreted as a comagmatic rock suite. Coarse-grained plutonic rocks may not represent the chemistry of the magmatic liquid from which they cooled (Wilcox, 1979). Crystal settling, volatile diffusion, or filter pressing may cause the remaining liquid to change its composition in unexpected ways.

Inspection of Figure 25 shows that analyses of the quartz latite-quartz diorite assemblage plot closely together between 65 and 70 percent SiO_2 for each oxide. These analyses also define linear trends for seven of nine major-element oxides. Pink granite, alaskite and rhyolite show linear trends for five major-element oxides. Although the trends are defined on the basis of a small number of points interpreting each of the Tertiary assemblages as comagmatic suites based strictly on these plots is tempting.

An unexpected, and perhaps coincidental, result of the whole-rock analyses is that all Tertiary samples, including the two plutonic and dike rock assemblages, plot on fairly tight linear trends. The trends are very well-defined for five major-oxides and less so for MgO , CaO , and Na_2O . The lack of tight fit on these four variation diagrams may be best explained as the result of syn-or post-plutonic

Figure 25. Variation diagram. Values from Table 4.

- △ Pink granite and alaskitic granite
- ▲ Rhyolite
- Quartz latite and latite
- Quartz diorite
- Cretaceous granitic rocks



emplacement hydrothermal alteration or may reflect real differences between the two plutono-dike associations. Mineralogical evidence for hydrothermal activity includes the alteration of feldspars to clays and carbonate, particularly in dike rocks, and biotite to chlorite and iron-oxides.

Plots of major-element oxide analyses of Cretaceous-age granitic rocks on the variation diagrams show significant linear trends for most elements. Two leucocratic granite samples contain the most silica and potassium of all Cretaceous batholithic rocks. Straight line variation of these analyses may be interpreted as an indication of comagmaticity for the Cretaceous rocks. The known or suspected order of intrusion of the four Cretaceous units is compatible with a mafic to felsic or "normal" differentiation scheme, culminating with the emplacement of leucocratic granite. Evidence of a discrete late-stage vapor phase within this unit may also indicate the highly evolved character of it. Field and petrographic evidence of this water-rich phase will be the subject of Chapter VI.

For several oxides, including MnO, CaO, and K_2O , linear trends of analysis of Tertiary and Cretaceous rocks show significant differences, either in slope or in relative positioning along the ordinate. These variations may reflect separate magmatic sources for the two groups of rocks. This interpretation is supported by abundant field and petrographic data which indicate widely different levels of emplacement for the Cretaceous and Tertiary intrusive suites. The relative enrichment of Cretaceous rocks in soda (Figure 23) relative to the Tertiary rocks may also indicate fundamental differences in their magma sources.

Depth of Emplacement of Tertiary Intrusions

Presence of miarolitic cavities within the pink granite-alaskite-rhyolite assemblage suggests emplacement of these rocks at depths of less than approximately 6 kilometers (Hyndman, 1972). An independent estimate of the depth of intrusion may be obtained by consideration of the quartz-albite-orthoclase ternary diagram.

Residual silicate liquids in the system $\text{NaAlSi}_3\text{O}_8\text{-KAlSi}_3\text{O}_8\text{-SiO}_2\text{-H}_2\text{O}$ (Ab-Or-Qtz-H₂O) reach the quartz-alkali feldspar boundary curve and approach an isobaric quaternary thermal minimum whose composition is dependent on $p\text{H}_2\text{O}$ (Tuttle and Bowen, 1958). A plot of the normative components albite, orthoclase, and quartz has been projected onto the Ab-Or-SiO₂ basal face of the quaternary Ab-Or-SiO₂-H₂O tetrahedron for two alaskite samples and is shown in Figure 26. The position of the isobaric quaternary minimum on the projection at various water pressures and its shift toward the Ab component with increasing $p\text{H}_2\text{O}$ is also shown (Jahns and Tuttle, 1963). Application of the Ab-Or-SiO₂-H₂O system to the alaskite is considered valid because the normative An content is less than one percent and because the alaskite is considered a product of crystallization at the quaternary eutectic as discussed in the last chapter.

Figure 26 shows that the alaskite compositions are close to the trend of the quaternary minimum; it also indicates that an average $p\text{H}_2\text{O}$ of less than 0.5 kilobars existed at the time the alaskite was liquid. If the average density for the overlying granitic and meta-sedimentary rocks is assumed to be about 2.7 gm/cc (Hyndman, ms) and

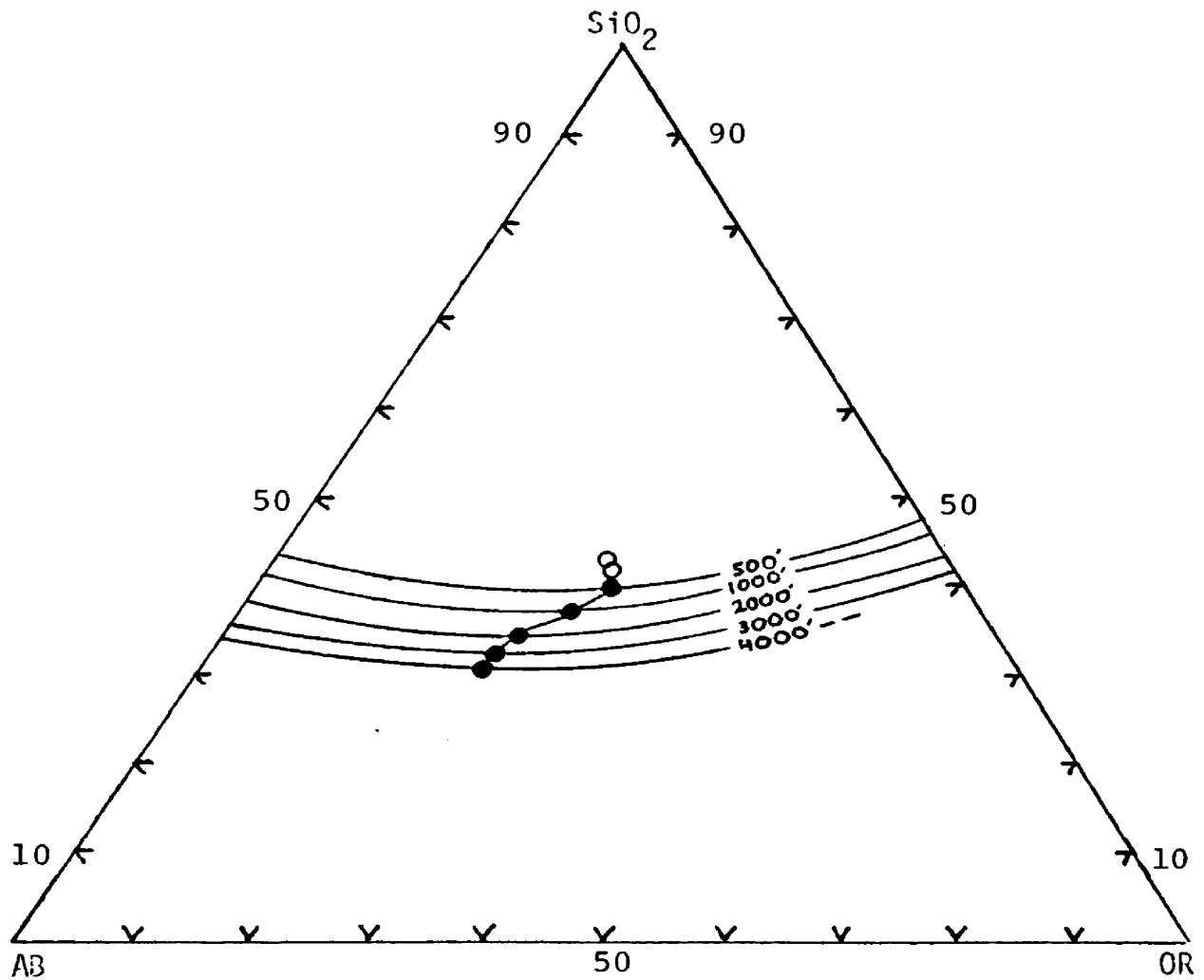


Figure 26. Effect of water pressure on the isobaric minimum in the system $\text{NaAlSi}_3\text{O}_8\text{-KAlSi}_3\text{O}_8\text{-SiO}_2\text{-H}_2\text{O}$.

the mechanical strength of the overlying rock mass is neglected, the calculated pH_2O is equivalent to a depth of less than 1.9 kilometers.

The indicated partial pressure of water may be subject to some revision because the effects of volatiles other than water and the small normative An content has not been evaluated. The probable error, however, is unlikely to exceed that involved in determining pH_2O from the experimentally derived position of the quaternary minimum. A critical assumption lies in the equivalence assumed between pH_2O and the load pressure. The load pressure during crystallization of the alaskite is considered here to be essentially static and due solely to the weight of the overlying rock mass, rather than being influenced by other stress fields resulting from tectonism, magma surge or faulting. This assumption may not be valid since the Tertiary intrusives were apparently emplaced into an extensional environment as discussed in the next chapter.

Summary

The important points in the preceding discussion may be summarized as follows:

- 1) Ab-Or-An, Na_2O - K_2O -CaO ternary plots and silica variation diagrams for analyses of Cretaceous and Tertiary intrusive rocks indicate separate magmatic sources for the two suites of rocks.
- 2) Similar chemical signatures separate Tertiary rocks into two distinct comagmatic suites: rhyolite, alaskitic granite, and pink granite; and latite, quartz latite, and quartz

diorite. In addition to their close chemical affinities, members of each of the two groups have a similar mineralogy, occur in close spatial proximity, and display consistent temporal relations. On the basis of these four criteria, I conclude that the two assemblages represent two comagmatic suites of rocks.

- 3) Based upon their outcrop distribution, the Tertiary porphyritic dike rocks appear to represent offshoots or "apophyses" of larger plutonic masses which subsequently intruded part of their own dike system. The two suites of dike rocks each show a relatively wide range of silica content which may indicate their derivation from several levels within differentiating magma chambers.
- 4) Variation diagrams for Al_2O_3 , Fe_{tot} , MnO , K_2O , P_2O_5 , and TiO_2 show good linear trends for all Tertiary samples. Such trends are commonly taken as evidence for comagmicity for the analysed samples. Further work concentrating on the geochemical, field, and petrographic relations may indicate a deeper comagmatic source for all Tertiary rocks.
- 5) Estimated depths of emplacement for all the Tertiary intrusions are less than 1.9 kilometers, provided relatively little time passed between emplacement of the two suites. An alaskite body, upon which this estimate is based, is interpreted as a high-silica, differentiated "cap" and marginal facies of the pink granite. This unit may be a

suitable target for base and precious metal exploration and, quite possibly, for rare earth minerals. Reid (1963) noted that aquamarine occurs largely as subhedral grains within alaskite of the Sawtooth area and suggests that "the rock seems to have been rich in volatiles" (p. 25). Volatile-rich magmas are likely candidates for the concentration of base and precious metals and rare earths owing to the depolymerized nature of the melt structure (Hildreth, 1980).

High-silica roof zones of biotite granites in the ring complexes of Northern Nigeria (MacLeod and others, 1971) contain major concentrations of disseminated accessory minerals enriched in Sn, W, Mo, Nb, Ta, Y, U, Th, Be, Li, and F. Much of the Nigerian mineralization remained dispersed within the subhorizontal roof zones of high Na/K granites rather than having been remobilized into major veins by postmagmatic fluids. Copper-poor "porphyry molybdenum" deposits tend to also occur in high-silica, alkali rich upper parts of certain granitic stocks in western North America.

CHAPTER V

STRUCTURAL FRAMEWORK

Three structural features define the dominant northeast structural grain in the area: 1) the elongate northeast-trending contact between Idaho batholithic rocks and Tertiary pink granite; 2) northeast-trending high-angle normal block faults; and 3) northeast-trending dikes.

Pink Granite-Cretaceous Granodiorite Contact

Although commonly obscured by vegetation, the contact between these two units appears to be dipping away from the Tertiary stock at between 50 and 80°. The contact is best exposed on the ridge southwest of the confluence between Cat Creek and South Fork Cat Creek (Fig. 27). Here the contact is marked by resistant, vertically to sub-horizontally jointed cliffs and ledges of pink granite overlain by rounded, deeply weathered exposures and gullies of batholithic rocks. The contact is also expressed by outwardly pointing V-shaped portions where it crosses stream channels and other localized topographic depressions. The contact may in part be a faulted contact as brecciation and granulation of the pink granite was noted along the contact near the mouth of Deadman Creek.

Pervasive green alteration several hundred meters wide is well developed in many places within both pink granite and surrounding

batholithic rocks near the contact. Thin section study reveals that the altered rock was subjected to strong, pervasive crushing or non-directional mylonitization (Reid, 1963). Alteration minerals include intensive clay development of feldspars and chloritization of biotite.

I interpret these features to indicate forcible emplacement of the pluton into rather cold, brittle rocks of the epizone and consequent localized argillic hydrothermal alteration in and near the contact. On-going hydrothermal activity near this contact is indicated by active hot springs along the lower reaches of Deadman Creek. Brecciation of pluton and country rock in and around the contact provided channelways for hot, corrosive fluids emanating from the pluton. Forcible emplacement of the other Tertiary stock has already been discussed in Chapter 3 and attests to the dominant emplacement mechanism for these epizonal plutons.

Faults

Prominent northeast-trending faults are visible within the eastern two-thirds of the map area. The faults have an average trend of about N35°E. Most of the observed faults trend within 10° of this average, and a few trend more than 15° away from it.

Exposures of fault planes are rare, and most of those seen represent minor movements too small to be shown on Plate 1. All of the faults display intermittent prominent bleached zones which vary from a few tens to a few hundred meters across. The bleached zones are

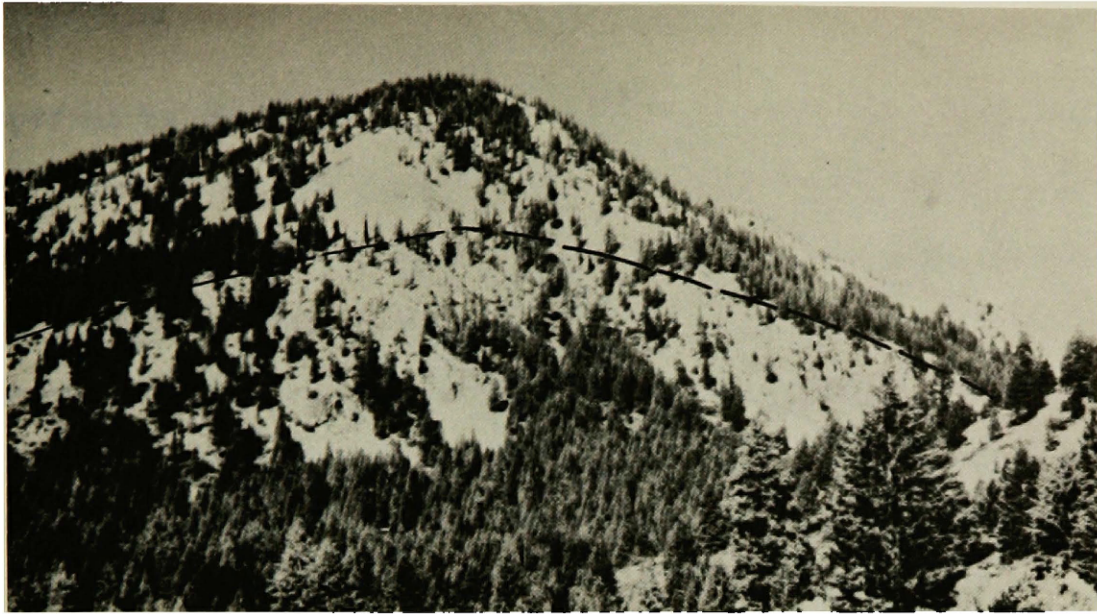


Figure 27. Photograph of outwardly-dipping contact between underlying pink granite and older granodiorite. View is southwest looking up Cat Creek.

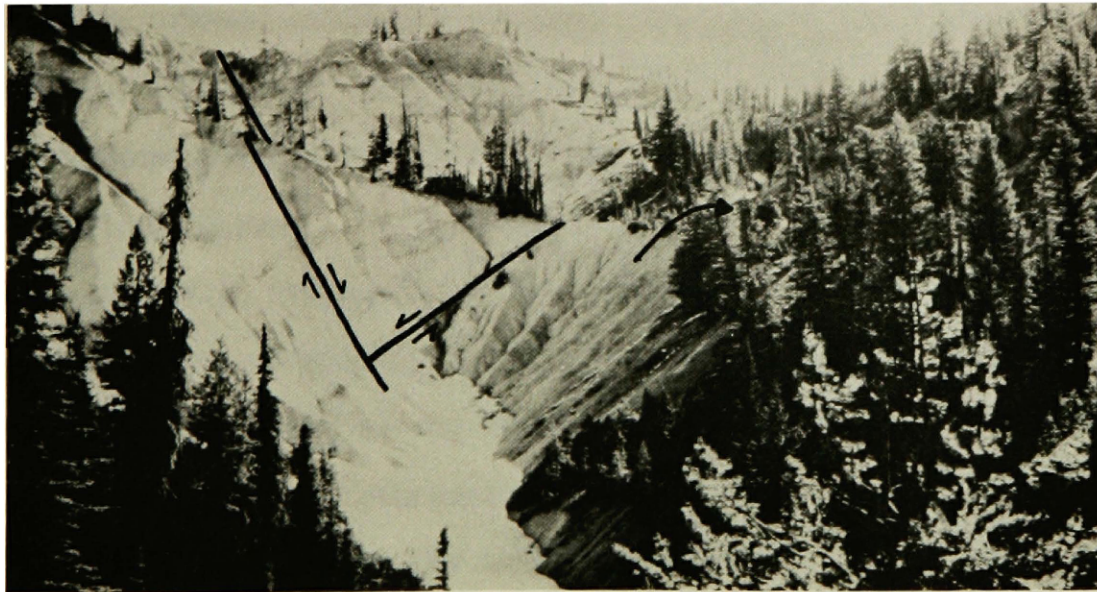


Figure 28. Photograph showing anomalous position of bedrock-floored stream drainage (at head of arrow) along west side of Cat Creek fault.

typified by those found at the head and along the southeast flank of Cat Creek (Fig. 28) and are characterized by white- to tan-colored non-resistant fault gouge commonly devoid of vegetative cover. The fault gouge normally consists of very friable bedrock debris which ranges from handsize fragments to finely comminuted rock powder reminiscent of rock flour. In a few places, fault breccia, in which angular fragments of widely different sizes have been recemented by silica, carbonate and iron-oxides, stands up in prominent relief. The best example of such breccia is found in rhyolite dikes along the eastern flank of Warm Springs Creek.

Some of the faults, such as the one which occupies the valley of South Fork Cat Creek, are in or approximately parallel to northeast-trending stream valleys. Others, like the fault along the southeast flank of Cat Creek, seem to have little or no relation to topography and follow along or slightly below ridgelines, commonly transversing several drainages. As shown on Plate 1, the faults dip northwest, or more commonly southeast, generally at high angles. The fault traces as mapped are slightly sinuous to nearly straight, and corroborate the conception of moderate to steep dips measured on slickensided fault surfaces during reconnaissance mapping south of the area. Several of the faults, including the Cat Creek and South Fork Cat Creek faults, were mapped continuously for distances of greater than 11 kilometers. Reconnaissance geological mapping in the Eightmile and Warm Springs Creek 7.5' quadrangles suggest that all faults extend several kilometers to the south.

Direct measurement of the amount of net slip is difficult because of the lack of reliable horizon markers, but movement along some of the faults is clearly substantial. For example, the horizontal component of displacement along the South Fork Cat Creek fault is approximately 800 meters. Assuming a 70° southward dip of the pink granite contact, approximately 2,200 meters of purely vertical separation is postulated along this fault. The same order of magnitude for displacement along north-northeast trending faults is reported by Ross (1934) in the Casto quadrangle, and Anderson (1947) in the Boise Basin.

Timing of movement along the faults is uncertain, but several periods of displacement are indicated. The greatest apparent displacement is demonstrated by the pink granite-granodiorite contact along the fault occupying the valley of South Fork Cat Creek. Smaller displacements of rhyolite and diabasic dikes were noted along faults on the east flank of Warm Springs Creek and in the Bull Trout Point area and indicate activity during early- or mid-Tertiary time.

Recent tectonic activity is indicated by terraces preserved on the downthrown block of the South Fork Cat Creek fault in the vicinity of Warm Springs Creek (Plate 1). The terraces are fairly flat level surfaces perched conspicuously 70 to 150 meters above the present-day stream level. These terraces are mantled with fine-grained clastic debris between 2 to 5 meters thick which support large, rounded glacial erratics. Within the same area, slide material was recently shed off the upthrown block and across the former channel of South Fork Cat

Creek. Ponding behind this slide has resulted in the accumulation of fine silt material which is visible on aerial photographs as a relatively wide flat area within the drainage basin. Near the head of Cat Creek, an active stream channel, incised into bedrock, is situated approximately 30 meters above the valley floor (Fig. 28). The channel is on the west side of the Cat Creek fault which can be traced along the base of the opposite stream bank. This section of the main valley is overfit and the valley walls are underlain primarily by easily weathered fault gouge.

Field relations, therefore, suggest two periods of mainly normal movement. The earlier and presumably major period of activity probably took place during emplacement of Tertiary intrusions. The extensional block-faulting may have provided "room" for upwardly-migrating plutons or acted as planes of structural weakness along which the plutons were forcibly emplaced. Strike-slip motion along these faults may have occurred at this time, however, their association with dikes and related extensional features may indicate dominantly normal movement. Sense of movement along the faults indicates downward-stepping block-faulting to the southeast. A minor amount of Quaternary offset along these faults is indicated by disruption or preservation of glacial or Recent landforms.

Dikes

The most distinctive structural element of the area is the north-northeast trending suite of dikes. As indicated earlier, most of the

dikes range in composition from latite to rhyolite. With the exception of volumetrically minor diabase, the dikes represent apophyses of related Tertiary plutons or were derived from common magmatic sources at depth.

The dikes have an average trend of about N 15° E. Most of the mapped dikes trend within 10° of this average and a few trend more than 15° away from it. Northwest-trending dikes, although uncommon, constitute a secondary dike-trend set. Most of these dikes are located along the western flank of Spring Creek.

Several features of the dikes suggest that they are injection features and not the products of metasomatic replacement. Contacts of the dikes are generally sharp and sub-parallel, and fine-grained border zones are common. Flow structures, including flow banding and trachytic texture, are commonly observed within the dikes. Exposures of wall rocks along dike contacts often contain sub-parallel striae reminiscent of slickensides and may indicate injection of dike material along pre-existing fault planes or abrasion of country rock during dike injection.

The remarkable uniformity of the trend of dikes in the area suggests that a pre-existing, regional stress field existed at the time of dike-pluton emplacement. Olson (1968) has demonstrated the existence of pervasive north-northeast fracturing in older batholithic rocks in the Red Mountain area. Reid (1963) shows dominantly north-east-trending fracture and joint systems in both Cretaceous and Tertiary granitic rocks of the Sawtooth area as does Kilsgaard (written comm., 1981) in the 10 Mile RARE II area.

Investigators who have studied fluid fracturing from both a theoretical and experimental standpoint generally conclude that fractures form normal to the direction of least compressive stress. Anderson (1951) stated that dikes form perpendicular to the least principle stress direction. Hubert and Willis (1957) have shown both theoretically and experimentally that fractures induced by fluid pressure form perpendicular to the least compressive stress direction.

The trend of extension fractures and the composite thickness of dikes in the field area indicate significant nearly east-west crustal extension. The minimum wall-rock extension produced by dike injection is 3,250 meters. This figure was calculated by multiplying the number of non-aligned dikes within 10° of N 15° E by 22.5 meters which is the average thickness of dikes plotted on Plate 1. A more reasonable estimate would also include that thickness of dikes too narrow to be shown at map scale. No more than 65 percent of all dikes in the area are shown on Plate 1. Assuming an average thickness of 4 meters for those dikes not shown gives a conservative total of approximately 3,450 meters of wall rock dilation. This corresponds to approximately 35 percent expansion of total rock volume.

Summary

Major structural elements within the area record regional north-west-southeast crustal extension during early and middle Eocene time. Forcible emplacement of high-level plutons was accompanied by high-angle normal faulting and the injection of dike material which, in

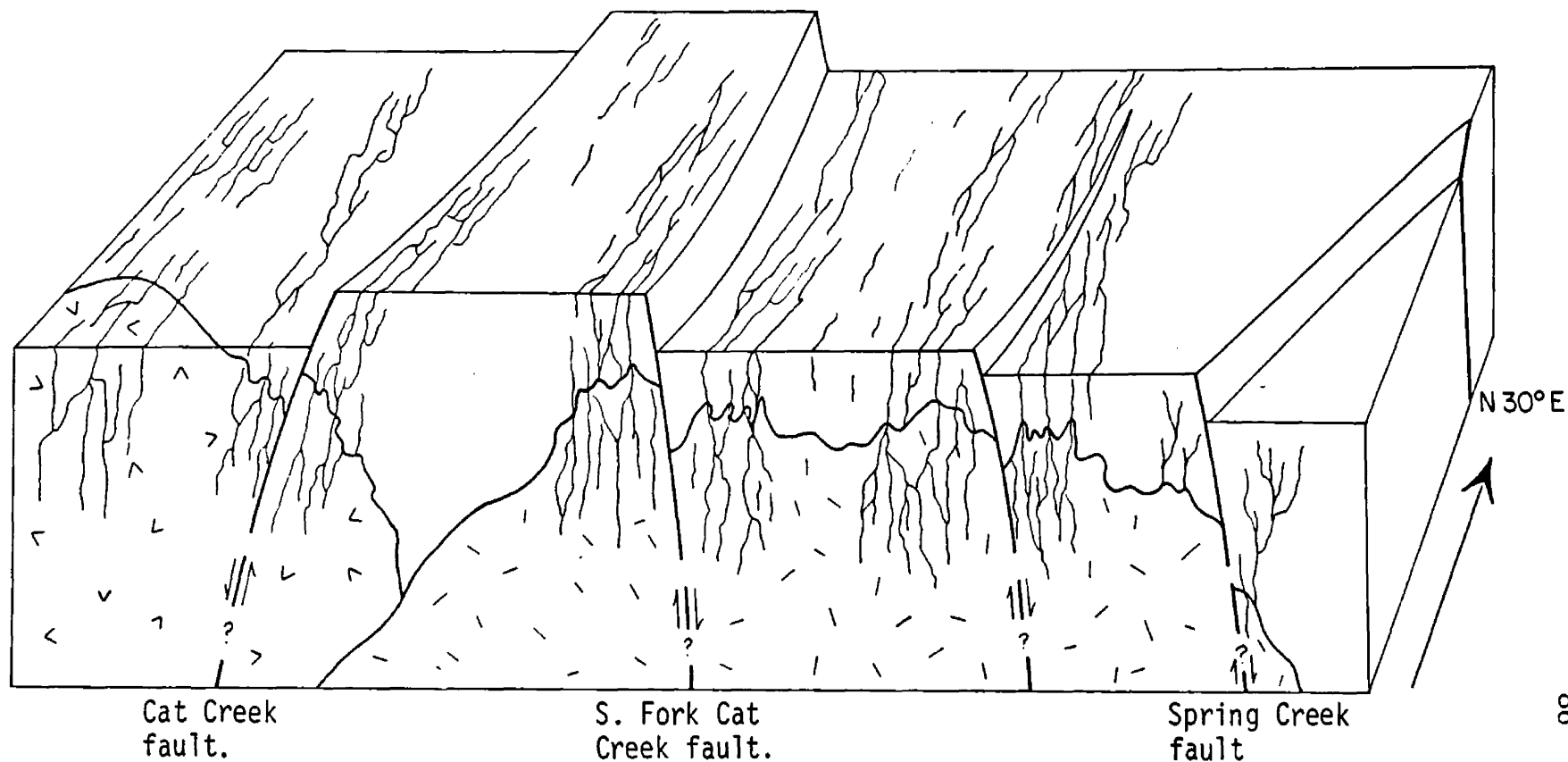


Figure 29. Schematic block diagram of Red Mountain-Bull Trout Point area showing relations of major structural features. Northwest-southeast crustal extension results in high-angle faulting and fracturing which localizes emplacement of Tertiary intrusions including pink granite (stippled), quartz diorite (V-pattern), and associated dikes. Some of the earlier dikes are subsequently intruded by their own plutonic source during final emplacement of the latter.

part, preceded emplacement of the plutons. Plutons presumably rose along deep-seated north-northeast trending planes of structural weakness, including some of the normal faults which produced fault-bounded contacts. Brittle extensional fracturing within this near-surface environment tapped deeper, presumably more mobile portions of the upwardly-migrating plutonic core magma and provided pathways for the emplacement of dike material before, during, and after final emplacement of the pluton. Few of the dikes penetrate into their own plutonic core, and it is likely that fracturing within the plutons was limited at this time. Presumably, the plutons were still relatively hot and may have reacted somewhat plastically to extensional forces placed upon them. Griggs (1960) has shown that higher temperatures enhance the ability of rocks to react plastically to stresses placed upon them.

Figure 29 is a schematic diagram showing the relations of structural elements discussed above. These relations suggest a major northeast-trending extensional tectonic feature, perhaps an incipient crustal rift, was active during Early Tertiary time and brought about at least 35 percent localized extension of the crust. The zone of rifting may have been responsible for generation of Tertiary calc-alkaline magma, and served as a foci for its final emplacement.

CHAPTER VI

VAPOR PHASE CRYSTALLIZATION IN LEUCOCRATIC GRANITE

During the course of detailed geologic mapping in the Red Mountain area, several consistent but peculiar features were noted in dikes of leucocratic Cretaceous-aged granite and in the surrounding country rocks. These features are significant in that they provide information as to the character of a discrete water-rich phase in the late cooling history of the leucocratic granite.

Leucocratic granite has been described by several workers within the Atlanta lobe of the Idaho batholith. All workers agree that the rock probably represents a late-stage differentiate or magmatic pulse related to the Idaho batholith.

The unit forms a discontinuous swarm of northwest-trending dikes and dikelets in the Cat Lakes-Lost Lakes region. The contact between a mass of Klg and underlying porphyritic granite on the divide between north and south forks of Cat Creek is nearly flat-lying. The two bodies, although offset along the fault parallel to Cat Creek, are similar in outcrop and mineralogy, and may be related.

These bodies cross-cut other units of Cretaceous Idaho batholith including foliated granite and porphyritic granite. Dikes of leucocratic granite discordantly cut and isolate angular blocks of porphyritic granite in the 10-Mile RARE 11 area. Leucocratic granite also truncates pegmatite of porphyritic granite indicating that the unit was

emplaced after consolidation of older batholithic phases.

Euhedral magnetite megacrysts exist within the swarm of west northwest-trending dikes of leucocratic granite north of Red Mountain. The megacrysts are surrounded by concentric bands of clear quartz and quartz-feldspar halos. The megacrysts are ubiquitous within the leucocratic rock and within older batholithic rock as far as 600 meters north of the swarm. Felsic halos range from .5 to 50 centimeters in width but commonly are between 1-4 centimeters across. Larger halos may contain several magnetite megacrysts up to .5 centimeters in length (Fig. 30) whereas smaller halos contain at most one.

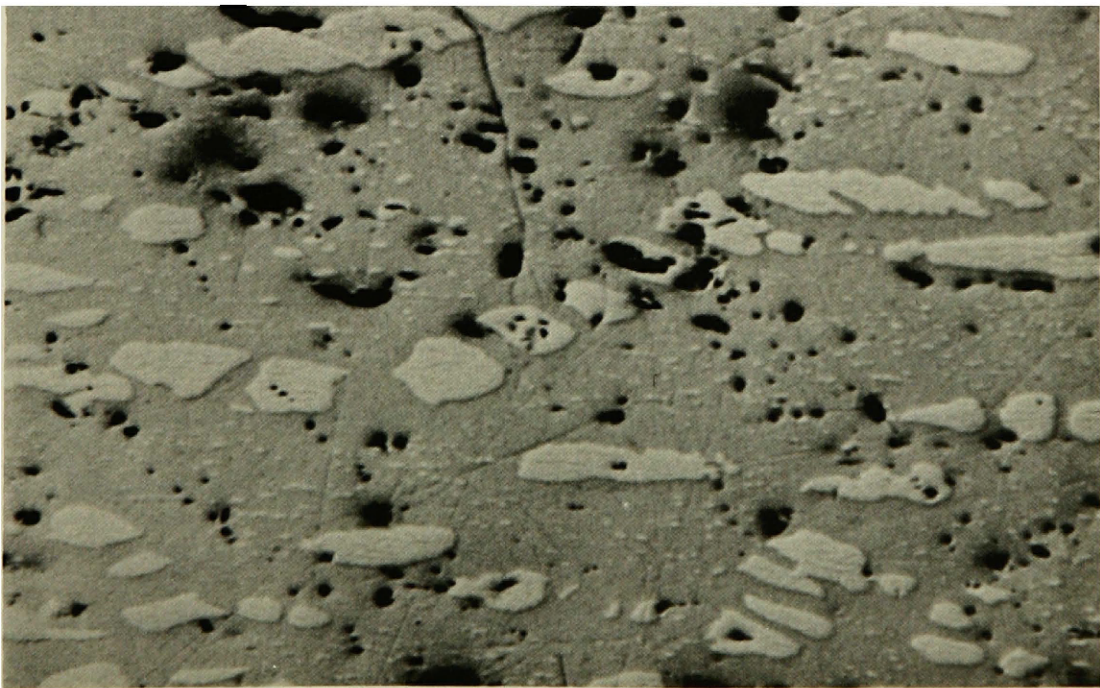
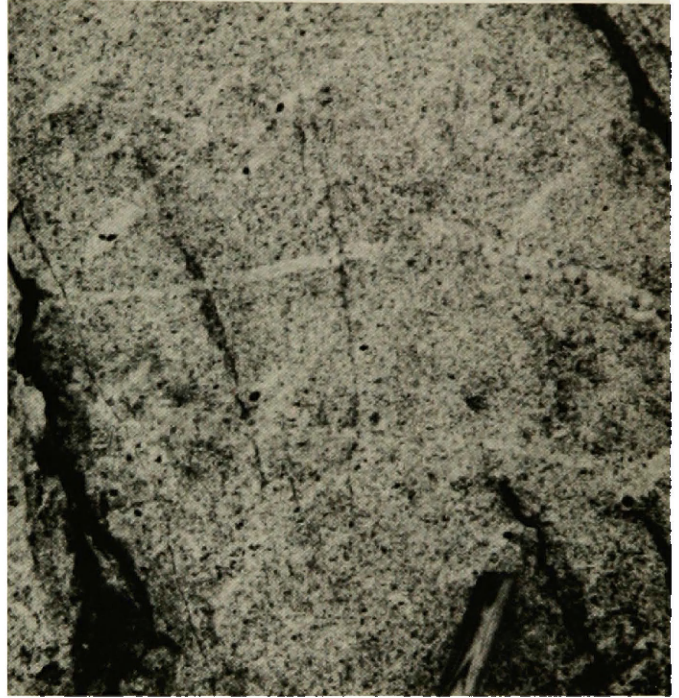
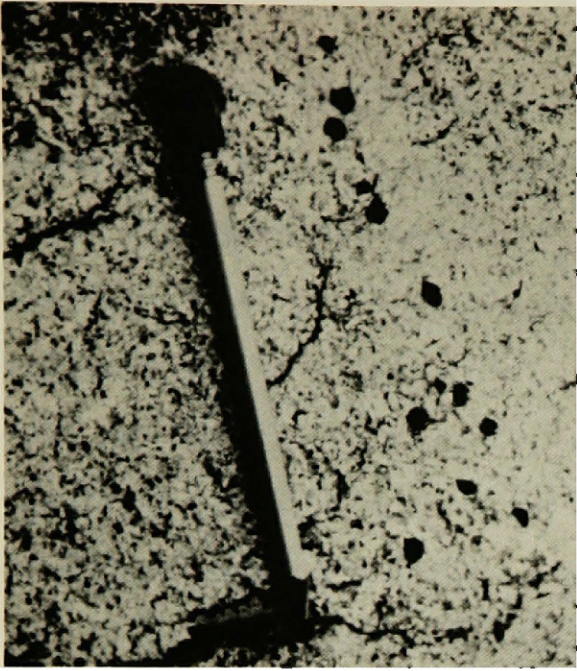
The megacrysts typically occur at or near the bottom of the felsic halos which are elliptical, teardrop, or tabular in shape. These features define a lineation which plunges steeply to the southeast and parallels foliation within the dike rocks defined by fine flakes of biotite (Fig. 31).

Examination of polished sections using a reflecting microscope showed that the magnetite grains range from tiny interstitial anhedral less than 1 mm in length to euhedral megacrysts up to 1 centimeter in diameter. Small interstitial grains are composed of a titanomagnetite host with between 5 and 10 percent ilmenite exsolution lamellae. In some grains two periods of sub-solidus exsolution are indicated by two sets of exsolution lamellae which are of widely different sizes (Fig. 32). Larger grains contain no exsolution lamellae and appear to be homogeneous Ti-rich magnetite or titanomagnetite.

Figure 30. Photograph showing cluster of magnetite megacrysts in large quartz-feldspar halo.

Figure 31. Photograph of lineation defined by elongate quartz-feldspar halos around magnetite megacrysts.

Figure 32. Reflecting microphotograph of two generations of ilmenite exsolution lamellae in titanomagnetite host.



Ilmenite-titanomagnetite intergrowths are well known in nature (Ramdohr, 1969). The existence of FeTiO_3 (ilmenite) - Fe_3O_4 (magnetite) solid solutions has been suggested experimentally by Wilson (1953) and Roy (1954) by successfully homogenizing magnetite-ilmenite intergrowths by heating rock samples. Buddington (1964) suggests that the intergrowths may form by oxidation of magnetite-ulvospinel (Fe_2TiO_4) solid solutions and concomitant exsolution of ilmenite due to decreasing temperatures.

Geothermometers have been proposed by several authors (Buddington, 1955; Buddington and Lindsley, 1964; and Carmichael, 1967) in which the compositions of magnetite-ulvospinel solid solutions in equilibrium with ilmenite varies directly with temperature. Buddington (1964) showed, however, that for a given temperature compositions of the solid-solution series become successively lower in TiO_2 with increasing $f\text{O}_2$. The compositions of these phases in mutual equilibrium are, therefore, dependent on oxygen fugacity ($f\text{O}_2$) as well as temperature. Analysis of both the magnetite-ulvospinel and coexisting ilmenite-hematite exsolution pairs permits estimation of both oxygen fugacity and temperature (Buddington, 1964).

A range of temperatures and oxygen fugacities may be estimated for the formation of the megacrysts by assuming "reasonable" compositions of magmatically-derived titaniferous magnetite and ferrian ilmenite. The shaded area in Figure 33 corresponds to the range of magmatically-derived calc-alkaline magnetite-ilmenite compositions reported by Buddington (1964). Temperatures of between 550 and 800°C

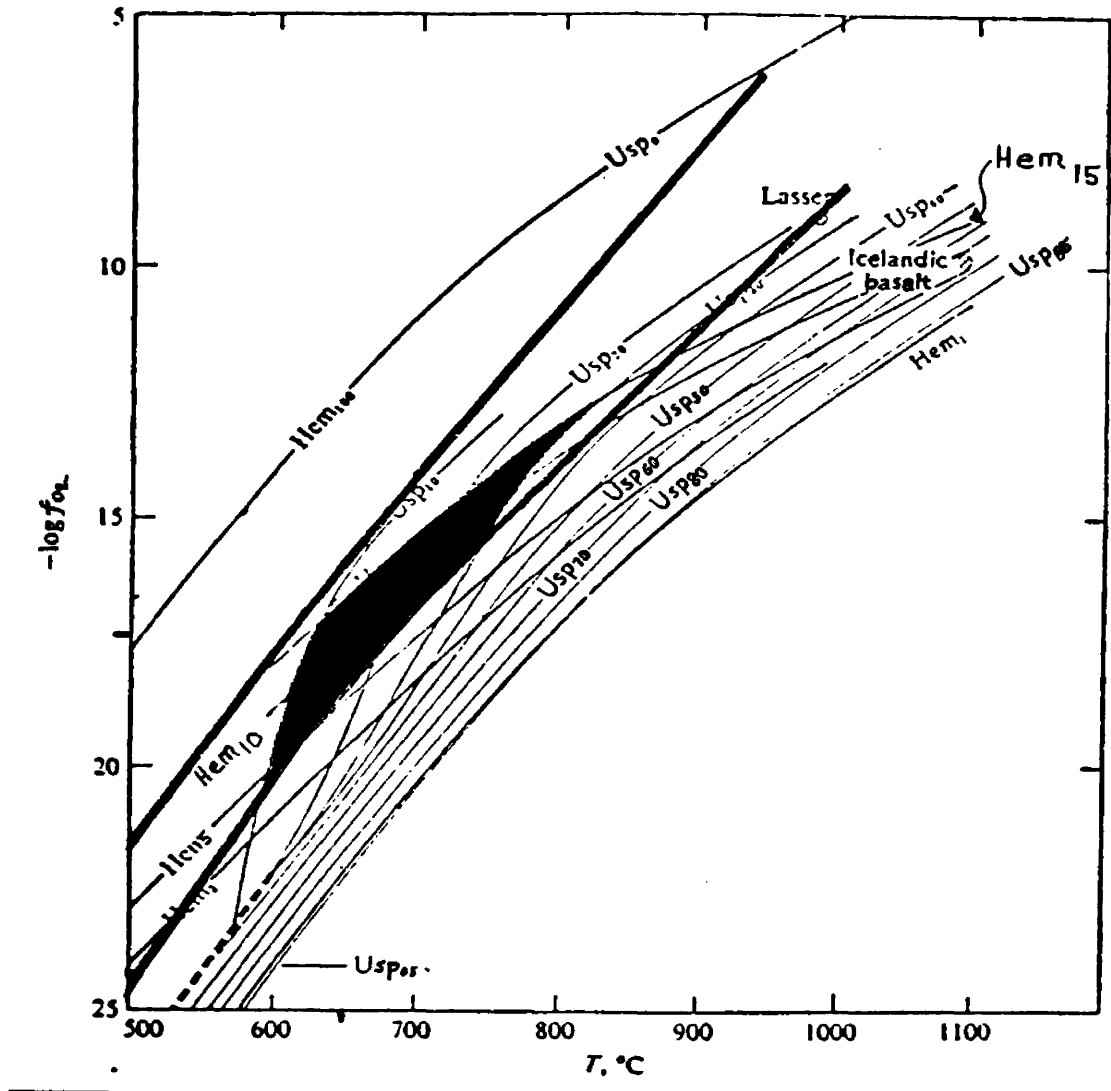


Figure 33. Compositions, in mole percent, of coexisting ilmenite-hematite and magnetite-ulvospinel solid solutions as a function of temperature and oxygen fugacity shown as $-\log f(\text{O}_2)$. (After Buddington and Lindsley, 1964). Bars are T - $f(\text{O}_2)$ stability boundaries for oxidation reaction $\text{biotite} + \text{O}_2 \rightarrow \text{magnetite} + \text{muscovite} + \text{quartz}$ using annite components of 0.5 (upper curve) and 1.0 (lower curve). (From Wones and Eugster, 1965.)

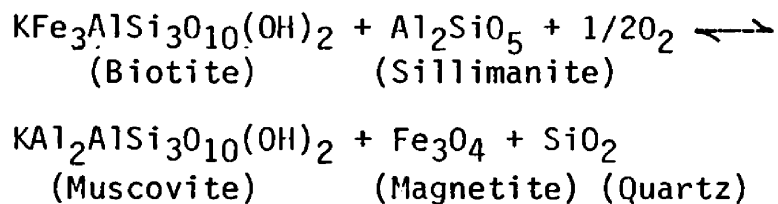
are indicated for the formation of the megacrysts with $\log fO_2$ values of between 12.5 and 20.

In thin section, the megacrysts are completely opaque ranging from small interstitial anheda to large, contiguous grains. Larger grains are poikilitic, including smaller anheda of quartz and feldspar. Very narrow selvages of pleochroic yellow-green to clear white mica commonly surround the megacrysts. Other minerals associated with the selvages are sphene and allanite. An irregular band of clear to smokey-color quartz generally surrounds large megacrysts. The bands are of variable thickness and where clusters of megacrysts occur within a single quartz-feldspar corona, the quartz bands are typically connected, forming a three-dimensional network of planar to irregular veins and veinlets.

Since the quartz-feldspar halos differ from surrounding granitic rock only in their complete lack of biotite, it seems reasonable to assume that the magnetite megacrysts grew at the expense of biotite. This conclusion is reinforced by the fact that the halos are parallel to a foliation defined by aligned flakes of biotite.

Eugster and Wones (1962) and Wones and Eugster (1965) have showed that biotite will react to increases in oxygen fugacity conditions to form a number of assemblages including the assemblage magnetite plus muscovite plus quartz; the same products as those most commonly seen within the quartz-feldspar halos. Biotite crystallizing from a magma may follow a more iron-rich trend or more magnesium-rich trend, depending upon the fO_2 conditions during cooling. If fO_2 is decreasing with

decreasing temperature, Mg/Fe ratios of anhydrous phases either decrease or change very little. Increasing fO_2 leads to the production of magnetite and an increase in the Mg/Fe ratios of biotite due to the oxidation of Fe^{2+} . In an aluminous environment, biotite is stable with muscovite, quartz, and magnetite over fairly limited and well-defined fO_2 - T regions. The reaction is:



Considerable substitution of Mg for Fe^{2+} in biotite and Al in muscovite would be expected in reactions involving biotite from calc-alkaline granitic rocks.

Wones and Eugster (1965) have plotted stability boundaries for this reaction against temperature and oxygen fugacity. The stability boundaries for this reaction involving annite components of 1 and .5 (covering the range of typical calc-alkaline biotite compositions) have been projected onto the geothermometer of Buddington and Lindsley (1964) and are shown in Figure 33. Note that the boundaries tightly bracket compositions of titanomagnetite-ilmenite pairs found in magmatically-derived calc-alkaline iron oxides.

The above considerations, while not conclusive, are permissible evidence for the conclusion that the megacrysts were derived during the late magmatic stage of the leucocratic granite and are the result of localized increases in fO_2 of its residual melt phase. Increases in fO_2 demonstrated by this reaction may most easily be explained by the

buildup of water within the leucocratic granitic melt due to early crystallization of anhydrous phases. That this period of crystallization may have occurred in the magmatic stage is also suggested by dilational pegmatite dikes which cut through, and are therefore later than, the quartz-feldspar halos surrounding the megacrysts. The pegmatite dikes presumably reflect the last residual melt phase of the leucocratic granitic melt. This conclusion is in agreement with Buddington and Lindsley (1964) who inferred that all such oxide mineral segregations which occur in igneous rocks are derived directly from magmas.

Separation of this water-rich phase to form miarolitic cavities did not occur indicating depths of emplacement greater than 6 kilometers (Hyndman, 1972). This fluid phase was locally pervasive, altering biotite flakes within nearby roof pendants to magnetite. One roof pendant, stopped directly into the leucocratic magma is completely altered to magnetite, feldspar and quartz demonstrating the alteration intensity of this fluid phase.

Discussion

Chemical analyses of leucocratic granite suggest that it represents a late stage differentiate of Cretaceous magma. The rock contains the highest concentrations of SiO_2 , K_2O and the lowest concentrations of all other oxide constituents except Na_2O and Al_2O_3 relative to all other Cretaceous-age map units. This conclusion is supported by abundant structural observations which show the unit as

intermediate in age between older batholithic rocks and intrusive rocks related to the Tertiary Challis thermal event. I concur with Anderson (1947) that the "compositon suggests a source in a deeper (more felsic) part of the batholith.....whereas its texture indicates relatively rapid cooling as though the magma had been injected into the solid and cooler part of the batholith" (p. 133).

The position of the magma may have been controlled by deep-seated faulting and fissuring within the batholith. A north northwest-trending linear swarm of roof pendants one kilometer north of the dike swarm may indicate local subsidence of the batholith along a north-west-trending shear. Possibly the leucocratic dikes were emplaced along this shear. This scheme, presented hypothetically in Figure 34, would allow initially for the symmetrical distribution of megacrysts both north and south of the dike swarm (#1 in Figure 34). Subsequent movement along this shear may have downdropped the northern block thus preserving the megacryst aureole only on the northern side of the dike swarm (#2 in Figure 34). Penecontemporaneous faulting associated with the emplacement of the dikes would also explain deformational fabrics in these rocks which include biotite foliation and schlieren, and augen-shaped, sub-parallel quartz-feldspar halos shown in Figure 31.

Perimeters of the felsic halos are fairly sharp and are defined by an abrupt change in biotite content. The sharp outline of the halos presumably indicate steep f_{O_2} gradients across their boundaries with markedly different f_{O_2} concentrations on either side of the

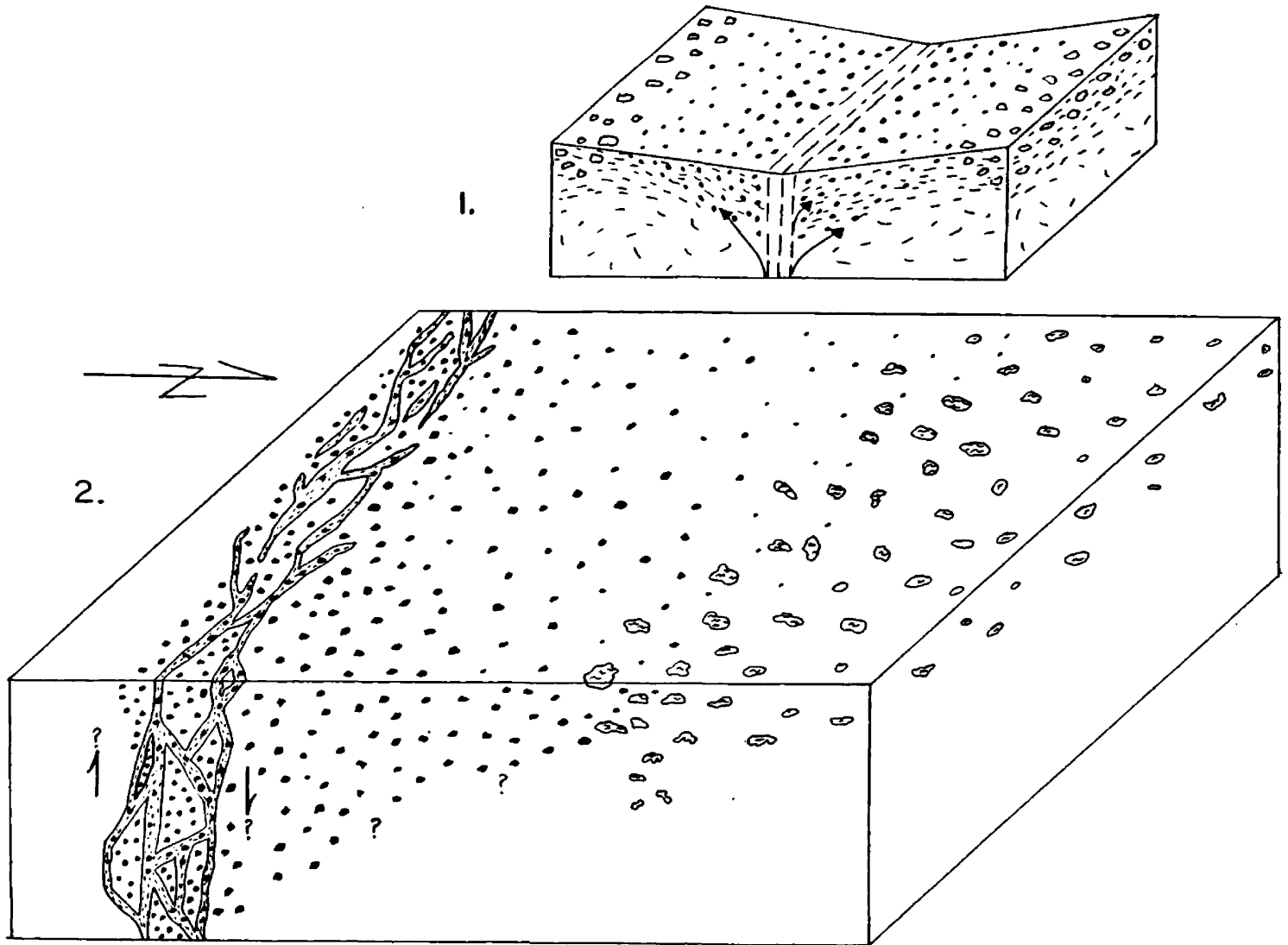


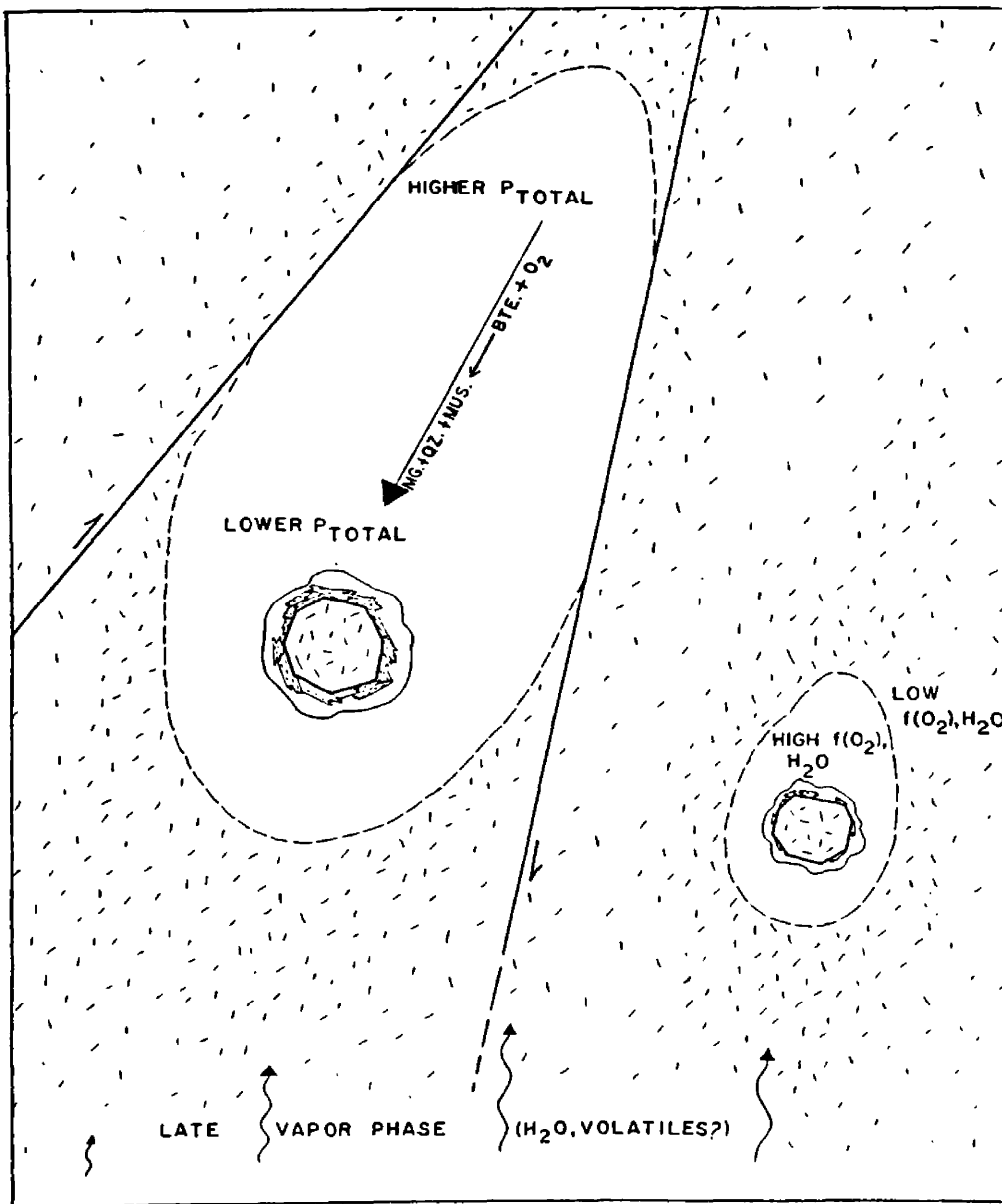
Figure 34.. Schematic diagram for emplacement of leucocratic granite dikes along west-northwest-trending shear in older batholithic rocks. Note the asymmetric distribution of magnetite megacrysts and foliated roof pendants with respect to the dike swarm in part 2. See text for further explanation.

boundaries. The megacrysts and associated depleted halos may be visualized as localized water-rich centers within the melt itself. Localization of the diffuse vapor phase may have been brought about by diffusion of water to zones of low pressure created by shear couples in the melt (Fig. 35).

In a relatively high-silica rock like the leucocratic granite dikes, melt structure must be dominantly controlled by the ratio of alkalis to network-forming cations and by the degree to which dissolved H_2O replaces bridging oxygens with nonbridging OH^- groups (D. Alt, pers. comm., 1980). Thus magma within these water-rich centers was probably less polymerized than the surrounding crystalliquid melt. Dissolved volatiles (e.g. water) would not only depolymerize the melt, but could enhance cation mobility (including Fe^{2+} and Fe^{3+} involved in the formation of the magnetite megacrysts) both through complexing and by increasing cation diffusivities.

Watson (1977) and Ryerson and Hess (1978) have shown that increased polymerization decreases the stability of high field-strength cations in silicate melts. Strongly polymerized silicic liquids provide relatively few suitable sites for highly charged species unable to "fit" within the alumino-silicate network. Hildreth (1980) has shown that the strongest enrichment factors for the high silica, water-rich roof zone of the Long Valley magma chamber were, in order of decreasing concentration: niobium (Nb), chlorine (Cl), antimony (Sb), tantalum (Ta), and uranium (U). These same enrichment trends might be expected within the water-rich portions

Figure 35. Schematic diagram for formation of magnetite megacrysts in the Red Mountain area. Shearing in leucocratic granite melt causes foliation of biotite and migration of water-rich phase to zones of lower pressure. Water-rich phase then reacts with biotite to form the assemblage magnetite muscovite, and quartz.



of the leucocratic granite melt now expressed by the magnetite megacrysts and associated felsic halos.

Extrapolation of the trend of the leucocratic dike swarm beyond the map area to the northwest indicates that these features may underlie the provenance area outlined by Truesdell (1977), and Mackin and Schmidt (1953) for the Bear Valley rare earth placer deposit. This placer contains significant quantities of euxenite, a "radioactive black" mineral containing niobium, tantalum, uranium, and other rare earths, and also columbite-tantalum, an oxide of niobium and tantalum. Contours of uranium concentrations in bedrock (Truesdell, 1977) within the Bear Valley area suggest one or perhaps two broadly linear source terranes for the placer which are roughly coincident with the extrapolated trend of the leucocratic dike swarm and associated megacrysts.

The provenance of the rare earth minerals may be those areas of leucocratic granite and older batholithic rocks affected by the late fluid phase of crystallization. Mapping of the leucocratic dike swarm to the northwest, and more detailed study of the mineralogy and petrology of these rocks and their heavy mineral suites may shed additional light on this tenuous connection.

CHAPTER VII

CONCLUSIONS

The Red Mountain-Bull Trout Point area contains a variety of textural and mineralogical phases of Idaho batholithic rocks which attest to separate Cretaceous and Tertiary thermo-magmatic events. Each event is characterized by a suite of related intrusive rocks which display an apparent evolution of magma from intermediate to felsic compositions.

Cretaceous Rocks

Four textural and compositional units of the Cretaceous Idaho batholith which are widespread units in the south-central and south-eastern portion of the Atlanta Lobe are found in the area. An earlier and partly remobilized mafic shell of foliated granodiorite is found as small, deformed, fault bounded slices near large metamorphic roof pendants in the far eastern portion of the map area. Although relations are obscure, successively more felsic rocks were intruded into the foliated granite including granodiorite porphyry and large amounts of porphyritic granodiorite. The Cretaceous intrusive episode culminated with the emplacement of leucocratic granite. Leucocratic granite is a late-stage differentiated phase which rose preferentially along major zones of weakness in the batholith from a more mobile and presumably more felsic core. This unit is now found as large discordant dike and sheet-like complexes

emplaced along northwest-trending faults and flat-lying joints in the Red Mountain area.

A discrete, pervasive water-rich phase late in the crystallization history of the leucocratic granite is manifested in the formation of magnetite megacrysts with biotite-depleted, quartz-feldspar coronas. The late magmatic phase contained appreciable amounts of dissolved H₂O, and may have also contained significant concentrations of base, precious, and rare-earth metals. Further to the northwest, these rocks may serve as provenance for the Bear Valley rare-earth placer deposit.

Tertiary Rocks

Two comagmatic suites of intrusive rocks of probably Eocene age have been identified in the Red Mountain-Bull Trout Point area. Intrusion of an earlier suite of quartz diorite to granodiorite and granitic plutonic rocks was accompanied by injection of related quartz latite to latite dikes. A later suite of pink granite, with a differentiated cap and marginal facies of alaskite, and associated rhyolitic dikes was emplaced in the vicinity of Bull Trout Point.

Dikes originated from their related plutonic source as upward and laterally injected apophyses of partly crystallized magma. The dikes were injected before, during and after final emplacement of their upwardly migrating plutonic source and some of the earlier dikes were subsequently intruded by the pluton. Linear trends on silica variation diagrams further indicate that both suites of Tertiary

intrusive rocks may be derived from a common magmatic source at depth.

Both intrusive suites were forcibly emplaced into relatively brittle crust within 2 kilometers of the surface. Plutons were in part emplaced along pre-existing or syntectonic northeast-trending high angle normal faults some of which show recurrent movement during Quaternary time. East-west extension was also promoted by intrusion of dikes along pervasive north- to northeast-trending fractures. Radial fractures, probably generated during emplacement of the two Tertiary masses, were not the primary structural controls for dike emplacement. It is suggested, therefore, that all intrusive rocks of known or suspected Eocene age, were generated and emplaced within a pre-existing zone of structural weakness characterized by nearly east-west crustal extension and interpreted here as a northeast-trending incipient crustal rift. Deep-seated north- to northeast-trending faulting and fissuring during this period of extension may have also provided circulation pathways for widespread hydrothermal systems centered around the Tertiary intrusions.

Relating Tertiary dikes with plutons in the Red Mountain-Bull Trout Point area may have important implications for the interpretation of subsurface geology and future mineral exploration in the Idaho Porphyry Belt. Chemical and petrographic analyses of dikes in isolated swarms may yield information as to the nature and composition of plutonic sources at depth. Similarly, dikes which contain significant amounts of base or precious metals may serve as indicators for buried or "blind" porphyry deposits.

REFERENCES CITED

- Anderson, A.L., 1947, Geology and ore deposits of the Boise Basin, Idaho: U.S. Geol. Survey Bull. 944-C, p. 119.
- Anderson, E.M., 1951, The dynamics of faulting and dike formation (2nd ed.): Oliver and Boyd, London, 206 p.
- Armstrong, R.L., 1975, The geochronometry of Idaho: Isochron/West, v. 14, 50 p.
- _____, 1976, The geochronometry of Idaho: Isochron/West, v. 15, 41 p.
- Axelrod, D.I., 1968, Tertiary floras and topographic history of the Snake River basin, Idaho: Geol. Soc. America Bull., v. 79, p. 713.
- Badgely, P.C., 1965, Structural and tectonic principles: Harper and Row, New York, 495 p.
- Badley, R.H., 1978, Petrography and chemistry of the East Fork dike swarm, Ravalli County, Montana: unpub. M.S. thesis, University of Montana, 54 p.
- Barrell, J., 1907, Geology of the Marysville Mining District, Montana, U.S. Geol. Survey Prof. Paper 57, 178 p.
- Bennett, E.H., 1973, The petrology and trace element distribution of part of the Idaho batholith compared to the White Cloud stock, Custer County, Idaho: unpub. Ph.D. Diss., Univ. of Idaho, Moscow, 172 p.
- _____, 1980, Granitic rocks of Tertiary age in the Idaho batholith and their relation to mineralization: Econ. Geol., v. 75, p. 278.
- Bond, J.G. (compiler), 1978, Geologic map of Idaho: Idaho Bur. Mines and Geol., scale 1:500,000.
- Buddington, A.F., 1959, Granite emplacement with special reference to North America: Geol. Soc. America Bull., v. 70, p. 671.
- _____; Fahey, J.J., Ulisidis, A.C., 1955, Thermometric and petrogenetic significance of titaniferous magnetite: Am. Jour. Sci., v. 253, p. 497.
- _____; Lindsley, D.H., 1964, Iron-titanium oxide minerals and synthetic equivalents: Jour. Petrology, v. 5, p. 310.

- Byers, F.M., Jr., Carr, W.J., Orkild, P.P., et al., 1976, Volcanic suites and related cauldrons of Timber Mountain-Oasis Valley caldera complex, southern Nevada: U.S. Geol. Survey Prof. Paper 919, 70 p.
- Carmichael, I.S.E., 1967, The iron-titanium oxides of salic volcanic rocks and their associated ferromagnesian silicates: *Contrib. Mineral. Petrol.*, v. 14, p. 36.
- Cater, F.W., 1969, The Cloudy Pass epizonal batholith and associated subvolcanic rocks: *Geol. Soc. America Spec. Paper* 116, 54 p.
- _____; Pinckney, D.M., Hamilton, W.B., Parker, R.L., 1973, Mineral resources of the Idaho Primitive Area and vicinity, Idaho: U.S. Geol. Survey Bull. 1304, 431 p.
- Criss, R.E., Taylor, H.P., Jr., 1978, Regional $^{18}\text{O}/^{16}\text{O}$ and D/H variations in granitic rocks of the southern half of the Idaho batholith and the dimensions of the giant hydrothermal systems associated with emplacement of the Eocene Sawtooth and Rocky Bar plutons: *Geol. Soc. America Abstr. with Programs*, v. 10, no. 7, p. 384.
- _____; Lanphere, M.A., Taylor, H.P., Jr., 1980, Effects of regional uplift, doming, and meteoric hydrothermal metamorphism on K/Ar ages of biotites in granitic rocks of the southern half (Atlanta Lobe) of the Idaho batholith: *Geol. Soc. America Abstr. with Programs*, v. 12, no. 7, p. 408.
- Donovan, P.R., 1962, The geology of the Little Falls area, Boise County, Idaho: M.S. Thesis, Colorado School of Mines.
- Dover, J.H., 1969, Bedrock geology of the Pioneer Mountains, Blaine and Custer Counties, Idaho: *Idaho Bur. Mines and Geol. Pamphlet* 142, 66 p.
- Dowty, E., 1980, Synneusis reconsidered: *Contrib. Miner. Petrol.*, v. 74, p. 74.
- Eaton, G.P., Wahl, R.R., Protska, H.J., et al., 1978, Regional gravity and tectonic patterns: Their relation to late Cenozoic epeirogeny and lateral spreading in the western Cordillera, *in*, Smith, R.B., and Eaton, G.P., (eds.), *Cenozoic tectonics and regional geophysics of the western cordillera*: *Geol. Soc. America Memoir* 152, 388 p.
- Erler, Elise L., 1980, Petrology and uranium mineralization of the Idaho batholith near Stanley, Custer County, Idaho: unpub. M.S. thesis, University of Montana, 98 p.

- Eugster, H.P., and Wones, D.R., 1962, Stability relations of the ferruginous biotite, annite: *Jour. Petrology*, v. 3, p. 82.
- Fiske, R.S., Hopson, C.A., and Waters, A.C., 1963, Geology of the Mount Rainier National Park, Washington: U.S. Geol. Survey Prof. Paper 444, 93 p.
- Griggs, D.T., and Handin, J., eds., 1960, Rock deformation: *Geol. Soc. America Memoir* 79, 382 p.
- Hildreth, W., 1979, The Bishop Tuff: Evidence for the origin of compositional zonation in silicic magma chambers, *in* Chapin, C.E., and Elston, W.E. eds., *Ash-flow tuffs*: *Geol. Soc. America Spec. Paper* 180, p. 43.
- Hubbert, M.K., and Willis, D.G., 1957, Mechanics of hydraulic fracturing: *AIME Transactions*, v. 210, p. 153.
- Hyndman, D.W., 1972, *Petrology of igneous and metamorphic rocks*: McGraw-Hill, New York, 533 p.
- _____ ; ms, *Petrology of igneous and metamorphic rocks*, 2nd Edition: McGraw-Hill, New York.
- _____ ; Badley, R., and Rebal, D., 1977, Northeast-trending early dike swarm in central Idaho and western Montana: *Geol. Soc. America Abstr. with Programs*, v. 9, p. 734.
- _____ ; and Williams, L.D., 1977, The Bitterroot Lobe of the Idaho Batholith: *Northwest Geology*, v. 6-1; p. 1.
- Kennedy, G.C., 1955, Some aspects of the role of water in rock melts: *Geol. Soc. America Spec. Paper* 62, p. 489.
- Kilsgaard, Thor H., Freeman, V.L., Coffman, J.S., 1970, Mineral resources of the Sawtooth Primitive Area, Idaho: *U.S. Geol. Survey Bull.* 1319-D, p. D-1.
- Mackin, J.H., and Schmidt, D.L., 1953, Reconnaissance geology of placer deposits containing radioactive minerals in the Bear Valley district, Valley County, Idaho: *U.S. Geol. Survey, TEM Report* 602, part 1, 32 p.
- MacLeod, W.N., Turner, D.C., and Wright, E.P., 1971, The geology of the Jos Plateau: *Geol. Sur. of Nigeria Bull.* 32, v. 1, 110 p.
- Nockolds, S.R., 1954, Average chemical compositions of some igneous rocks: *Geol. Soc. America Bull.*, v. 65, p. 1007.

- Nold, J.L., 1974, Geology of the northeastern border zone of the Idaho batholith: Northwest Geology, v. 3, p. 47.
- Olson, H.J., 1968, The geology and tectonics of the Idaho Porphyry Belt from the Boise Basin to the Casto quadrangle: unpub. Ph.D. thesis dissertation, University of Arizona.
- Ramdohr, P., 1969, The ore minerals and their intergrowths: Pergamon Press, English translation, 3rd Edition, Oxford, England.
- Reid, R.R., 1963, Reconnaissance geology of the Sawtooth Range: Idaho Bur. Mines and Geology Pamph. 129, 37 p.
- Rember, W.C., and Bennett, E.H., 1979, Geologic map of the Challis quadrangle, Idaho: Idaho Bur. Mines and Geology. Geologic Map Series, Challis two-degree quadrangle.
- Ross, C.P., 1934, Geology and ore deposits of the Casto quadrangle, Idaho: U.S. Geol. Survey Bull. 854, 135 p.
- _____, 1937, Geology and ore deposits of the Bayhorse region, Custer County, Idaho: U.S. Geol. Survey Bull. 877, 161 p.
- _____, 1962, Stratified rocks in south-central Idaho: Idaho Bur. Mines and Geology Pamph. 125, 126 p.
- Roy, S., 1954, Ore microscopic studies of the vanadium-bearing titaniferous iron ores of Mayurbhan, with a detailed note on their texture: Nat. Inst. Sci. India, Proc. 20, p. 691.
- Ryerson, F.J., and Hess, R.C., 1978, Implications of liquid distribution coefficients to mineral-liquid partitioning: Geochimica et Cosmochimica Acta, v. 42, p. 921.
- Schmidt, D.L., 1964, Reconnaissance petrographic cross section of the Idaho batholith in Adams and Valley Counties, Idaho: U.S. Geol. Survey Bull. 1181-G.
- Smith, R., 1967, A regional gravity survey of western and central Montana: unpub. Ph.D. dissertation, University of Utah.
- Smith, R.L., 1979, Ash-flow magmatism, in, Chapin, C.E., and Elston, W.E., eds., Ash-flow tuffs: Geol. Soc. America Spec. Paper 180, p. 5.
- Streckeisen, A., 1976, To each plutonic rock its proper name: Earth-Science Reviews, v. 12, p. 1.

- Sylvester, A.G., Oertel, G., Nelson, C.A., and Christie, J.M., 1978, Papoose Flat pluton: A granitic blister in the Inyo Mountains, California: *Geol. Soc. America Bull.*, v. 89, p. 1205.
- Treves, S.B., and Melear, J.D., 1953, The geology and ore deposits of the Seafoam Mining District, Custer County, Idaho: *Idaho Bur. Mines and Geology Pamphlet 96*, 19 p.
- Truesdell, P., Wegrzyn, R., and Dixon, M., 1977, Provenance of radioactive placers, Big Meadow area, Valley and Boise Counties, Idaho: U.S. Energy Research and Development Administration Report GJBX-15(77), 52 p.
- Tuttle, O.F., and Bowen, N.L., 1958, Origin of granite in the light of experimental studies in the system $\text{NaAlSi}_3\text{O}_8\text{-KAlSi}_3\text{O}_8\text{-SiO}_2\text{-H}_2\text{O}$: *Geol. Soc. America Memoir 74*, 153 p.
- Vance, J.A., 1969, On synneusis: *Contrib. Mineral. and Petrology*, v. 24, p. 7.
- Walker, F., 1957, Ophitic texture and basaltic crystallization, *Jour. of Geol.*, v. 65, p. 1.
- Watson, E.B., 1977, Partitioning of manganese between forsterite and silicate liquid: *Geochim. et Cosmochimica acta*, v. 41, p. 1363.
- Whitney, J.A., 1975, The effects of pressure, temperature and XH_2O on phase assemblage in four synthetic rock compositions: *Jour. of Geol.*, v. 83, p. 1.
- Wilcox, R.E., 1979, The liquid line of descent and variation diagrams, in, Yoder, H.S. (ed.), *The evolution of the igneous rocks, 50th anniversary perspectives*, p. 205.
- Williams, L.D., 1977, Petrology and petrography of a section across the Bitterroot lobe of the Idaho batholith: unpub. Ph.D. thesis dissertation, University of Montana, 221 p.
- Wilson, H.D.B., 1953, Geology and geochemistry of base metal deposits: *Econ. Geol.*, v. 48, p. 370.
- Wones, D.R., and Eugster, H.P., 1965, Stability of biotite: Experiment, theory, and application: *American Mineralogist*, v. 50, p. 1228.